Study of the non linear behaviour of concrete structures

Auteur : Dumoulin, Kevin
Promoteur(s) : De Ville De Goyet, Vincent
Faculté : Faculté des Sciences appliquées
Diplôme : Master en ingénieur civil des constructions, à finalité approfondie
Année académique : 2015-2016
URI/URL : http://hdl.handle.net/2268.2/1379

Université de Liège - Faculté des Sciences Appliquées

Comportement non-linéaire des structures en béton

Mémoire de fin d'études réalisé en vue de l'obtention du grade de master Ingénieur Civil des constructions par Dumoulin Kévin

Jury Members : Vincent De Ville De Goyet, Jean-Marc Franssen, Boyan Mihaylov, Yves Duchêne

Année académique 2015-2016

Université de Liège

Study of the non linear behaviour of concrete structures

Graduation Studies conducted for obtaining the Master's degree in Civil Engineering in Construction by Dumoulin Kévin

Academic year 2015-2016

Summary

Running complete non linear analysis in concrete structure requires still some thinking. Which properties of the concrete and the reinforcement steel should be used for the analysis ? This question is more likely problematic for the concrete for which the uncertainties on the material strength are higher than for the reinforcement steel. Several approaches using different material properties exist in the literature and are here investigated and compared. The approaches of the partial safety factor (using design properties) and of the global resistance factor (using modified mean properties) appear to be correlated and nearly similar. In contrast, real benefits that can reach 20 % of extra load margin compared to the two first, can be done using the estimation of the coefficient of variation approach.

In addition, where do we have to put the uncertainties safety factors on the model of actions and resistances in the verification process ? Depending of the type of structure, the position of these safety factors can be argued and discussed. Indeed, for a non linear analysis, the relation between the force and the displacement is by definition non linear. The position of the safety factors (on the load or on the displacement) has then an importance and depends on the behaviour of the structure (under or over-proportional). For each approach, different relations are then proposed in function of the position of these factors of uncertainties.

The different relations of each approaches are here studied thanks to different numerical models. Models on cubes, columns, frames and beams with the catenary effect are made in this work using the non linear analysis software Finelg.

Université de Liège

Comportement non-linéaire des structures en béton

Mémoire de fin d'études réalisé en vue de l'obtention du grade de master Ingénieur Civil des constructions par Dumoulin Kévin

Année académique 2015-2016

Résumé

Utiliser une analyse non linéaire complète pour une structure en béton requiert encore quelques interrogations. Quelles propriétés pour le béton et l'acier de renforcement doivent être utilisées pour l'analyse ? Cette question est plus problématique pour le béton pour lequel les incertitudes sur la résistance sont plus grandes que pour l'acier de renforcement. Plusieurs approches, utilisant différentes propriétés du matériau, présentes dans la littérature sont ici étudiées et comparées. Les approches de coefficient partiel de sécurité (utilisant des propriétés de dimensionnement) et d'un coefficient global de sécurité (utilisant des propriétés moyennes modifiées) apparaissent comme étant fort corrélées et similaires. Par contre, de réels avantages, qui peuvent atteindre 20 % de charges en plus comparé aux deux premières, peuvent être fait en utilisant l'approche de l'estimation du coefficient de variation.

De plus, où est-il nécessaire de placer les coefficients de sécurité sur les incertitudes du modèle des actions et de la résistance dans le processus de vérification ? Dépendant du type de structure, la position de ces coefficients peut être discutée. De fait, pour une analyse non linéaire, la relation entre la charge et le déplacement est par définition non linéaire. La position de ces coefficients de sécurité (sur la charge ou sur le déplacement) a donc une importance et dépend du comportement de la structure (sous ou sur-proportionnel). Pour chaque approche, différentes relations sont donc proposées en fonction de la position de ces coefficients d'incertitudes.

Les différentes relations de chaque approche sont donc ici étudiées grâce à différents modèles numériques. Des modèles de cubes, colonnes, portiques ainsi que de poutres avec l'effet chainette sont réalisés dans ce travail en utilisant le programme d'analyse non linéaire Finelg.

Remerciement

Je tiens de manière général à remercier toutes les personnes qui ont contribué de près ou de loin à la réalisation de mon travail de fin d'études.

Plus particulièrement,

Je voudrais remercier Vincent de Ville de Goyet, mon promoteur, pour tout d'abord avoir proposé ce sujet mais surtout pour m'avoir suivi et guidé tout au long du travail.

Ensuite, je tiens à remercier Mr Jean-Marc Franssen, Mr Boyan Mihaylov ainsi que Mr Thomas Gernay pour leur contributions, aides et avis dans le processus d'évolution de mon travail de fin d'étude. De même, je tiens à addresser mes remerciement à Mr Corentin Pesesse qui a m'a aidé à quelques reprises dans l'utilisation du logiciel de calcul FINELG et CINELU.

En avance, je tiens à remercier les différents membres du jury pour l'intérêt qu'ils portent au travail ainsi que pour le temps qu'ils consacreront à sa lecture et à son évaluation.

Finalement, je cloturerais en remerciant mes parents pour leur soutien inépuisable ainsi que l'ensemble de mes camarades de promotion.

Table of Contents

1 Symbols

The following symbols are valid for the present work and are mostly taking from the Eurocode.

Latin letters :

E_{cm}	Secant/Mean value of the modulus of elasticity for the concrete.
E_s	Modulus of elasticity for the reinforcement steel.
E_{cd}	Design value of modulus of elasticity for the concrete.
L_{fl}	Buckling length of one element.
f_c	Compressive strength of the concrete.
f_{cd}	Design value of the concrete compressive strength.
f_{ck}	Characteristic compressive cylinder strength of the concrete at 28 days.
$f_{c\tilde{m}}$	Modified mean value of the concrete cylinder compressive strength.
f_{cm}	Mean value of the concrete cylinder compressive strength.
f_y	Yield strength of the steel reinforcement.
f_{yd}	Design yield strength of the steel reinforcement.
f_{yk}	Characteristic yield strength of the steel reinforcement.
f_{ym}	Mean yield strength of the steel reinforcement.
q_{ud}	Design ultimate load limit.
$q_{u\tilde{m}}$	Modified mean ultimate load limit.
q_{uk}	Characteristic ultimate load limit.
q_{um}	Mean ultimate load limit.
q_{demand}	Demand value of the load (without partial safety factor).
V_R	Coefficient of variation of the resistance.
V_m	Coefficient of variation of the model uncertainty.
V_g	Coefficient of variation of the geometrical uncertainty.
V_f	Coefficient of variation of the material strength.

Greek symbols :

α_{cc}	Coefficient taken into account the long term effects on the compressive strength and the unfavourable effects resulting from the way the load is applied.
α_R	Sensitivity factor on the resistance.
α_h	Coefficient of reduction related to the length/high - Geometrical imperfections.
α_m	Coefficient of reduction related to the number of elements - Geometrical imperfections.
β	Reliability index.
γ_c	Partial safety factor forthe concrete material.
γ_g	Partial safety factor for the permanent actions without the model uncertainties.
γ_G	Partial safety factor for the permanent actions G.
γ_M	Partial safety factor on the material properties.
γ_q	Partial safety factor for the variable actions without the model uncertainties.
γ_Q	Partial safety factor for the variable actions Q.
γ_{Rd}	Partial safety factor associated to the uncertainties of the model resistance.
γ_{sd}	Partial safety factor associated to the uncertainties of the model action and/or the effect.
γ_O	Global safety coefficient on the resistance.
$\gamma_{O'}$	Global safety coefficient on the resistance when γ_{Rd} and γ_{sd} are unit values.
γ_{Om}	Global safety coefficient on the resistance for the ECOV approach.
γ_s	Partial safety factor for the reinforcement steel material.
λ	Slenderness coefficient.
χ	Factor representing the demand load over the resistance load.
ϵ	Deformation of the material (steel and concrete).
ρ_s	Reinforcement steel ratio.
θ_0	Basic inclination.
θ_i	Calculated inclination.

2 Introduction

Non linear analysis of concrete structure has still some uncertainties and issues to be solved. Different types of approaches are here detailed and compare using the non linear finite element software Finelg.

The procedure of designing a structure can be usually separated into two major steps. First the analysis of the structure has to be done in order to obtain the internal forces in each elements for different load cases. Secondly and finally, the verification of the sections of each elements for the obtained internal forces is computed. A complete non linear analysis advantage is to gather these two separated steps into one by introducing the material laws, and the geometrical non linearity into the analysis.

Complete non linear analysis are frequently used for steel structures especially thanks to the simple stress-strain relationship of the steel material. For concrete structures, such analysis are rare. Indeed, the stress-strain relationship of the concrete is not unique and dependent of the strength. Concerning the steel, the Young modulus is constant for all types of quality where the concrete presents different modulus. Even for the same quality of concrete, the modulus of elasticity changes if the mean or the design strength is used. The variability of the concrete gives also some issues and questions on the material law to be used (mean, characteristic or design curve).

Several approaches are provided by the codes and the literature to compute a complete non linear analysis for a concrete structure. A focus on the approaches from the Eurocode 1992 [1][2] and the concrete model code [3] is done in this work. Approaches of partial safety factor and global resistance factor are explained in the Eurocode 1992 [1][2]. The estimation of the coefficient of variation approach is introduced in the concrete model code [3].

An other aspect to turn to is concerning the position of the different safety factor in the verification process. In fact, the safety factor that represents the uncertainties on the model of actions and resistances can be placed on different position (on the load or on the effect of the load) depending on the structure.

In this rapport, first a brief summary of the important input parameters as the material properties and the geometrical imperfections is done. Then, the next section focuses on the different approaches available in the code and in the literature in a static approach. Also a section on the code rules on the dynamic analysis issues are briefly introduced. The main part of this work consists on the modelling test. Models of cubes, columns, frames and a beam with the catenary effect are investigated in order to compare the different approaches and the relations available. Finally a brief conclusion is done.

3 Problematic

As explained in the introduction, computing an complete non linear analysis on concrete structure has still some issues. The major questions are the material laws to be used in such analysis. Indeed, it has an importance especially concerning the modulus of elasticity. If the modulus is decreased in order to take into account the uncertainties on it, the structure becomes more flexible that leads to an increase of the second order effect. This fact is observe when design value for the material law are used. Indeed, the modulus of elasticity E_{cm} has to be divided by 1,2.

The same idea can be extrapolated to a dynamic analysis for concrete structure. Indeed, if the young modulus changes and decreases, it increases the period of the structures. In the case of seismic analysis, the increase of the period of the structure leads to a decrease of the seismic loads. So for a design, reducing the loads is not really a conservative method. Concerning now the wind analysis, the gust have a period of more or less 4 seconds. By increasing the period of the structure, the structure can become highly sensitive to the wind.

These issues are solved by choosing one approach over an other. In fact, each approach proposed and detailed in the following sections are based on different assumption concerning the material properties (design properties, mean properties,...).

The next issue concerns now the position of the different safety factors in the verification process. Indeed, different relations with a difference in the position for the safety factors are formulated in the codes. Sometimes, the safety factor are placed on the load, and sometimes on the effect of the load. Because non linear analysis are studied in this work, the position of the safety factor influences the verification of the structure. For each approaches, a clear definition of these different relations are done with then in the modelling part a comparison and an explanation of the results obtained.

4 Input parameters

The report begins with an introduction to the different input parameters needed for one nonlinear analysis. Indeed, the further discussions will refer to these parameters. The input parameters concern the stress-strain relationships (material laws) and the geometrical imperfections required for a complete non linear analysis. Some rules are provided in the Eurocode 1992-1-1 [1] for the concrete and the reinforcement steel relationships. The Eurocode 1992-1-1 [1] gives also the rules concerning the introduction of the imperfections into the model.

4.1 Concrete material law

The stress-strain relationship for the concrete in compression proposed in the Eurocode 1992-1-1 [1] in the case of a non linear analysis has for general expression :

$$\frac{\sigma_c}{f_c} = \frac{k\eta - \eta^2}{1 + (k-2)\eta} \tag{1}$$

with

— $\eta = \epsilon_c/\epsilon_{c1}$.

— ϵ_{c1} is the deformation at the peak stress.

— f_c is the compressive strength of the concrete.

— $k = 1{,}05\, E_c|\epsilon_{c1}|/f_c$ with E_c is the young modulus. Values of the young modulus can be obtained in the Eurocode 1992-1-1 [1] or directly in the table 68 in the annex.

The representation of this relation can be observed in figure 1 below :

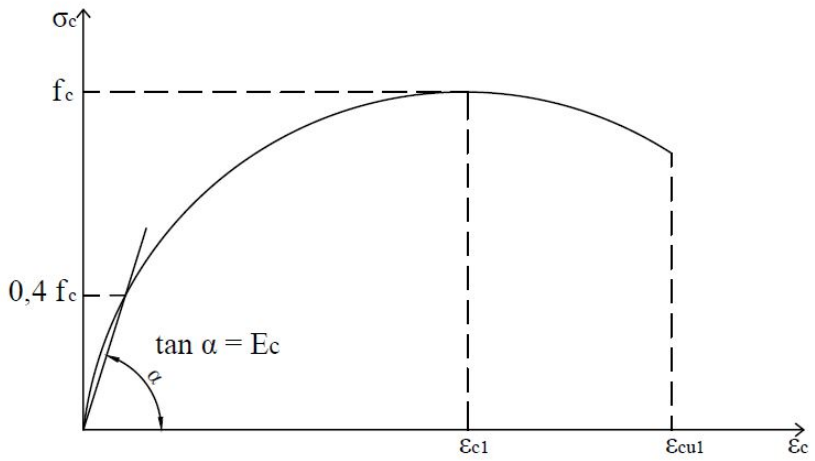

FIGURE 1 – Stress-strain relationship used in the non linear analysis for the concrete material.

This relation is only valid for deformation from 0 to ϵ_{cu1}. Indeed, when the deformation increases too much, tension appears in the relationship which is not possible. An other relation can be used if this relation represents well the behaviour of the considered concrete, however in our case, a change of the material law has not been studied. The possible tension in the concrete is not investigate in this work.

4.2 Reinforcement steel material law

Concerning the reinforcement steel, two stress-strain relationships can be chosen. Some different hypothesis can be made according to the Eurocode 1992-1-1 [1] :

— Hardening after yielding with a limit on the deformation equal to ϵ_{uk} and a maximal stress of k f_{yk} for ϵ_{uk} with k and ϵ_{uk} that can be found in the annex C of the Eurocode 1992-1-1 [1] and in the table 1 below.

— No hardening and no limitation on the deformation limit. The non-necessity of limitation can be discussed and for example in the national annex for Belgium [4], a limitation as in the first case has to be taken.

In a design analysis, the limitation corresponds to ϵ_{ud}. The recommended value of ϵ_{ud} is equal to 0,9 ϵ_{uk}, however, the national annex for Belgium [4] recommends to use a value of $\epsilon_{ud} = 0{,}8\ \epsilon_{uk}$. The young modulus of the reinforcement steel is always equal to 200 GPa.

The representation of this relationship can be seen in figure 2 below :

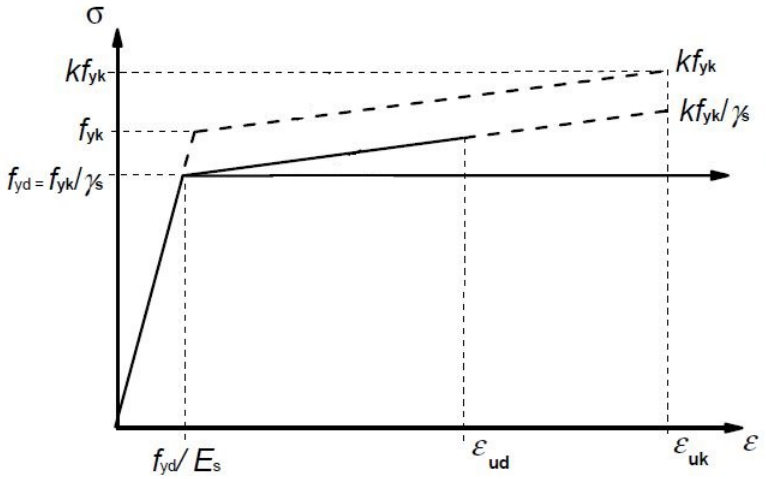

FIGURE 2 – Stress-strain relationship for the reinforcement steel material [1].

The table 1 below summarizes the properties of the reinforcement steel based on the type of the steel.

Product form	Bars and de-coiled rods or Wire Fabrics		
Class	A	B	C
Characteristic yield strength f_{yk} or $f_{0,2k}$ [MPa]	400 to 600		
Minimum Value of k = $\frac{f_{t1}}{f_y}$	$\geq$ 1,05	$\geq$ 1,08	1,15 $\leq$ k $\leq$ 1,35

TABLE 1 – Properties of the steel reinforcement [1].

4.3 Geometrical imperfections

The analysis has to take into account the unfavourable effect of the geometrical imperfections on the structure. Concerning the uncertainties of the dimension of the sections, they are directly embedded into the material safety factor γ_M. But the imperfection of the construction has to be taken into account into the analysis. The Eurocode 1992-1-1 [1] provides the rules and the guidelines for these imperfections :

The imperfections can be represented thanks to an inclination θ_i of the element :

$$\theta_i = \theta_0 \alpha_h \alpha_m \tag{2}$$

with

- θ_0 is the basic inclination. The value to use can also vary for the different countries. The recommended value in the Eurocode 1992 [1] is $\theta_0 = 1/200$.
- α_h is the coefficient of reduction related to the length/high : $\alpha_h = 2/\sqrt{l}$ with $2/3 \leq \alpha_h \leq 1$.
- α_m is the coefficient of reduction related to the number of elements : $\alpha_m = \sqrt{0,5(1+1/m)}$.
- l is the length/high of the element.
- m is the number of vertical elements contributing to the global effect.

In the case of isolated members and here more especially for a cantilever column, the effect of the geometrical imperfections can be taken in two manners :

1) with an eccentricities $e_i = \theta_i l_0/2$ where l_0 is the effective length of the members. In the case of a cantilever column, l_0 is equal to $2l$.
2) with a lateral load H_i resulting in the same first order moment. H_i l = N e_i $\rightarrow$ H_i = N $\frac{\theta_i l_0/2}{l_0/2}$ = Nθ_i.

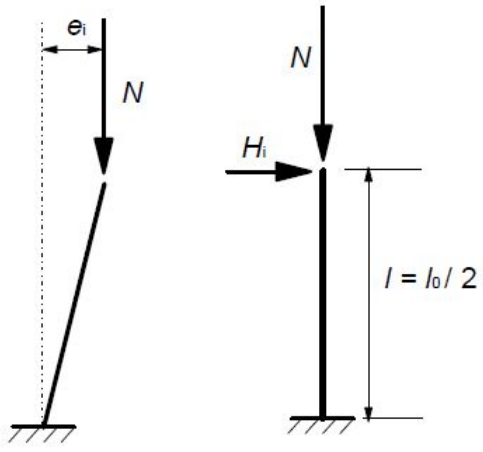

FIGURE 3 – Effect of the geometrical imperfections on isolated members [1].

5 Codes and rules available (static approach)

In this part, the different codes available (Eurocode 1992 [1], [2] and the Concrete model code [3]) are investigated for the non linear analysis rules. Moreover, some approaches on the non linear analysis for concrete structure provided in the literature are also studied. First, some general remarks on the safety format are introduced. Then, the different approaches are explained and detailed. Finally, a comparison between these approaches and an illustration are done.

5.1 Safety format

First of all, some general remarks about the design process and the different safety coefficient is done. The general design condition that has to be fulfilled is :

$$F_d \leq R_d \tag{3}$$

where F_d corresponds to the design value of the actions and R_d the design resistance. This relation imposed a condition on the load whatever the safety factors. An other way of thinking would be to compare the effect of these loads (displacements or also stresses). For a non linear analysis, the relation between the load and the effect of it is by definition not linear. This non linearity brings an other question on the position of the safety factors hidden behind F_d and R_d. Several approaches exist to obtain the design resistance R_d and are explained in the following parts. The different condition relation are also mentioned for each approaches.

5.2 Global resistance factor approach

The global resistance factor (GRF) approach's principle is to compute a non linear analysis with modified mean values of the stress-strain relationship. This approach's principle is similar to the method proposed in the Eurocode 1992-2 [2].

- Mean stress-strain relationship is used for the reinforcement steel (f_{ym} = 1,1 f_{yk}).
- For the concrete properties, E_{cm} is used for the Young modulus and modified mean strength is used for the compressive limit ($f_{c\tilde{m}}$ = 1,1 α_{cc} γ_s/γ_c f_{ck}).
- The favourable effect of the tensile resistance of the concrete cannot be used.

The coefficient α_{cc} takes into account the long term effect and the unfavourable position of the loads. The recommended value in the Eurocode 1992-1-1 [1] is 1, but it can be furnished by the national annex. Concerning the Belgium [4], α_{cc} is taken as 0,85. For record, the United-Kingdom [5] and the France [6] recommend a value of 0,85 and 1 respectively.

The reason behind this modified value used for the concrete material comes from the global safety factor obtained when considering separately both material and their respective safety factor. Indeed, when $\alpha_{cc} = 1$, we obtain as the ratio between the mean and the design strength :

$$\frac{f_{ym}}{f_{yd}} = \frac{1,1 f_{yk}}{f_{yk}/\gamma_s} = 1,1 \times 1,15 = 1,265- \tag{4}$$

$$\frac{f_{cm}}{f_{cd}} = \frac{1,1 f_{ck}}{f_{ck}/\gamma_c} = 1,1 \times 1,5 = 1,65- \tag{5}$$

Where γ_s and γ_c are the partial safety factor on the material properties. 1,1 is the factor to convert characteristic to mean strength. Noted that this 1,1 factor is valid for the steel but not really for the concrete where $f_{cm} = f_{ck} + 8$ [MPa]. The global factor is different in case of steel failure or concrete failure. Or the partial factor used in equations 4 and 5 formulated the same failure probability. In order to obtain an unique global factor, a modified formulation for the mean value is computed :

$$\frac{f_{c\tilde{m}}}{f_{cd}} = \frac{1,1\gamma_s/\gamma_c f_{ck}}{f_{ck}/1,5} = \frac{1,1 \times 1,15 \times 1,5}{1,5} = 1,265- \tag{6}$$

Then, an unique safety factor is obtained and equals 1,265.

The output of the non linear analysis is the ultimate load limit, called $q_{u\tilde{m}}$. The Eurocode 1992-2 [2] provides these following inequalities, on the effects of the loads (E) or on the loads (q), that have to be verified :

$$E(\gamma_{sd} q_{demand}) \leq E\left(\frac{q_{u\tilde{m}}}{\gamma_O \gamma_{Rd}}\right) \quad or \quad \gamma_{sd} q_{demand} \leq \frac{q_{u\tilde{m}}}{\gamma_O \gamma_{Rd}} \tag{7}$$

$$\gamma_{Rd} E(\gamma_{sd} q_{demand}) \leq E\left(\frac{q_{u\tilde{m}}}{\gamma_O}\right) \quad or \quad q\left[\gamma_{Rd} E(\gamma_{sd} q_{demand})\right] \leq \frac{q_{u\tilde{m}}}{\gamma_O} \tag{8}$$

$$\gamma_{Rd}\gamma_{sd} E(q_{demand}) \leq E\left(\frac{q_{u\tilde{m}}}{\gamma_O}\right) \quad or \quad q\left[\gamma_{Rd}\gamma_{sd} E(q_{demand})\right] \leq \frac{q_{u\tilde{m}}}{\gamma_O} \tag{9}$$

$$E(q_{demand}) \leq E\left(\frac{q_{u\tilde{m}}}{\gamma_{O'}}\right) \quad or \quad q_{demand} \leq \frac{q_{u\tilde{m}}}{\gamma_{O'}} \tag{10}$$

with

— γ_{Rd} is the partial coefficient represented the uncertainties of the resistance model, the recommended value is γ_{Rd} = 1,06 [2]. Note that the value of γ_{Rd} can vary with the uncertainties of the model. Indeed, the model code of concrete [3] proposes 1,0 for no uncertainties, 1,06 for low and 1,1 for high uncertainties. However the concrete model code [3] also recommends to use 1,06 in the case of a non linear finite element analysis.

— γ_{sd} is the partial coefficient represented the uncertainties of the actions model and/or their effects. The value should be taken from 1,05 to 1,15. The recommended value in the Eurocode 1992-2 [2] is γ_{sd} = 1,15. In the national annex of Belgium [4], additional remarks are provided :γ_{sd} = 1,05 for the model with few uncertainties, as for example the actions applied on isostatic structures, γ_{sd} = 1,15 is applied then to the model of structures highly hyperstatic, γ_{sd} = 1,10 is applied finally for the intermediary structures.

— γ_O is the global resistance factor, its value is taken as 1,20 [2]. Note that $\gamma_O\gamma_{Rd} = 1,272$ and equals more or less the global factor obtained in the equation 5 and 6. γ'_O is also the global resistance factor but when γ_{Rd} and γ_{sd} are not directly taken into account, $\gamma'_O = 1{,}27$. We see that this coefficient γ'_O covers γ_{Rd} but not γ_{sd}. Indeed, $\gamma'_O = 1{,}27 \approx \gamma_O\gamma_{Rd}$.

— q_{demand} is defined as the load value, $q_{demand} = \gamma_g G + \gamma_q Q = F_d/\gamma_{sd}$. $F_d = \gamma_G G + \gamma_Q Q$ or $\gamma_g = \gamma_G/\gamma_{sd}$; $\gamma_q = \gamma_Q/\gamma_{sd}$, in fact, it is γ_G and γ_Q that are provided in the Eurocode 1990 [7].

— $q_{u\tilde{m}}$ corresponds to the ultimate limit load in the non linear analysis using modified mean value for the concrete material and mean properties for the reinforcement steel.

The difference between these relations is simply the position of the safety coefficients. Sometimes they multiply or divide the actions, and sometimes their effects. But for a non linear analysis, the relation between the action and their effects is not especially linear so dividing the actions or the effects has not especially the same impact. Three types of curves depending on the behaviour can be extracted and are illustrated in figure 4(a) : linear behaviour, underproportional behaviour and overproportional behaviour. The Eurocode 1990 [7] discuss that problematic :

a) When the action effect (E,R) increases more than the action (q) (overproportional behaviour), the partial safety factor should be applied to the value of the action.

b) When the action effect (E,R) increases less than the action (q) (underproportional behaviour), the partial safety factor should be applied to the value of the action effect.

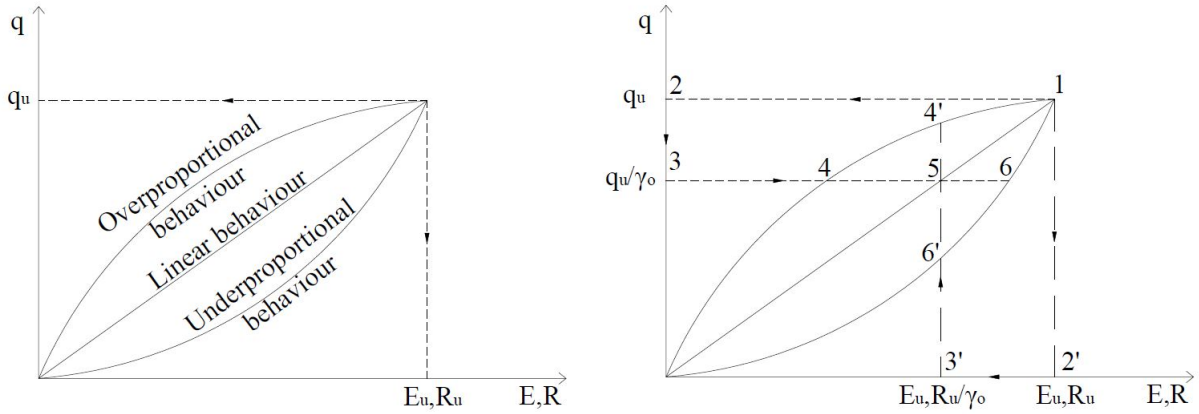

(a) Different behaviour illustration (b) Strategy impact for the verification

FIGURE 4 – Non linear curve illustration - Behaviour illustration and strategy of the verification.

Most of the common structures present a behaviour as a) except for cable or membrane. The figure 4(b), shows the difference between both strategy.

As explained, for an overproportional behaviour, the partial safety factor should be applied to the value of the action in order to obtain to most unfavourable effect. Indeed, we see in figure 4(b) that the point 4 (dividing the action value) appears earlier than the point 4' (dividing the action effect value) on the non linear curve which means that the effect is highly impacted. This observation can also be done for the underproportional behaviour where the conclusion are reversed. It is also obvious that for a linear behaviour, dividing the action or the action effect leads to the same result (point 5 in figure 4(b)).

The figure 5 below illustrates in a theoretical manner the procedure of the different relation presented. The relation are illustrated thanks to the path (in dashed line and with numbers) needed to make the verification. The points without prime represent the right member path (resistance) and the points with prime the left member path (demand). The verification can be done with the load but also with the effect of the load. The verification of one leads obviously to the other but not with the same safety margin.

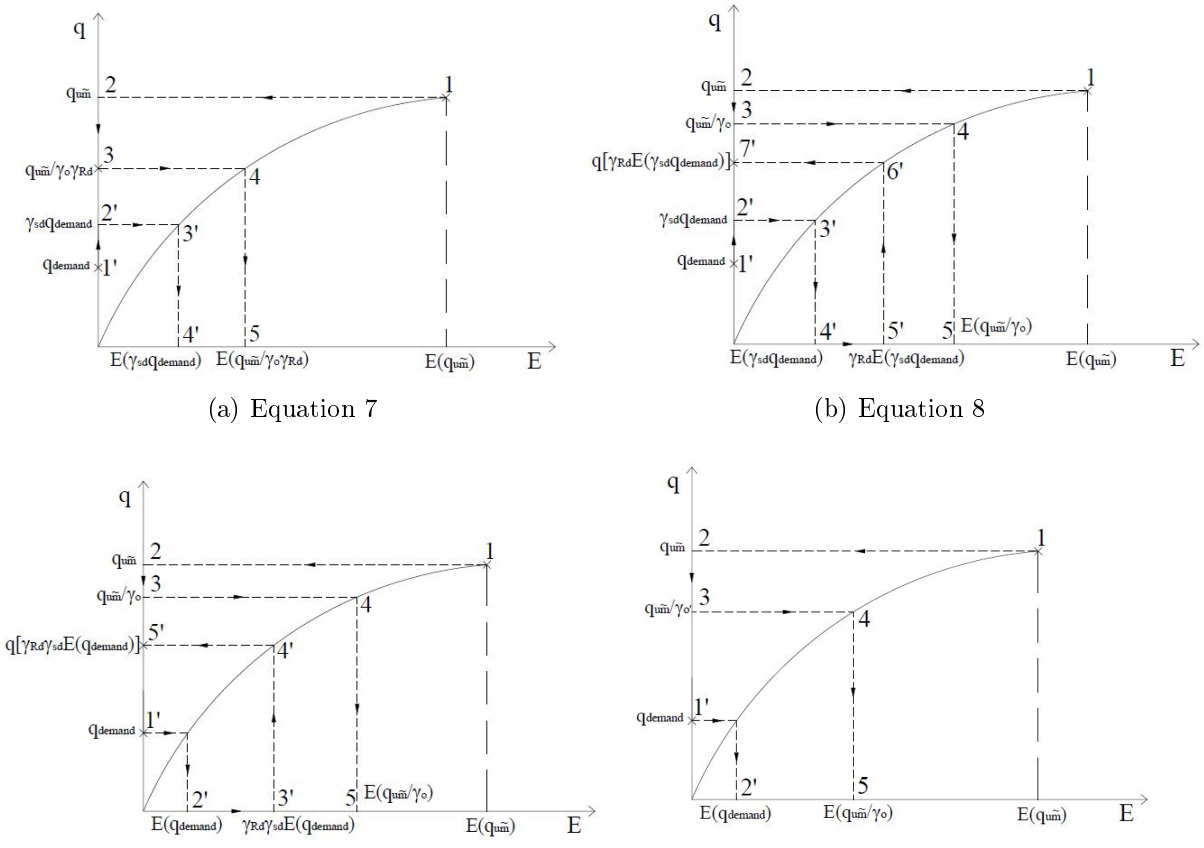

FIGURE 5 – Illustration of the different relations of verification for the GRF approach.

5.3 Estimation of the coefficient of variation of resistance (ECOV)

This approach (ECOV) [3] uses mean value for the concrete material properties to calculate the ultimate resistance q_{um}. Then, to obtain the value of the global resistance coefficient $\gamma_{Om} = \frac{R_m}{R_d}$, it proposes to estimate the coefficient of variation of resistance. To do that, an estimate of the mean and characteristic values of the resistance has to be calculated using the corresponding material properties. Concerning the characteristic properties of the concrete, also mean Young modulus is used.

$$R_m = (f_{cm}, f_{ym}, E_{cm}) \quad \& \quad R_k = (f_{ck}, f_{yk}, E_{cm}) \tag{11}$$

The coefficient of variation of the resistance (σ_R/μ_R) is then obtained thanks to :

$$V_R = \frac{1}{1,65} \ln\left(\frac{R_m}{R_k}\right) \quad \text{or also} \quad R_k = R_m \exp(-1,65 V_R) \tag{12}$$

The coefficient 1,65 assumes the probability of the characteristic load limit as 0,05 and a lognormal distribution of the resistance of the structure. Finally the global resistance coefficient γ_{Om} is determined by the following expression :

$$\gamma_{Om} = \frac{R_m}{R_d} = \exp(\alpha_R \beta V_R) \tag{13}$$

with α_R is the sensitivity factor for the reliability of resistance and β the reliability index. These coefficients can be obtained from the Eurocode 1990 [7].

— *The reliability index β :* We can adapt the reliability index in function of the reference period and of the consequences of a failure. Three consequences classes are defined in the Eurocode 1990 [7]. The table 2 defines these classes :

Consequences class	Description	Examples of buildings and civil engineering works
CC3	High consequence for loss of human life, or economic, social or environmental consequences very great.	Grandstands, public buildings where consequences of failure are high (e.g. a concert hall).
CC2	Medium consequence for loss of human life, economic, social or environmental consequences considerable.	Residential and office buildings, public buildings where consequences of failure are medium (e.g. an office building).
CC1	Low consequence for loss of human life, and economic, social or environmental consequences small or negligible.	Agricultural building where people do not normally enter (e.g. storage buildings), greenhouses.

TABLE 2 – Definition of the consequences classes [7].

Three classes of reliability RC1, RC2 and RC3 that define the β reliability index concept can be associated with the three classes of consequences CC1, CC2 and CC3. The table 3 gives the recommended minimum values for that reliability index β in function of the class of reliability.

Reliability class	1 year reference period	50 years reference period
RC3	5,2	4,3
RC2	4,7	3,8
RC1	4,2	3,3

TABLE 3 – Recommended minimum values for reliability index β (ultimate limit states) [7].

The reliability index is also related to the probability of failure of the structure by $P_f = \Phi$ (-β) where Φ is the cumulative distribution function of the standardised normal distribution. The relation is given in the table 4.

P_f	10^{-1}	10^{-2}	10^{-3}	10^{-4}	10^{-5}	10^{-6}	10^{-7}
β	1,28	2,32	3,09	3,72	4,27	4,75	5,2

TABLE 4 – Relation between β and P_f [7].

— *The sensitivity factor α_R :* The index R means that this factor is applied on the resistance side. There is also a sensitivity factor α_E that affect the actions. The value α is positive for the resistance and negative for the unfavourable actions (convention). α_R and α_E equals 0,8 and -0,7 respectively if $0{,}16 < \frac{\sigma_E}{\sigma_R} < 7{,}6$. σ_E and σ_R are respectively the standard deviation of the actions and the resistance. When this condition is not satisfied, it should use $\alpha = \pm\ 1$ for the part that have the higher standard deviation and $\alpha = \pm\ 0{,}4$ for the other one.

Finally the relations that has to be fulfilled are :

$$E(\gamma_{sd} q_{demand}) \leq R\left(\frac{q_{um}}{\gamma_{Om}\gamma_{Rd}}\right) \quad or \quad \gamma_{sd} q_{demand} \leq \frac{q_{um}}{\gamma_{Om}\gamma_{Rd}} \tag{14}$$

$$\gamma_{Rd} E(\gamma_{sd} q_{demand}) \leq R\left(\frac{q_{um}}{\gamma_{Om}}\right) \quad or \quad q\left[\gamma_{Rd} E(\gamma_{sd} q_{demand})\right] \leq \frac{q_{um}}{\gamma_{Om}} \tag{15}$$

$$\gamma_{Rd}\gamma_{sd} E(q_{demand}) \leq R\left(\frac{q_{um}}{\gamma_{Om}}\right) \quad or \quad q\left[\gamma_{Rd}\gamma_{sd} E(q_{demand})\right] \leq \frac{q_{um}}{\gamma_{Om}} \tag{16}$$

where q_{um} is here equivalent to R_m and represents the mean capacity or mean ultimate load limit obtained thanks to a complete non linear analysis with mean properties.

The figure 6 illustrates these three relations in a theoretical manner as for the previous approach.

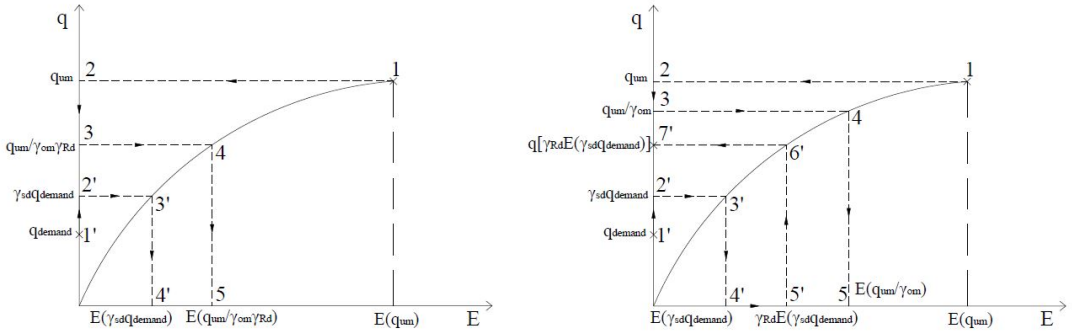

(a) Equation 14

(b) Equation 15

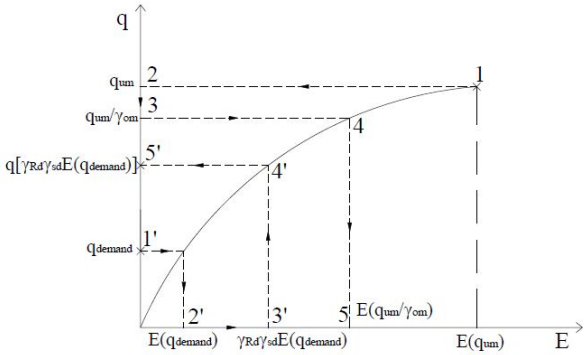

(c) Equation 16

FIGURE 6 – Illustration of the different relations of verification for the ECOV approach.

5.4 Partial safety factor approach

The approach of partial safety factor (PSF) corresponds to the method proposed by the Eurocode 1992-1-1 [1]. In summary, this approach consists of using design values for the stress-strain relationships :

— Design stress-strain relationships are used : $f_{cd} = \alpha_{cc} f_{ck}/\gamma_c$ and $f_{yd} = f_{yk}/\gamma_s$. γ_c and γ_s are the partial safety factor on the material strength. The Eurocode 1992-1-1 [1] provides recommended value for both factor. $\gamma_c = 1{,}5$ and $\gamma_s = 1{,}15$ for a common project. $E_{cd} = E_{cm}/\gamma_{CE}$ with $\gamma_{CE} = 1{,}2$.

— The favourable effect of the tensile resistance of the concrete can be used. In this work, the tensile resistance has not been taken into account.

— The creep effect has to be taking into account either by a precise model either by multiplying all relative deformation values of the concrete stress-strain relationship by a factor $(1 + \phi_{ef})$, where ϕ_{ef} is called the effective coefficient of creep. Again, this effect has not been studied in this work.

The value of the safety factor γ_c and γ_s can be explained thanks to the European Concrete Platform (2008)[8]. The coefficient of variation in the table 5 can be used to determine the partial safety factor.

Type of uncertainties	Steel	Concrete
Modelling	$V_m = 2{,}5\ \%$	$V_m = 5\ \%$
Geometry	$V_g = 5\ \%$	$V_g = 5\ \%$
Material	$V_f = 4\ \%$	$V_f = 15\ \%$

TABLE 5 – Coefficient of variation needed to determine the partial safety factor for the steel and concrete material [8].

The partial safety factor on the material strength γ_M can be then determined with :

$$\frac{f_k}{f_d} = \gamma_M = \exp(3,04V_R - 1,64V_f) \tag{17}$$

with

$$V_R = \sqrt{V_m^2 + V_G^2 + V_f^2} \tag{18}$$

where

— V_R is the coefficient of variation of resistance.
— V_m is the coefficient of variation of the model uncertainty.
— V_g is the coefficient of variation of the geometrical uncertainty.
— V_f is the coefficient of variation of the material strength.

The equation 17 gives then the determination of the partial safety factor on the material. Using the value from the table 5, we obtain $\gamma_M = \gamma_c = 1{,}30$. By using an additional factor of 1,15 in order to take into account the uncertainties from the concrete test made and cured especially for test and not from the finished structure. Then $\gamma_c = 1{,}15 \times 1{,}30 = 1{,}50$. For the steel material, the equations give $\gamma_M = \gamma_s = 1{,}154$.

A brief explanation of the equation 17 is done here.

$$\frac{f_k}{f_d} = \gamma_M = \exp(3,04V_R - 1,64V_f) \tag{19}$$

Knowing that :

$$f_k = f_m \exp(-1,64V_f) \tag{20}$$

The value of 1,64 assumes the probability of the characteristic resistance as 0,05. Noted that on the relation 12, this value is equal to 1,65 and has the same definition. By replacing the equation 20 into the equation 19, we obtain :

$$\frac{f_m \exp(-1,64V_f)}{f_d} = \exp(3,04V_R)\exp(-1,64V_f) \tag{21}$$

$$\frac{f_m}{f_d} = \exp(3,04V_R) \tag{22}$$

Where 3,04 corresponds to $\alpha_R\beta$ that are the sensitivity factor for the reliability of resistance times the reliability index. $\alpha_R = 0{,}8$ and β is here taken as 3,8 which corresponds to a reliability class RC2 for 50 years of reference period (see table 3).

The equation 22 gives the relation between the mean and the design resistance. This equation is similar and on the same assumption to the equation 13 proposed in the ECOV approach but concerns the resistance of the concrete and not the structure.

The output of this method is a non linear curve until the failure of the structure (q_{ud}). If the failure of the structure appears for a load lower than the applied load, the structure is not well designed. In contrast, if the structure fails after that applied load, the structure presents a good design. The following two relations have to be fulfilled to assure a good design :

$$E(\gamma_{sd} q_{demand}) \leq R\left(q_{ud}\right) \quad or \quad \gamma_{sd} q_{demand} \leq q_{ud} \tag{23}$$

$$\gamma_{sd} E(q_{demand}) \leq R\left(q_{ud}\right) \quad or \quad q\left[\gamma_{sd} E(q_{demand})\right] \leq q_{ud} \tag{24}$$

The figure 7 illustrates these two relations in a theoretical manner as previously.

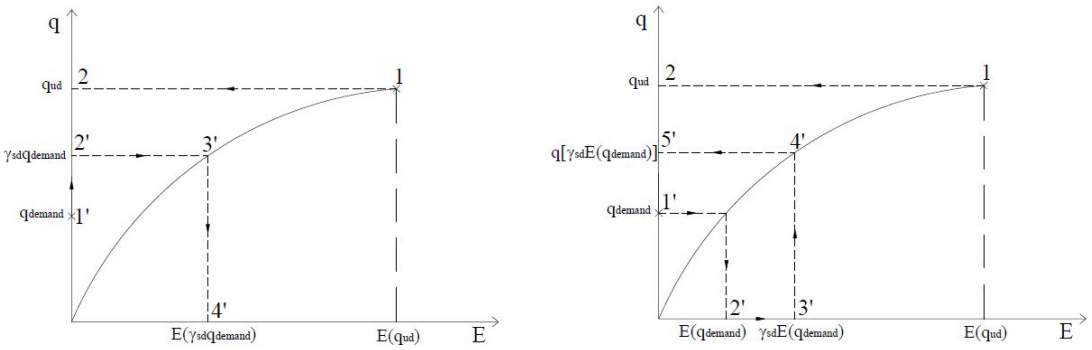

(a) Equation 23 (b) Equation 24

FIGURE 7 – Illustration of the different relations of verification for the PSF approach.

5.5 Probabilistic approach

The last approach proposed by the concrete model code [3] is a full probabilistic analysis. The safety can also be evaluated thanks to the reliability index β linked to the failure probability P_f.

$$R_d = \frac{1}{\gamma_{Rd}} R(\alpha\beta) \tag{25}$$

The probabilistic approach can be summarized as follows [3] :

1) Randomization of input variables : The properties are obtained thanks to random distribution with mean and standard deviation value.
2) Probabilistic analysis of the resistance : Series of analysis with the method of Monte Carlo. The results of this analysis are the random parameters of the resistance (mean, standard deviation, type of distribution function,...).
3) Evaluation of the design resistance : Once we have the random distribution of the resistance, we can obtain thanks to the probability of failure, the design resistance.

5.6 Other methods

In this section, a brief introduction of some alternatives and approaches coming from the literature is done.

An approach is proposed by Six M. in 2001 [9] in order to calculate a global resistance factor γ_O for slender columns. His approach requires one non linear analysis with as properties for the materials : $f_y = 1{,}1\ f_{yk}$ and $f_c = 1{,}1\ \alpha_{cc} f_{ck}$ ($\approx$ mean value).

A second approach is proposed by Henriques et al. in 2002 [10] and calculates also a global resistance factor γ_O but here for beam structures. The approach is quite simple to implement and requires only one non linear analysis using mean value for the material properties.

A third more complete approach is proposed by Schlune et al. in 2011 [11]. The goal of his approach is to obtain also a global resistance factor γ_O here based on the coefficient of variation. This global resistance factor divides the result of one non linear analysis using mean properties for the steel and in situ compressive strength for the concrete. This approach is more or less similar to the ECOV approach except that in Schlune's approach, the calcul of the coefficient of variation is more complex. Indeed, it requires three more non linear analysis and depends on the type of structure. This method has then the disadvantages to be not systematic.

5.7 Summary and comparison

A brief summary and a comparison between the different approaches investigated is done here. A focus on the three major approaches (GRF, ECOV and PSF) is presented. The partial safety factor approach is the simplest approach studied, indeed, it requires only one analysis without any further computation in order to obtain the resistance of the structure. The global resistance factor approach requires also one analysis but additional computation. Finally, the estimation of the coefficient of variation needs two non linear analysis also with computation.

Concerning the assumption of the different approaches, the figure 8 illustrates and summarizes the material properties needed and the resistance of the structure obtained for each approaches. The GRF and ECOV approaches are global and requires a global resistance factor γ_O or γ_{Om}. For the GRF, γ_O is a constant and independent of the structure. That is the reason modified properties are needed. In contrast, γ_{Om} changes in function of the resistance of the structure. If the failure is more guided by the concrete, γ_{Om} will have a higher value than if the failure appears more in the reinforcement steel.

An other comparison can be made between the PSF and the GRF approaches. The basis of the GRF approach is the design value of the material properties. These design properties are multiplied by the same factor for the steel and the concrete in order to obtain modified mean properties.

The last comment concerns the PSF approach for which the partial safety factor on the material are independent of the structure. Indeed, γ_c and γ_s have constant values and are calculated based on constant coefficient of variation. This is the main difference between the PSF and the ECOV approaches for which the coefficient of variation is calculated in order to obtain the global resistance factor γ_{Om}.

FIGURE 8 – Comparison between the different assumptions made for the three approaches studied and summary.

6 Codes and rules available (dynamic approach)

This section introduces the literature review concerning the dynamic analysis for a concrete structure and its possible issues in the case of seismic and wind analysis.

6.1 Basics

The basics of a dynamic analysis regroups the determination of the mass and the stiffness of the structure. The mass of the structure is taken as constant and is composed of the dead load and sometimes some variable loads. It has however a high uncertainties. Concerning the stiffness, the uncertainties comes from the Young modulus of the concrete itself and also of the inertia of the section (cracked section or not).

In the previous section, we discussed the possible reduction of the modulus of elasticity in the case of a design non linear analysis ($E_{cd} = E_{cm}/\gamma_{CE}$). The figure 9 illustrates the effect of a decrease of the Young modulus of the concrete on a structure. The structure becomes more flexible which leads to an higher natural period of the structure (T) or a smaller frequency (f).

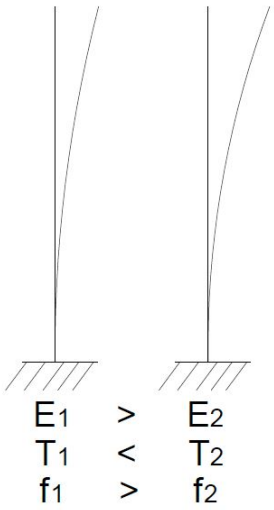

FIGURE 9 – Illustration of the Young modulus decrease's effect on a structure.

Thanks to the experience or also thanks to the Eurocode 1998-1 [12], some simplified formulas provide the period of one building structure based on the high or on the stage number. The Eurocode 1998 [12] provides a formula (equation 26) based on the high for a structure until 40 meters high :

$$T = C_t H^{3/4} \tag{26}$$

where C_t corresponds to a coefficient depending on the type of structure. For a concrete frame structure, the coefficient C_t is equal to 0,075. For the other type of concrete structure, C_t = 0,05. H corresponds naturally to the high of the structure.

An other relation more simplified and based on the experience corresponds to :

$$T = CN \tag{27}$$

where N corresponds to the number of stage of the structure and C corresponds to a coefficient depending on the type of structure. C = 0,1 for a concrete frame structure and C = 0,05 for a concrete wall structure that is more rigid.

6.2 Seismic

For the seismic analysis, if the period of the structure increases, the load on the structure can become smaller depending on the period. The figure 10 below illustrates the type of building situated in the different part of one typical response spectrum.

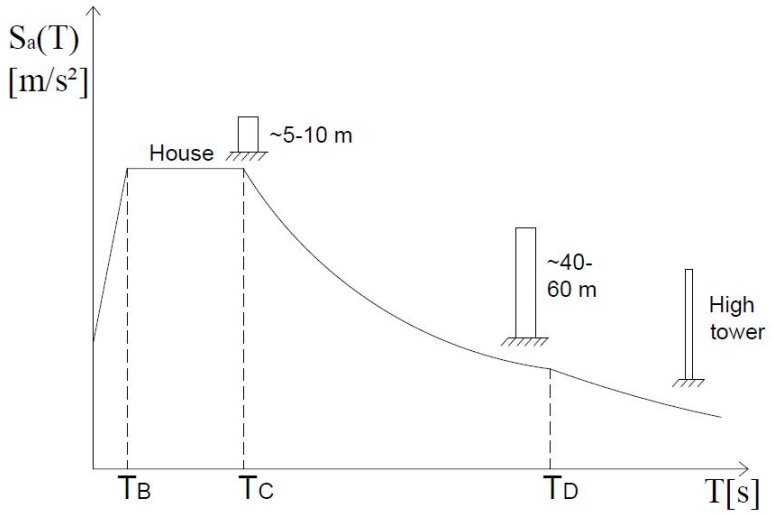

FIGURE 10 – Response spectrum illustrating the building type periods.

The key point of the two types of response spectra are summarized in the table 6 below depending on the subsoil classes :

/	Type 1				Type 2			
Soil Classes	S	T_B [s]	T_C [s]	T_D [s]	S	T_B [s]	T_C [s]	T_D [s]
A	1,0	0,15	0,4	2,0	1,0	0,05	0,25	1,2
B	1,2	0,15	0,5	2,0	1,35	0,05	0,25	1,2
C	1,15	0,20	0,6	2,0	1,5	0,10	0,25	1,2
D	1,35	0,20	0,8	2,0	1,8	0,10	0,30	1,2
E	1,4	0,15	0,5	2,0	1,6	0,05	0,25	1,2

TABLE 6 – Parameters describing the response spectrum of type 1 and 2 regarding the subsoil classes [12].

If the increased period of the structure T_2 appears to be less than T_C, the increase of the period has no influence on the seismic load. Indeed, the period is situated on the plateau, see figure 11. But concerning the more flexible structure, a diminution of the rigidity of the structure leads to a diminution of the seismic force acting on the structure.

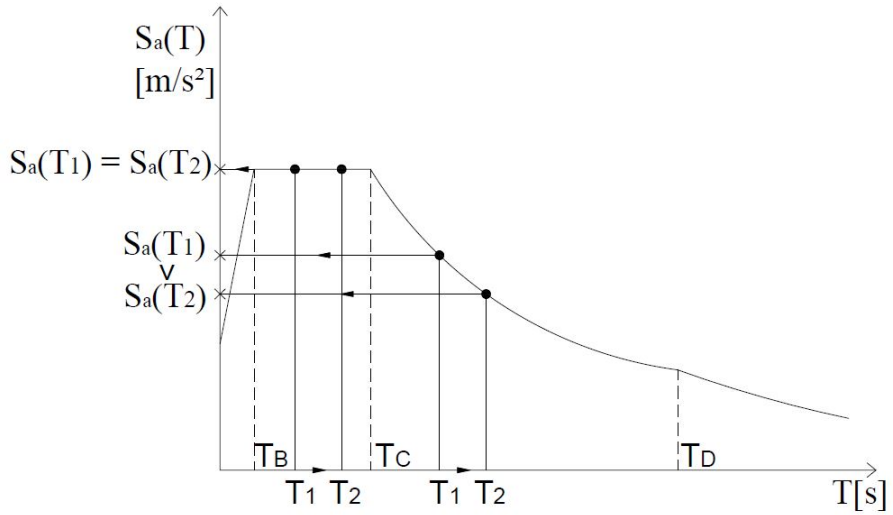

FIGURE 11 – Response spectrum illustrating the effect of a period increasing.

These observations are against the logic of the design. Indeed, decrease the Young modulus appears to be not conservative because the loads decreases as well.

In the codes [12], no clear answers to this issue are provided. However, it is specified that mean properties should be used in the case of non liner analysis without any further precision.

6.3 Wind

In the case of a wind analysis, the reduction of the Young modulus increases the likelihood of the possible vibration of the structure. The reduction of Young modulus increases then the period of the concrete structure and get closer to the period of the gust that is approximately equal to 4 seconds. In this case then, decreasing the rigidity of the structure appears to be conservative in the analysis. Moreover, no rules founded as [13] provide guidelines or comments on this process of analysis. However, using mean properties for the material seems to be a good approach.

6.4 Conclusion

Concerning a dynamic analysis, a careful attention has to be done for the use of material properties. Moreover, the conclusion is not unequivocal because the decreasing of the Young modulus does not give the same safety in the analysis for a seismic or a wind analysis.

7 Numerical modelling

In this section, the numerical simulations are presented and explained. First the software used, Finelg is briefly introduced and the input parameters are detailed. Then, several tests are done from the simple cube where the second order effect has no influence to a frame structure where the second order effect can be important and hyperstaticity plays a role. Finally a simple beam is studied where a chain or catenary effect appears. Several analysis are performed on the same model in order to calculate the different approaches and to compare the results.

7.1 Finelg and Cinelu

Finelg [14] is a software of finite element analysis developed in collaboration between the University of Liège and the Engineering Office Greisch. Finelg is able to perform non linear analysis with the geometrical and material non linearity. Finelg has also the ability to solve dynamic problems and stability analysis.

The non linear analysis is performed step by step. The incrementation from step to step can be done by several methods [15]. First the load can be imposed but this approach becomes problematic for the convergence when the load reaches a maximum. The second approach concerns the imposed displacement which solves the previous issue but has also problem when the displacement reaches a maximum. A combination of these two methods can be one solution. One better method concerns the arc length method that consist to a spherical step. Whatever the increment, the sphere will always intercept the equilibrium curve. In this work, the arc length method is used for all the models except for the beam with the catenary effect for which imposed displacement is used. In our work, beam elements are used for the models investigated but Finelg gives also the possibility to model shell elements.

Cinelu [16] is a software of verification at ultimate limit state (ULS) for section in reinforced concrete. The main advantage of Cinelu is its ability to verify sections on unsymmetrical bending. It allows also the possibility of defining the section properties and geometry for later an exportation in Finelg.

7.2 Material laws

For the material laws, Finelg has already several relations directly available for the users.

Concerning the concrete material, one relation availabe (equation 28) is more or less similar to the relation provided in the Eurocode 2 [1] (defined in the equation 1).

$$\frac{\sigma_c}{f_c} = \frac{k\eta + (k' - 1)\eta^2}{1 + (k - 2)\eta + k'\eta^2} \tag{28}$$

if $k' = 0$ (k' is a parameter of the law), we obtain the same relation as in the equation 1. The coefficient k defines in Finelg has also one slight difference, $k = E_c|\epsilon_{c1}|/f_c$ for which it misses one factor of 1,05. For the further tests, C25/30 concrete class is used in the numerical model.

The following table 7 summarizes the different properties of material that has to be modelled. Indeed, in order to compute the several approaches studied, different material properties have to be studied. A difference is also made for the design and the modified mean properties regarding on the value of α_{cc} (the Eurocode 1992-1-1 [1] and the Belgium annex [4] recommend a value of 1 and 0,85 respectively).

/	f_c [MPa]	k [-]	E_c [MPa]
Design ($\alpha_{cc} = 0{,}85$)	14,67	3,83	25833
Design ($\alpha_{cc} = 1$)	16,67	3,255	25833
Modified Mean ($\alpha_{cc} = 0{,}85$)	17,92	3,633	31000
Modified Mean ($\alpha_{cc} = 1$)	21,08	3,088	31000
Characteristic	25	2,604	31000
Mean	33	1,973	31000

TABLE 7 – Concrete properties required for computing the different approaches.

The figure 12 represents the different stress-strain curves for the different material properties defined in the table 7 for a C25/30 concrete :

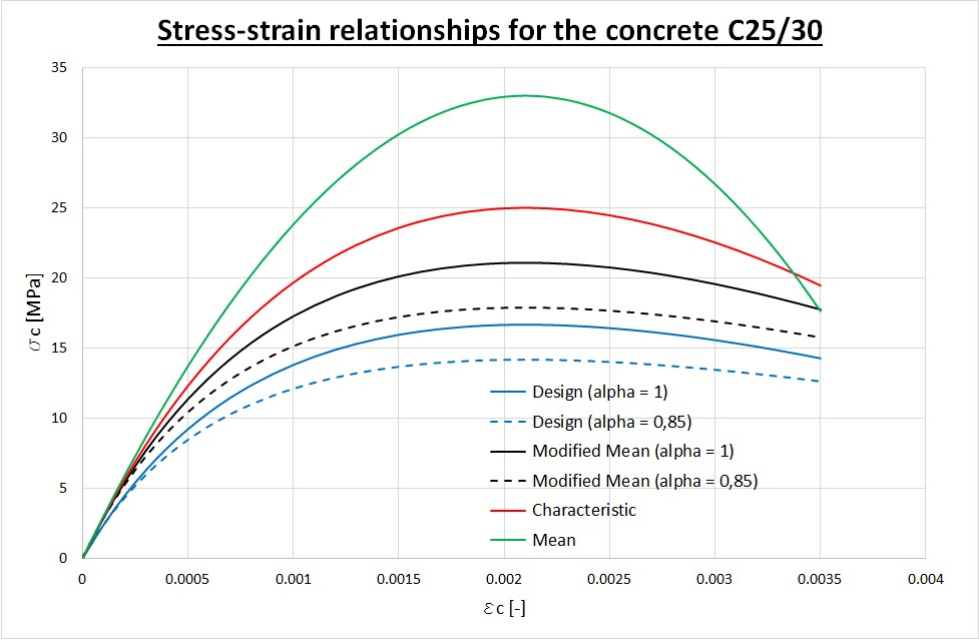

FIGURE 12 – Stress-strain relationship for the concrete C25/30 for the different concrete properties.

For the reinforcement steel, a classical elastic-perfectly plastic or a bilinear relationship are used. Steel of quality B500S is used in the further numerical models. For the class B of steel, the characteristic ultimate deformation and the coefficient k can be larger than 5 % and 1,08 respectively (see table 1). For our case, $\epsilon_{uk} = 5$ % and k = 1,08.

The table 8 summarizes the reinforcement steel properties for the different cases. We observe only 4 different properties. Indeed, the influence of α_{cc} has no more effect and there is no modified mean properties of the steel. Moreover, there are two possibilities to represent the reinforcement steel behaviour with the design value (with or without hardening).

/	f_y [MPa]	E_s [MPa]	E_t [MPa]
Design	434,8	200000	727,27
Design bis	434,8	200000	0
Characteristic	500	200000	842,10
Mean	550	200000	931,22

TABLE 8 – Reinforcement steel properties for the different properties.

The figure 13 illustrates the four different stress-strain relationships studied. Concerning the design analysis, two possibilities are available (with and without hardening) both with a limitation of the deformation to $\epsilon_{ud} = 0{,}8\ \epsilon_{uk}$ as recommended in the national annex of Belgium [4].

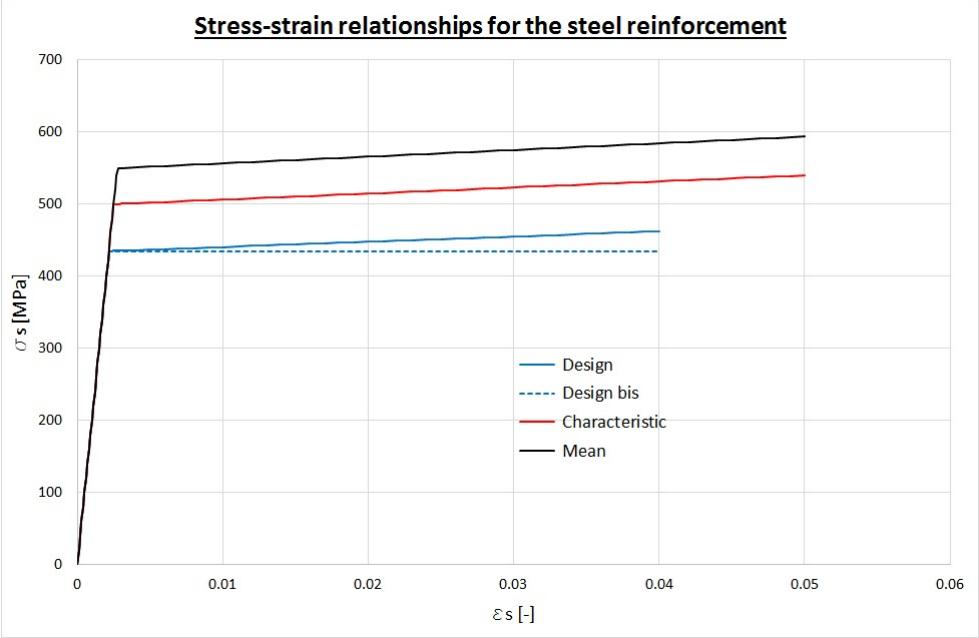

FIGURE 13 – Stress-strain relationships for the different reinforcement steel properties.

For every test performed in the following report, hardening of the steel is represented. Only the reinforced cube in tension is investigated with both possibilities in order to see its influence.

7.3 Cube models

The first models studied in this work is small cubes. This simple model is performed in order to investigate the difference between the different approaches available when the second order effect has no influence. The results obtained from the software Finelg can also be compared to analytical solution and so validate the non linear analysis computed by the Finelg. A cube of 50 cm with an illustration of that cube with the reinforcement in figure 14 is chosen to make that model.

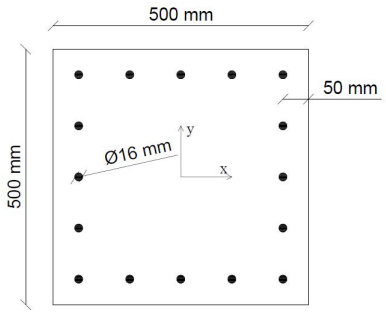

FIGURE 14 – Illustration of the section of the reinforced concrete cube.

In the following, three subsections are separated. First the cube without any reinforcement is modelled for which the different approaches studied are detailed. Then a reinforced concrete cube is investigated first in compression then in tension.

7.3.1 Concrete cube

The first model represents then a concrete cube (without any reinforcement). Non linear analysis are performed with different material properties as discussed previously in order to compute the different approaches investigated. Then, a comparison between the non linear analysis obtained analytically (Equilibrium equation) and numerically (Finelg) is done to verify the model in figure 15.

The comparison between the numerical and analytical solution is done for the mean, characteristic, design and the modified mean analysis. The design and the modified mean analysis comparison is performed only with a unit value for α_{cc}. We observe that the numerical results are matching the analytical results. This assures good results obtained numerically for the further analysis.

$\alpha_{cc} = 0{,}85$		$\alpha_{cc} = 1$		/	
q_{ud} [kN]	$q_{u\tilde{m}}$[kN]	q_{ud} [kN]	$q_{u\tilde{m}}$ [kN]	q_{uk} [kN]	q_{um} [kN]
3542	4480	4167	5271	6250	8250

TABLE 9 – Ultimate load limits for the concrete cube test for each material properties.

The next step consists of the evaluation of the different approaches investigated. The figure 16 illustrates the different non linear curves with their respective load limit. The maximal value of the force gives the ultimate load limit for the different

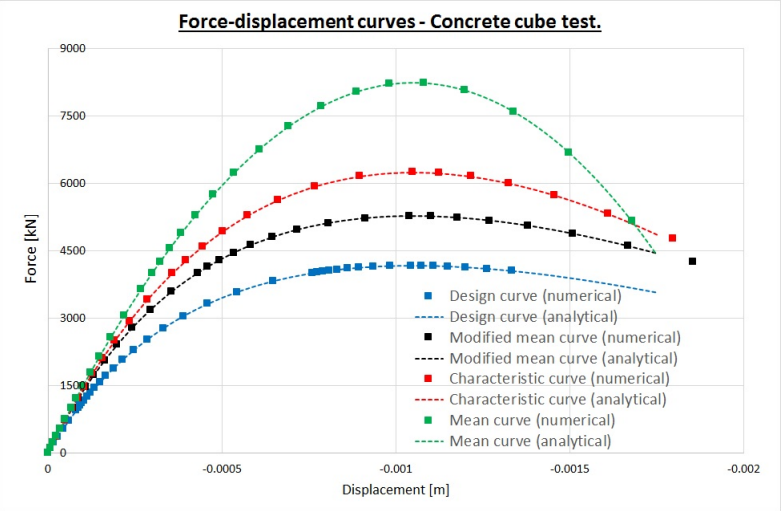

FIGURE 15 – Numerical and analytical force-displacement curves for the different material properties (concrete cube).

curves ($q_{ud}(\alpha_{cc})$, $q_{u\tilde{m}}(\alpha_{cc})$, q_{uk} and q_{um}). The table 9 summarizes these ultimate load limits obtained numerically for each material properties. The table 10 contains the verification results obtained with the different approaches available using a factor $\chi = \frac{F_d}{R_d}$ here for the concrete cube test. Moreover, the value of γ_{Rd} and γ_{sd} are fixed to 1,06 and 1,15 respectively as recommended in the Eurocode 1992 [2].

Concerning the ECOV approach, the global resistance coefficient γ_{Om} has to be calculated using the characteristic and mean analysis :

$$V_R = \frac{1}{1,65} \ln \frac{q_{um}}{q_{uk}} = \frac{1}{1,65} \ln \frac{8250}{6250} = 0,16826- \tag{29}$$

$$\gamma_{Om} = \exp(\alpha_R \beta V_R) = \exp(3,04 \times 0,16826) = 1,668 \tag{30}$$

The value of $\alpha_R\beta$ are taken as 0,8 and 3,8 respectively in order to be situated in the reliability classes RC2 for a reference period of 50 years. In our case, $\gamma_{Om} =$ 1,668 is much higher than the $\gamma_O = 1,2$ of the GRF approach. But concerning the ECOV approach, γ_{Om} takes directly into account which material has an influence, and here obviously there is only the concrete. We observe that the global factor has the same order of magnitude as the factor obtained in the equation 5.

The value of q_{demand} is fixed at 3062 kN in order to fix the χ factor to 1 for the first relation of the global resistance factor (GRF) approach in the table 10. This relation has all the safety coefficient placed on the action. This type of relation is chosen because in theory, it is the one with the less safety margin (see figure 4). We see in comparison with the other relations that this assumption is right for each approaches. The partial safety factor approach has also a more or less similar result when the safety factor are placed on the action. A major difference of 15 % appears between the results of the GRF and the PSF approaches regarding the value of α_{cc}. Indeed, this coefficient varies from 0,85 to 1 that explains the difference of 15 %. Concerning the ECOV approach, we observe a larger safety margin in the result (around 25 %).

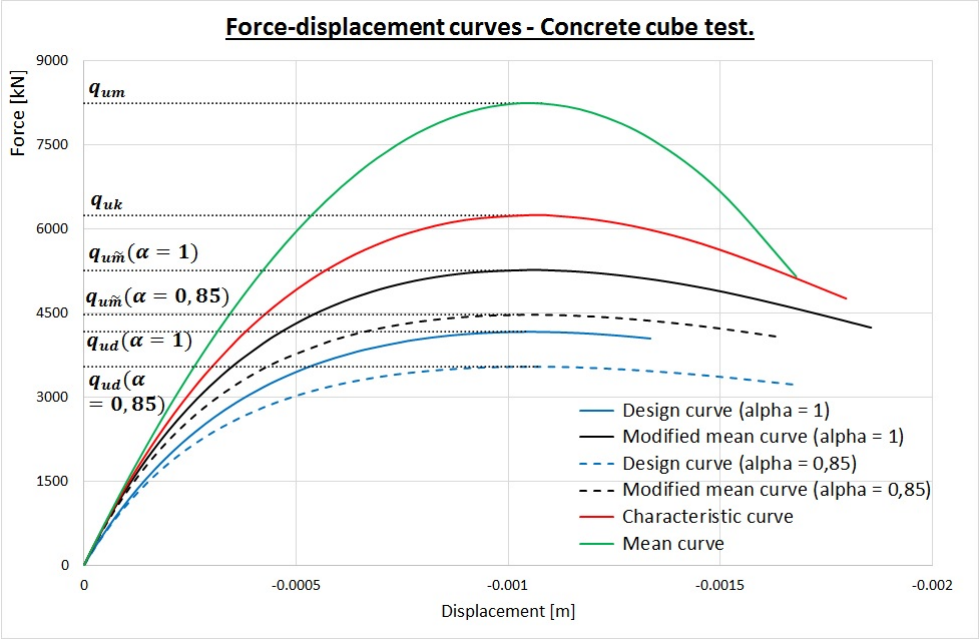

FIGURE 16 – Force-displacement curves for the concrete cube model for each material properties.

Concrete cube model				
Approach		LM	RM	χ [-]
GRF $\underline{\alpha_{cc} = 0,85}$	$\gamma_{sd} q_{demand} \leq \frac{q_{u\tilde{m}}}{\gamma_O \gamma_{Rd}}$	3522	3522	**1,0000**
	$q\left[\gamma_{Rd} E(\gamma_{sd} q_{demand})\right] \leq \frac{q_{u\tilde{m}}}{\gamma_O}$	3622	3733	0,9703
	$q\left[\gamma_{Rd} \gamma_{sd} E(q_{demand})\right] \leq \frac{q_{u\tilde{m}}}{\gamma_O}$	3401	3733	0,9112
	$q_{demand} \leq \frac{q_{u\tilde{m}}}{\gamma_{O'}}$	3062	3527	0,8682
PSF $\underline{\alpha_{cc} = 0,85}$	$\gamma_{sd} q_{demand} \leq q_{ud}$	3522	3541	**0,9945**
	$q\left[\gamma_{sd} E(q_{demand})\right] \leq q_{ud}$	3212	3541	0,9069
GRF $\underline{\alpha_{cc} = 1}$	$\gamma_{sd} q_{demand} \leq \frac{q_{u\tilde{m}}}{\gamma_O \gamma_{Rd}}$	3522	4144	**0,8499**
	$q\left[\gamma_{Rd} E(\gamma_{sd} q_{demand})\right] \leq \frac{q_{u\tilde{m}}}{\gamma_O}$	3660	4392	0,8332
	$q\left[\gamma_{Rd} \gamma_{sd} E(q_{demand})\right] \leq \frac{q_{u\tilde{m}}}{\gamma_O}$	3485	4392	0,7935
	$q_{demand} \leq \frac{q_{u\tilde{m}}}{\gamma_{O'}}$	3062	4150	0,7379
PSF $\underline{\alpha_{cc} = 1}$	$\gamma_{sd} q_{demand} \leq q_{ud}$	3522	4167	**0,8452**
	$q\left[\gamma_{sd} E(q_{demand})\right] \leq q_{ud}$	3295	4167	0,7907
ECOV	$\gamma_{sd} q_{demand} \leq \frac{q_{um}}{\gamma_O \gamma_{Rd}}$	3522	4670	**0,7541**
	$q\left[\gamma_{Rd} E(\gamma_{sd} q_{demand})\right] \leq \frac{q_{um}}{\gamma_O}$	3708	4950	0,7490
	$q\left[\gamma_{Rd} \gamma_{sd} E(q_{demand})\right] \leq \frac{q_{um}}{\gamma_O}$	3641	4950	0,7354

TABLE 10 – χ factor for the different approaches for the concrete cube model (LM $\equiv$ Left Member and RM $\equiv$ Right Member).

A detail of the different relations is done here for the concrete cube test in order to fix the procedure once. Each relation of the different approaches is explained and detailed. Concerning the global resistance factor and the partial safety factor approaches, only the relations with $\alpha_{cc} = 0{,}85$ are detailed (the principle is the same for $\alpha_{cc} = 1$). The effect of the load E(q) is here the displacement in centimetres.

1) Global resistance factor (GRF) approach :

— Relation 1 : $E(\gamma_{sd} q_{demand}) \leq E\left(\frac{q_{u\tilde{m}}}{\gamma_O \gamma_{Rd}}\right)$ *or* $\gamma_{sd} q_{demand} \leq \frac{q_{u\tilde{m}}}{\gamma_O \gamma_{Rd}}$.
For the relation 1, the different safety coefficients are placed on the load and not on the effect of the load. This format gives an easy verification, see the table 11 and figure 17 :

/	q [kN]	E(q) [cm]
q_{demand}	3062 (1)	/
$\gamma_{sd} q_{demand}$	3522 (2)	-0,4264 (3)
I∧	I∧	I∧
$\frac{q_{u\tilde{m}}}{\gamma_O \gamma_{Rd}}$	3522 (2')	-0,4264 (3')
$q_{u\tilde{m}}$	4480 (1')	/

TABLE 11 – Global Resistance Factor approach : Relation 1 - Table

The shape has no influence on the factor χ. Indeed, only the ultimate load limit $q_{u\tilde{m}}$ and the demand load q_{demand} are used and not the displacement. The χ coefficient is equal and imposed to 1 for this relation.

— Relation 2 : $\gamma_{Rd} E(\gamma_{sd} q_{demand}) \leq E\left(\frac{q_{u\tilde{m}}}{\gamma_O}\right)$ *or* $q\left[\gamma_{Rd} E(\gamma_{sd} q_{demand})\right] \leq \frac{q_{u\tilde{m}}}{\gamma_O}$.
For the relation 2, the safety coefficients are placed as well on the load and on the effect of the load. This format gives a more complicated verification, see the table 12 and figure 18.

/	q [kN]	E(q) [cm]
q_{demand}	3062 (1)	/
$\gamma_{sd} q_{demand}$	3522 (2)	-0,4264 (3)
$\gamma_{Rd} E(\gamma_{sd} q_{demand})$	3622 (5)	-0,4520 (4)
I∧	I∧	I∧
$\frac{q_{u\tilde{m}}}{\gamma_O}$	3733 (2')	-0,4856 (3')
$q_{u\tilde{m}}$	4480 (1')	/

TABLE 12 – Global Resistance Factor approach : Relation 2 - Table.

In this case, the shape of the curve has an influence on the results. Indeed, the safety coefficients γ_{Rd} and γ_{sd} are placed on the displacement and on the load respectively. The χ coefficient is here equal to 0,9703.

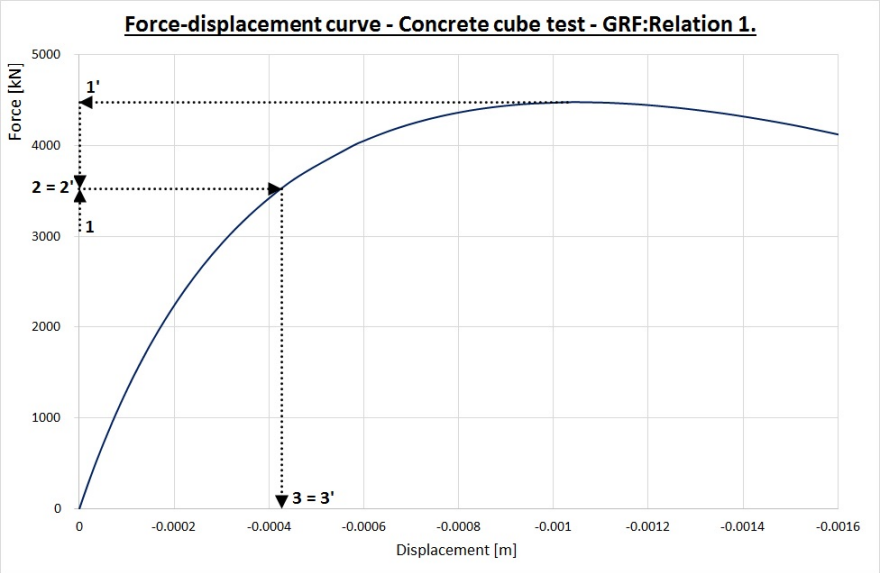

FIGURE 17 – Global Resistance Factor approach : Relation 1 - Procedure.

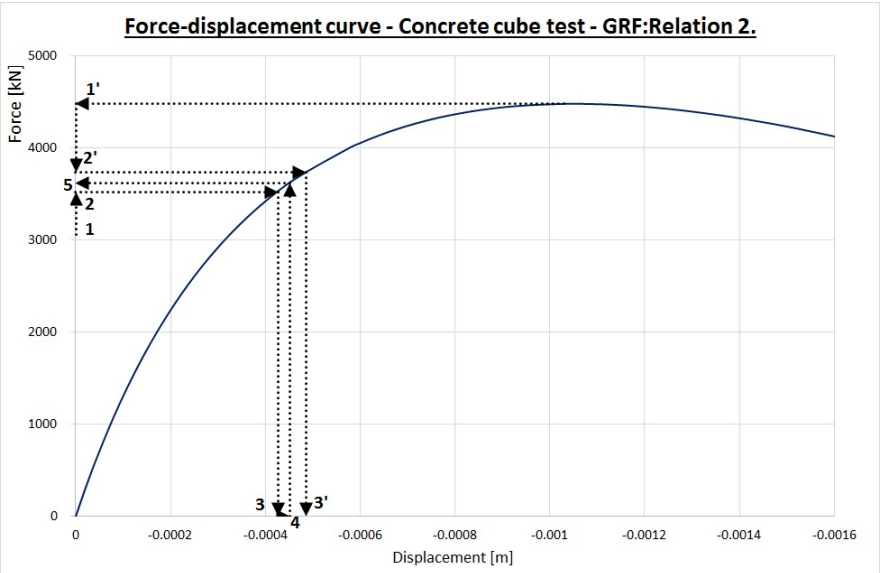

FIGURE 18 – Global Resistance Factor approach : Relation 2 - Procedure.

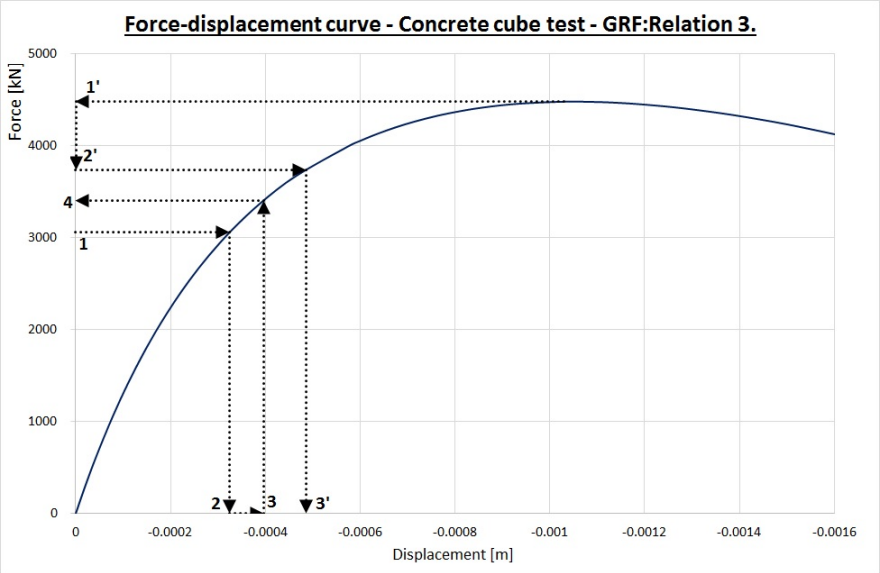

FIGURE 19 – Global Resistance Factor approach : Relation 3 - Procedure.

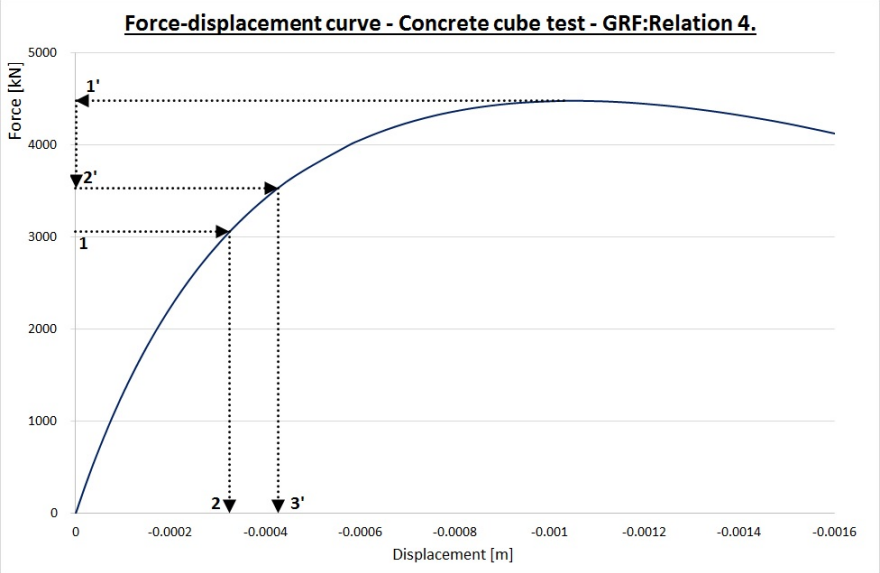

FIGURE 20 – Global Resistance Factor approach : Relation 4 - Procedure.

— Relation 3 : $\gamma_{Rd}\gamma_{sd}E(q_{demand}) \leq E\left(\frac{q_{u\tilde{m}}}{\gamma_O}\right)$ *or* $q\left[\gamma_{Rd}\gamma_{sd}E(q_{demand})\right] \leq \frac{q_{u\tilde{m}}}{\gamma_O}$
For the relation 3, the safety coefficients γ_{Rd} and γ_{sd} are both placed on the effect of the load (the displacement here), see the table 13 and figure 19. The χ coefficient is here equal to 0,9112.

/	q [kN]	E(q) [cm]
q_{demand}	3062 (1)	-0,3247 (2)
$\gamma_{Rd}\gamma_{sd}E(q_{demand})$	3401 (4)	-0,3958 (3)
I∧	I∧	I∧
$\frac{q_{u\tilde{m}}}{\gamma_O}$	3733 (2')	-0,4856 (3')
$q_{u\tilde{m}}$	4480 (1')	/

TABLE 13 – Global Resistance Factor approach : Relation 3 - Table.

— Relation 4 : $E(q_{demand}) \leq E\left(\frac{q_{u\tilde{m}}}{\gamma_{O'}}\right)$ *or* $q_{demand} \leq \frac{q_{u\tilde{m}}}{\gamma_{O'}}$
For the relation 4, the safety coefficients γ_{sd} and γ_{Rd} are unit values but $\gamma_{O'} = 1,27$. This simplifies the verification, see the table 14 and figure 20 :

/	q [kN]	E(q) [cm]
q_{demand}	3062 (1)	-0,3247 (2)
I∧	I∧	I∧
$\frac{q_{u\tilde{m}}}{\gamma'_O}$	3527 (2')	-0,4278 (3')
$q_{u\tilde{m}}$	4480 (1')	/

TABLE 14 – Global Resistance Factor approach : Relation 4 - Table.

The shape of the curve has no influence on the factor χ. Indeed, the same procedure as for the relation 1 is done except for the unit value of the safety coefficients. The χ coefficient is then equal to 0,8682.

2) Partial safety factor (PSF) approach :

— Relation 1 : $E(\gamma_{sd}q_{demand}) \leq R\left(q_{ud}\right)$ *or* $\gamma_{sd}q_{demand} \leq q_{ud}$

/	q [kN]	E(q) [cm]
q_{demand}	3062 (1)	/
$\gamma_{sd}q_{demand}$	3522 (2)	-0,9238 (3)
I∧	I∧	I∧
q_{ud}	3541(1')	-1,0723 (2')

TABLE 15 – Partial Safety Factor approach : Relation 1 - Table.

For the first relation, the safety coefficient γ_{sd} is imposed on the action directly, see the table 15 and figure 21 for the procedure.

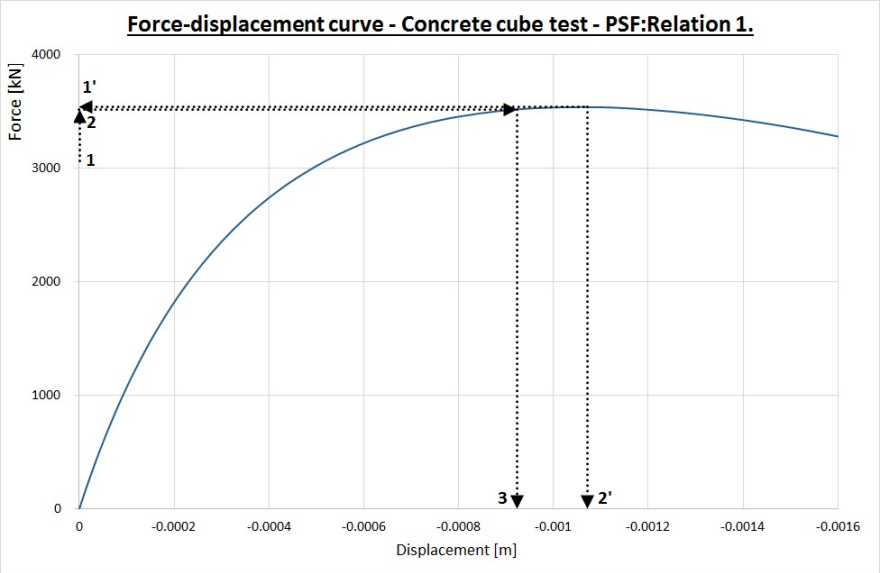

FIGURE 21 – Partial Safety Factor approach : Relation 1 - Procedure.

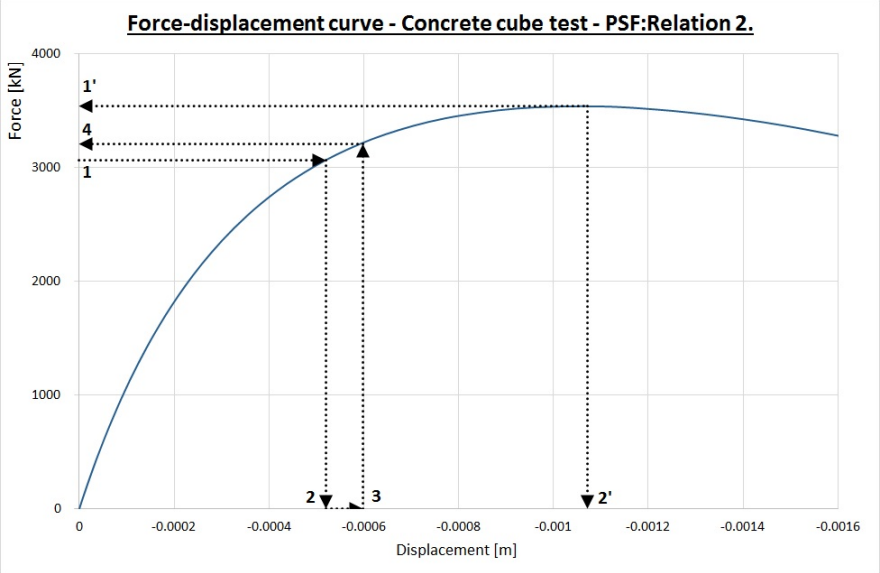

FIGURE 22 – Partial Safety Factor approach : Relation 2 - Procedure.

For this relation, the shape of the curve has also no importance, only the demand load is multiplied by the safety coefficient. The χ factor equals 0,9945.

— Relation 2 : $\gamma_{sd}E(q_{demand}) \leq R\left(q_{ud}\right) \quad or \quad q\left[\gamma_{sd}E(q_{demand})\right] \leq q_{ud}$
For the second relation, the safety coefficient γ_{sd} is imposed on the displacement, see the table 16 and figure 21 for the procedure :

/	q [kN]	E(q) [cm]
q_{demand}	3062 (1)	-0,5197 (2)
$\gamma_{sd}E(q_{demand})$	3212 (4)	-0,5977 (3)
I∧	I∧	I∧
q_{ud}	3541(1')	-1,0723 (2')

TABLE 16 – Partial Safety Factor approach : Relation 2 - Table.

For this relation, the shape of the curve has an importance, indeed the displacement is here multiplied by γ_{sd}. The χ factor equals then 0,9069 which is more or less 10% lower than the previous relation.

3) Estimation of the coefficient of variation (ECOV) approach :

— Relation 1 : $E(\gamma_{sd}q_{demand}) \leq R\left(\frac{q_{um}}{\gamma_{Om}\gamma_{Rd}}\right) \quad or \quad \gamma_{sd}q_{demand} \leq \frac{q_{um}}{\gamma_{Om}\gamma_{Rd}}$
For the relation 1, the different safety coefficients are placed on the load and not on the effect of the load. This format gives an easy verification, see the table 17 and figure 23 :

/	q [kN]	E(q) [cm]
q_{demand}	3062 (1)	/
$\gamma_{sd}q_{demand}$	3522 (2)	-0,2580 (3)
I∧	I∧	I∧
$\frac{q_{um}}{\gamma_O\gamma_{Rd}}$	4670 (2')	-0,3617 (3')
q_{um}	8242 (1')	/

TABLE 17 – Estimation of Coefficient of Variation approach : Relation 1 - Table

The shape has no influence on the factor χ. Indeed, only the ultimate load limit q_{um} and the demand load q_{demand} are used and not the displacement. The χ coefficient is equal to 0,7541 for this relation.

— Relation 2 : $\gamma_{Rd}E(\gamma_{sd}q_{demand}) \leq R\left(\frac{q_{um}}{\gamma_{Om}}\right) \quad or \quad q\left[\gamma_{Rd}E(\gamma_{sd}q_{demand})\right] \leq \frac{q_{um}}{\gamma_{Om}}$
For the relation 2, the safety coefficients are placed as well on the load and on the effect of the load. This format gives a more complicated verification, see the table 18 and figure 24.

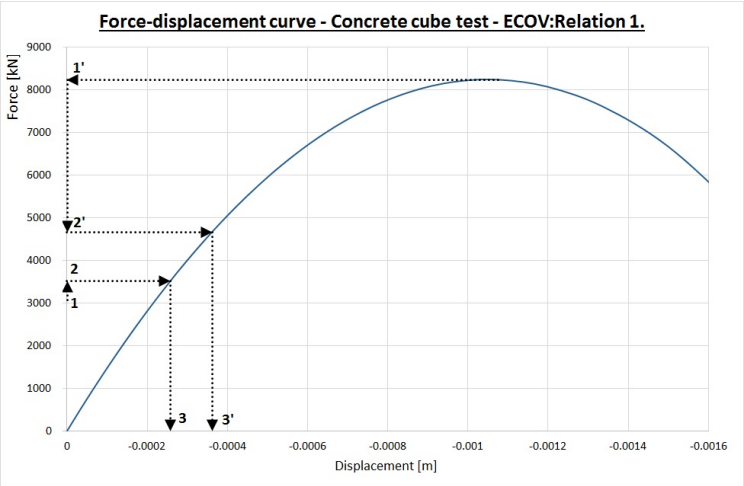

FIGURE 23 – Estimation of Coefficient of Variation approach : Relation 1 - Procedure.

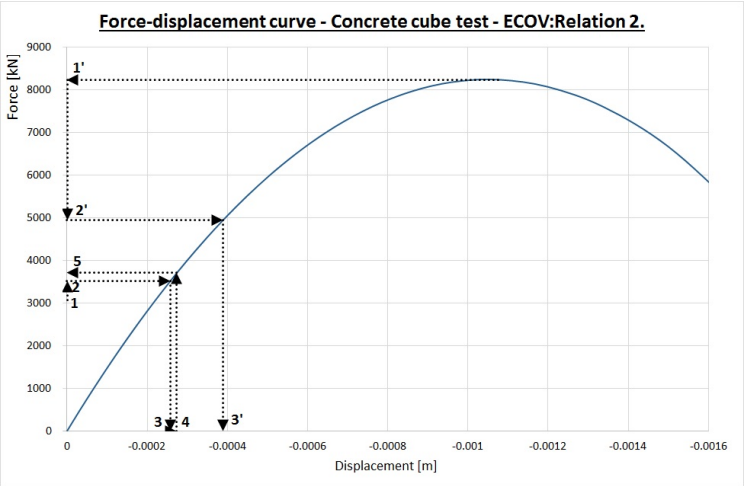

FIGURE 24 – Estimation of Coefficient of Variation approach : Relation 2 - Procedure.

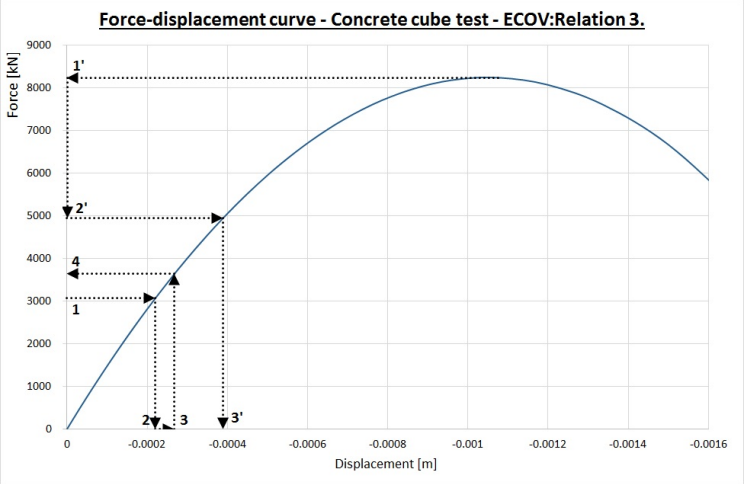

FIGURE 25 – Estimation of Coefficient of Variation approach : Relation 3 - Procedure.

/	q [kN]	E(q) [cm]
q_{demand}	3062 (1)	/
$\gamma_{sd}q_{demand}$	3522 (2)	-0,2580 (3)
$\gamma_{Rd}E(\gamma_{sd}q_{demand})$	3708 (5)	-0,2735 (4)
I∧	I∧	I∧
$\frac{q_{um}}{\gamma_O}$	4950 (2')	-0,3894(3')
q_{um}	8242 (1')	/

TABLE 18 – Estimation of Coefficient of Variation approach : Relation 2 - Table.

In this case, the shape of the curve has an influence on the results. Indeed, the safety coefficients γ_{Rd} and γ_{sd} are placed on the displacement and on the load respectively. The χ coefficient is here equal to 0,7490.

— Relation 3 : $\gamma_{Rd}\gamma_{sd}E(q_{demand}) \leq R\left(\frac{q_{um}}{\gamma_{Om}}\right)$ *or* $q\left[\gamma_{Rd}\gamma_{sd}E(q_{demand})\right] \leq \frac{q_{um}}{\gamma_{Om}}$
For the relation 3, the safety coefficients γ_{Rd} and γ_{sd} are both placed on the effect of the load (the displacement here), see the table 19 and figure 25.

/	q [kN]	E(q) [cm]
q_{demand}	3062 (1)	-0,2198 (2)
$\gamma_{Rd}\gamma_{sd}E(q_{demand})$	3641 (4)	-0,2679 (3)
I∧	I∧	I∧
$\frac{q_{um}}{\gamma_O}$	4950 (2')	-0,3894(3')
q_{um}	8242 (1')	/

TABLE 19 – Estimation of Coefficient of Variation approach : Relation 3 - Table.

The shape of the curve has then also an importance. The χ factor is here equal to 0,7354.

7.3.2 Reinforced concrete cube

The second model consists of a reinforced concrete cube (as illustrate in figure 14). The percentage of reinforcement in the cube is equal to 1,3%. Again a comparison between the numerical and analytical curves is done. The comparison between the analytical and numerical curve in figure 26 shows a nice fitting of both numerical and analytical analysis.

The next step consists of the evaluation of the different approaches investigated. The figure 27 illustrates the different non linear curves with their respective load limits. The maximal values of the force give the ultimate load limit for the different curves ($q_{ud}(\alpha_{cc})$, $q_{u\tilde{m}}(\alpha_{cc})$, q_{uk} and q_{um}) and are summarized in the table 20.

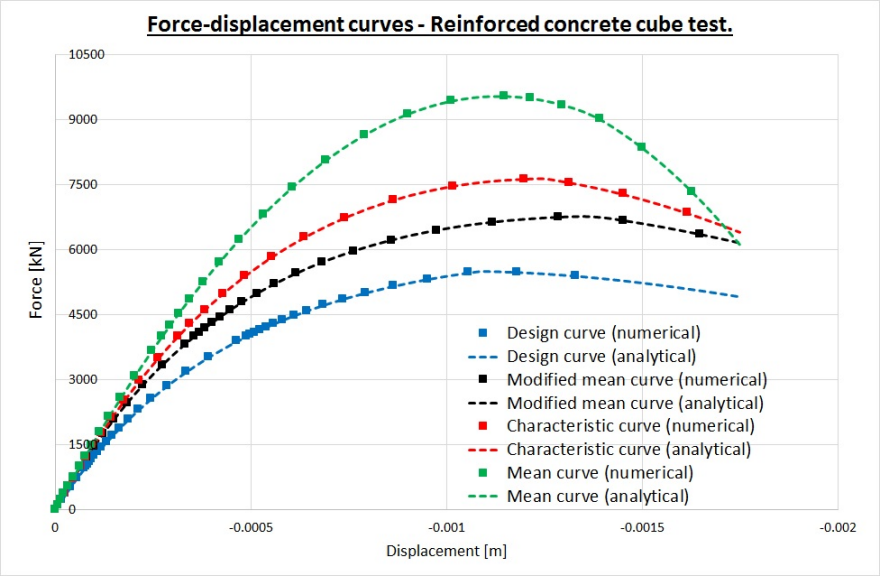

FIGURE 26 – Numerical and analytical force-displacement curves for the different material properties (reinforced concrete cube in compression).

$\alpha_{cc} = 0{,}85$		$\alpha_{cc} = 1$		/	
q_{ud} [kN]	$q_{u\tilde{m}}$[kN]	q_{ud} [kN]	$q_{u\tilde{m}}$ [kN]	q_{uk} [kN]	q_{um} [kN]
4888	6022	5483	6745	7638	9548

TABLE 20 – Ultimate load limit for the reinforced concrete cube test for each material properties.

The table 21 summarizes the results of the verification obtained with the different approaches available using the factor $\chi = \frac{F_d}{R_d}$ and the figure 27 illustrates the force-displacement curves.

The value of q_{demand} is fixed at 4117 kN in order to fix the χ coefficient to 1 for the first relation of the GRF approach in table 21. For this relation, the safety coefficients are placed on the action and not on the displacement.

Concerning the ECOV approach, the global resistance coefficient γ_{Om} has to be calculated using the characteristic and mean analysis as explained previously :

$$V_R = \frac{1}{1,65} \ln \frac{q_{um}}{q_{uk}} = \frac{1}{1,65} \ln \frac{9548}{7638} = 0,1352- \tag{31}$$

$$\gamma_{Om} = \exp(\alpha\beta V_R) = \exp(3,04 \times 0,1352) = 1,508 \tag{32}$$

We observe that the global factor γ_{Om} decreases when reinforcement steel is added in the section. For a concrete cube, γ_{Om} is equal to 1,668 where here γ_{Om} is only equal to 1,508 which shows the influence of the steel. The GRF approach has always a higher value of χ especially compared to the ECOV approach. The partial safety factor approach has also a more or less similar result when the safety factor are placed on the action (only 3% of difference). The last remark concerns the smaller difference between the GRF and PSF regarding of the α_{cc} value (10% of difference compared to 15% for the concrete cube model).

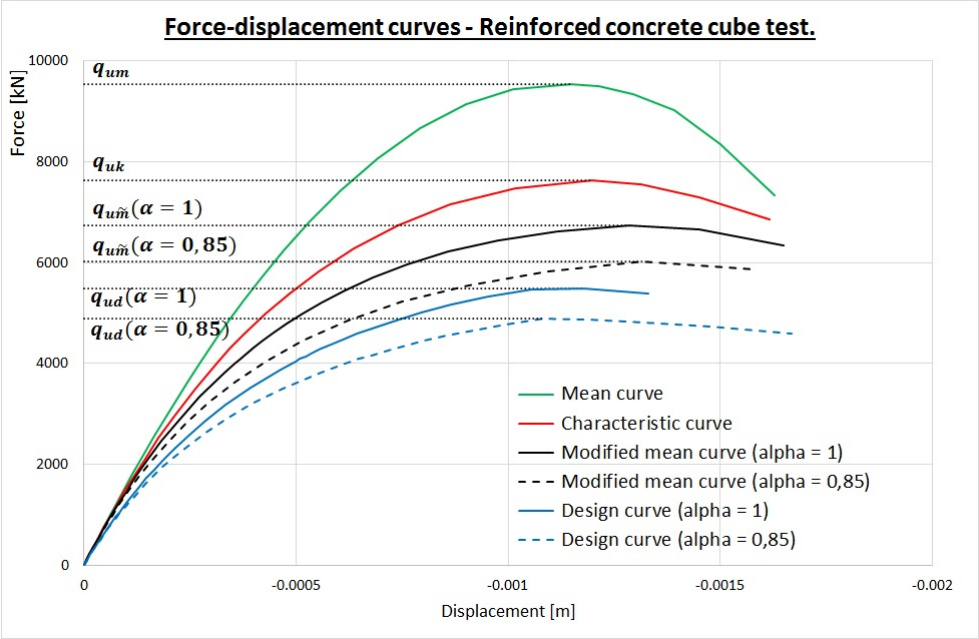

FIGURE 27 – Force-displacement curves for the reinforced concrete cube model in compression.

Reinforce concrete cube model - Compression				
Approach		LM	RM	χ
GRF $\underline{\alpha_{cc} = 0,85}$	$\gamma_{sd} q_{demand} \leq \frac{q_{u\tilde{m}}}{\gamma_O \gamma_{Rd}}$	4735	4735	**1,0000**
	$q\left[\gamma_{Rd} E(\gamma_{sd} q_{demand})\right] \leq \frac{q_{u\tilde{m}}}{\gamma_O}$	4868	5019	0,9699
	$q\left[\gamma_{Rd} \gamma_{sd} E(q_{demand})\right] \leq \frac{q_{u\tilde{m}}}{\gamma_O}$	4547	5019	0,9060
	$q_{demand} \leq \frac{q_{u\tilde{m}}}{\gamma_{O'}}$	4117	4742	0,8682
PSF $\underline{\alpha_{cc} = 0,85}$	$\gamma_{sd} q_{demand} \leq q_{ud}$	4735	4889	**0,9686**
	$q\left[\gamma_{sd} E(q_{demand})\right] \leq q_{ud}$	4354	4889	0,8906
GRF $\underline{\alpha_{cc} = 1}$	$\gamma_{sd} q_{demand} \leq \frac{q_{u\tilde{m}}}{\gamma_O \gamma_{Rd}}$	4735	5303	**0,8929**
	$q\left[\gamma_{Rd} E(\gamma_{sd} q_{demand})\right] \leq \frac{q_{u\tilde{m}}}{\gamma_O}$	4892	5621	0,8704
	$q\left[\gamma_{Rd} \gamma_{sd} E(q_{demand})\right] \leq \frac{q_{u\tilde{m}}}{\gamma_O}$	4643	5621	0,8261
	$q_{demand} \leq \frac{q_{u\tilde{m}}}{\gamma_{O'}}$	4117	5311	0,7752
PSF $\underline{\alpha_{cc} = 1}$	$\gamma_{sd} q_{demand} \leq q_{ud}$	4735	5483	**0,8635**
	$q\left[\gamma_{sd} E(q_{demand})\right] \leq q_{ud}$	4419	5483	0,8060
ECOV	$\gamma_{sd} q_{demand} \leq \frac{q_{um}}{\gamma_{Om} \gamma_{Rd}}$	4735	5972	**0,7929**
	$q\left[\gamma_{Rd} E(\gamma_{sd} q_{demand})\right] \leq \frac{q_{um}}{\gamma_{Om}}$	4973	6330	0,7856
	$q\left[\gamma_{Rd} \gamma_{sd} E(q_{demand})\right] \leq \frac{q_{um}}{\gamma_{Om}}$	4869	6330	0,7692

TABLE 21 – χ factor for the different approaches for the reinforced concrete cube test in compression.

7.3.3 Rupture by tension

The second test on the reinforced concrete cube consists of changing the force from compression to tension. The assumption that no tensile strength is present in the concrete is also made so only the reinforcement takes the forces acting on the cube. The number of analysis decreases then to 4 and no more 6 when concrete are acting. Indeed, the coefficient α_{cc} does not affect the ultimate load anymore. Moreover, there is not modified mean properties for the steel reinforcement. However concerning the design analysis, two options can be activated. Indeed, hardening can be neglected by modelling an yielding plateau. The required analysis are then with design (hardening), design bis (no hardening), characteristic and mean values.

The maximal value of the force gives the ultimate load limit for the different curves (q_{ud}, q_{ud} (bis), q_{uk} and q_{um} see table 22).

q_{ud} [kN]	q_{ud} (bis) [kN]	q_{uk} [kN]	q_{um} [kN]
1487	1399	1737	1911

TABLE 22 – Ultimate load limits for the reinforced concrete cube test in tension.

Again a comparison between the analytical and numerical analysis is done here (see the figure 28). We observe a good match between them except concerning the ability of Finelg to reach the ultimate possible strain in a certain step.

The global resistance factor (GRF) and the estimation of the coefficient of variation (ECOV) approach have then the same load limit. The only difference between these two approaches is the global resistance coefficient γ_O or γ_{Om}. For the GRF approach, γ_O is fixed at 1,2. Concerning the ECOV approach, the global resistance coefficient γ_{Om} has to be calculated based on the characteristic and the mean analysis. It equals here :

$$V_R = \frac{1}{1,65} \ln \frac{q_{um}}{q_{uk}} = \frac{1}{1,65} \ln \frac{1911}{1737} = 0,05776- \tag{33}$$

$$\gamma_{Om} = \exp(\alpha\beta V_R) = \exp(3,04 \times 0,05776) = 1,192. \tag{34}$$

γ_{Om} is more or less equal to γ_O. This fact is quite logical because only the reinforcement steel is acting. This results in a quasi equality between the GRF and the ECOV approach for this test. In that case, just the GRF approach is investigated.

The table 23 summarizes the results obtained with the different approaches available using the factor χ and the figure 28 illustrates the force-displacement curves for the model in tension. The value of q_{demand} is fixed at 1306 kN in order again to fix the χ coefficient to 1 for the first relation of the GRF approach in the table 23.

A really important remark concerning the design model corresponds to the reduced limit of the deformation available (see in figure 28). Indeed, a limit of 0,8 ϵ_{uk} has to be done for a design calculation. Because of that reduced value of the deformation, we observed that the χ coefficient for the partial safety factor approach is

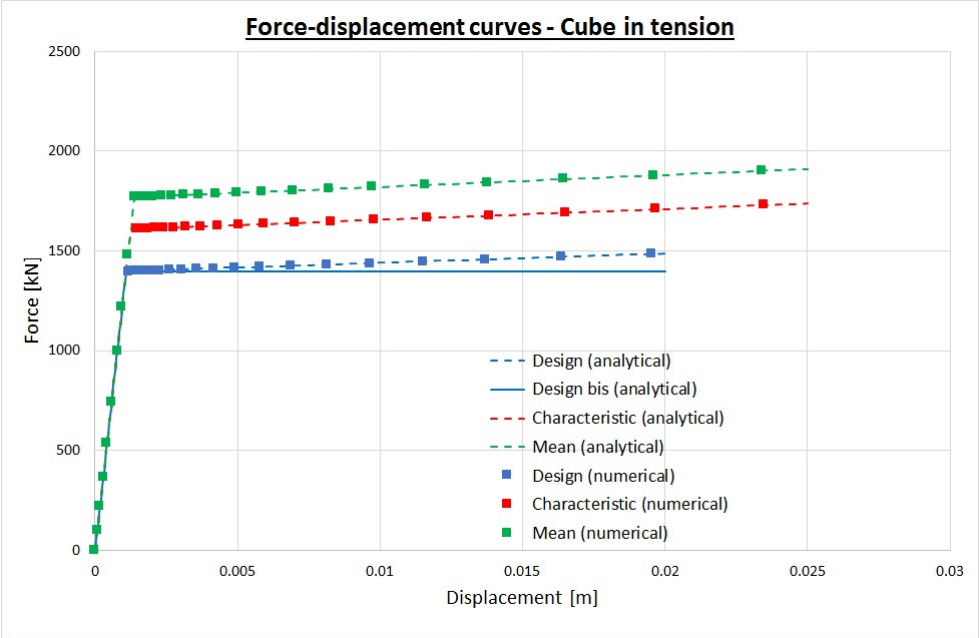

FIGURE 28 – Force-displacement curves for the reinforced concrete cube test in tension.

Reinforce concrete cube model - Tension				
Approach		LM	RM	χ
GRF	$\gamma_{sd} q_{demand} \leq \frac{q_{u\tilde{m}}}{\gamma_O \gamma_{Rd}}$	1502	1502	**1,0000**
	$q\left[\gamma_{Rd} E(\gamma_{sd} q_{demand})\right] \leq \frac{q_{u\tilde{m}}}{\gamma_O}$	1582	1592	0,9933
	$q\left[\gamma_{Rd} \gamma_{sd} E(q_{demand})\right] \leq \frac{q_{u\tilde{m}}}{\gamma_O}$	1579	1592	0,9913
	$q_{demand} \leq \frac{q_{u\tilde{m}}}{\gamma_{O'}}$	1306	1505	0,8682
PSF Design	$\gamma_{sd} q_{demand} \leq q_{ud}$	1502	1487	**1,0101**
	$q\left[\gamma_{sd} E(q_{demand})\right] \leq q_{ud}$	1397	1487	0,9392
PSF Design bis	$\gamma_{sd} q_{demand} \leq q_{ud}(bis)$	1502	1399	**1,0736**
	$q\left[\gamma_{sd} E(q_{demand})\right] \leq q_{ud}(bis)$	1399	1399	**1,0000**

TABLE 23 – χ factor for the different approaches for the reinforced concrete cube test in tension.

larger than 1 for the first relation (safety factor on the load). Indeed, if the deformation was not limited, the maximum load in the design analysis would be 1399 × 1,08 = 1511 kN > 1502 kN. The value 1,08 is the k factor that multiplies the yielding stress (see table 2). An other important remark is concerning the second relation for the design analysis without hardening. Indeed, the χ factor equals 1 because of the yielding plateau. The value of q_{demand} is equal to 1306 kN which is lower than the yielding force 1399 kN. But when the displacement for q = 1306 kN is multiplied by the safety factor γ_{sd}, the point reached the yielding plateau naturally and q is then equal to 1399 kN that is also equal to q_{ud}(bis).

7.3.4 Discussion of the results and comparison

We observed from these previous test on cubes that the safety factor should be applied on the load and not on the load effect which corresponds to the most restrictive method.

Also a good correlation between the GRF and PSF approaches is seen. Indeed, the difference between these approaches is not higher than 3 % (always when compare the same kind of relations - with the safety factor on the load or the others). This correlation comes from the theory behind these approaches. In fact the GRF approach's principle is the design value of the material multiplied by a certain factor (the same for the steel and the concrete). Then a global resistance factor divides the resistance of the structure using the material properties defined. So the GRF approach begins with as basis the design value of the material properties.

Concerning now the ECOV approach, the basis are no more the design value but the mean value of the material properties. Moreover the global resistance factor is calculated depending on the resistance of the structure (dependant of the structure). This explains the difference with the GRF and PSF approaches for which the partial safety factor of the material are independent of the structure.

For the structure in pure compression, we clearly see the advantage to use the ECOV approach over the PSF and the GRF approaches. Indeed, a gain of 20 to 25 % is obtained in comparison with the GRF (α_{cc} = 0,85) and of 10 % with the GRF (α_{cc} = 1). A small attention has to be done concerning the ECOV approach that does not include that α_{cc} coefficient in the verification.

7.4 Column models

The next test consists of the analysis of several type of cantilever columns with the geometry based on a real example (the 4th European school situated in Brussels and design by the engineering office Greisch). For this building, circular columns with a diameter of 1,6 meters are used and an high of around 7 to 9 meters. The figure 29 shows the column model and the details of the section studied :

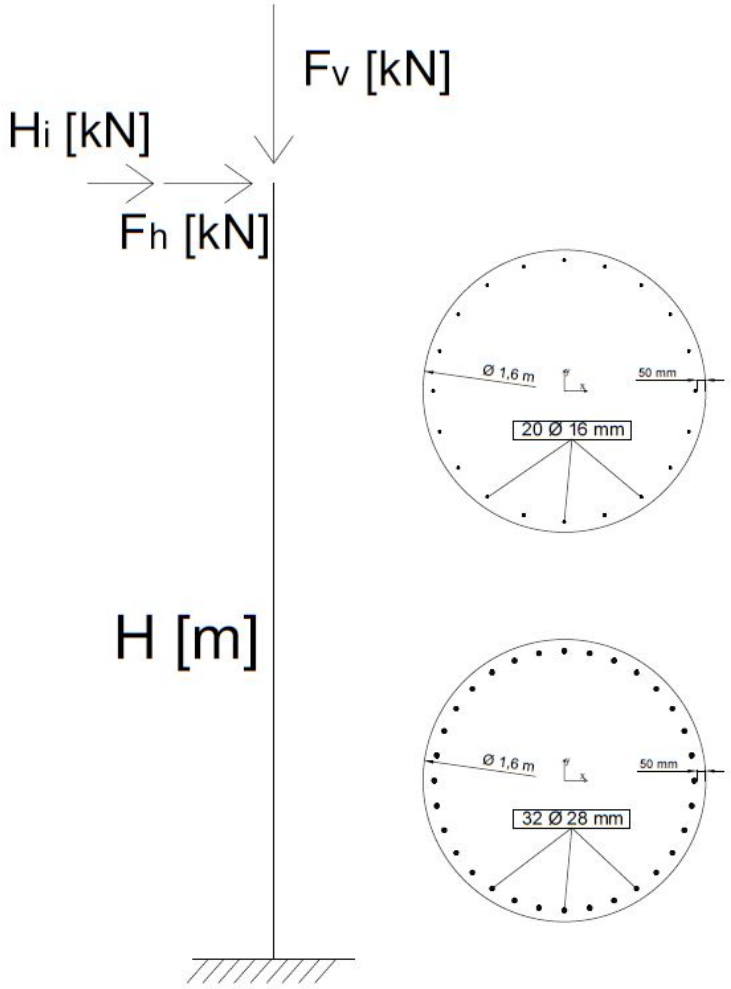

FIGURE 29 – Model of the column and geometry of the section studied.

A set of columns with two type of sections is then investigated. One section is composed of 20 bars of diameter 16 mm that corresponds to 0,2 % for the ratio of reinforcement and the other section with 32 bars of 28 mm of diameter that makes 1 %. These ratio of reinforcement can be discussed a bit longer. Indeed, the codes provides some rules about the minimum amount of reinforcement needed in a section [12]. This minimum ratio can be linked to the seismic class of the structure. For a high or medium class(DCH or DCM), the minimum amount of reinforcement ρ_{min} is equal to 1 %. In the case of low seismicity (class DCL), the minimum ratio

can decrease and depends on the axial load on the column. The ratio is the minimum value between 0,2 % and 0,1 $N_{Ed}/A_c f_{yd}$. On this last formula, we clearly observe that the minimum reinforcement is proportional to the normal force on the column. If the normal force does not exceed in our case 17500 kN, the minimum of reinforcement is still 0,2%. More the normal force increases, more ρ_{min} increases too.

The high, the initial eccentricities and the loads are variables. High of 5, 10 and 30 meters are studied and compared. The first step is to calculate the geometrical imperfections of the column. The basic inclination θ_0 varies from 1/100, 1/200 to 1/300. The following equation gives the geometrical imperfection based on that basic inclination and the table 24 summarizes the inclination obtained for each height of column :

$$\theta_i = \theta_0 \alpha_h \alpha_m \tag{35}$$

High [m]	θ_0 [rad]	α_h [-]	α_m [-]	θ_i [10^{-3} rad]
5	1/100	$2/\sqrt{5} = 0,8944$	$\sqrt{0,5(1+1/1)} = 1$	8,944
5	1/200	0,8944	1	4,472
5	1/300	0,8944	1	2,981
10	1/100	$2/\sqrt{10} = 0,6324$	$\sqrt{0,5(1+1/1)} = 1$	6,324
10	1/200	0,6324	1	3,162
10	1/300	0,6324	1	2,108
30	1/200	$2/\sqrt{30} = 0,365$	$\sqrt{0,5(1+1/1)} = 1$	1,826

TABLE 24 – Summary of the eccentricities values obtained for each height of columns.

The eccentricities are taking into account thanks to an equivalent lateral force. In the case of a cantilever column, this equivalent lateral force is equal to the vertical force times the inclination ($H_i = F_V \times \theta_i$).

The next step is to define the variation of the lateral loads. This variation is modelled with the ratio of the lateral loads over the vertical loads, ratio = $\frac{F_H}{F_V}$. The table 25 summarizes the different cases investigated for the study of columns. For the columns of 5 and 10 meters, first mostly vertical load are acting with a change of the geometrical imperfections and then columns with higher horizontal loads (with the recommended basic inclination of 1/200) are modelled. For all these load configurations, two tests are performed regarding on different ratio of reinforcement. For each cases, simplified names are given and are summarized in the table 25.

An other test is also investigated by imposing only horizontal load at the top of the column. The high of the column has no real influence on the curve obtained because the failure is caused only by bending. Indeed, the load limit decreases with the high, but the capacity of the section stays similar. For these tests, columns of 5 meters are then modelled with also both type of section. 5F1 corresponds to the 5 meters column subjected to horizontal load at the top for the section with 0,2% of steel reinforcement and 5F2 with 1%.

H [m]	5									
$\frac{F_H}{F_V}$ [-]	2,9813 10^{-3}		4,4721 10^{-3}		8,944 10^{-3}		0,1044721		0,2044721	
ρ_s [%]	0,2	1	0,2	1	0,2	1	0,2	1	0,2	1
Cases	5A1	5A2	5B1	5B2	5C1	5C2	5D1	5D2	5E1	5E2
H [m]	10									
$\frac{F_H}{F_V}$ [-]	2,1082 10^{-3}		3,162 10^{-3}		6,324 10^{-3}		0,103162		0,203162	
ρ_s [%]	0,2	1	0,2	1	0,2	1	0,2	1	0,2	1
Cases	10A1	10A2	10B1	10B2	10C1	10C2	10D1	10D2	10E1	10E2

TABLE 25 – Summary of the set cases for the columns of 5 and 10 meters.

Finally, a column of 30 meters high is modelled with again the recommended basic inclination of 1/200. The goal of this column is to obtain a failure by buckling and not of the section. Again, both types of section are studied.

An interesting parameters to study for columns is the slenderness factor (λ). Indeed, the Eurocode 1992-1-1 [1] provides the limit value of the slenderness (λ_{lim}) above what the second order effects are not negligible.

$$\lambda_{lim} = 20.A.B.C/\sqrt{n} = 10,78/\sqrt{n} \tag{36}$$

with A, B and C can be taken as 0,7, 1,1 and 0,7 respectively. n is equal to the ratio between the normal force N_{Ed} and $A_c f_{cd}$ that corresponds to the capacity of the concrete section in compression, n is called the relative normal effort. Knowing the slenderness (λ) of the different columns tested here, the coefficient n can be obtained.

$$\lambda = \frac{l_0}{i} = \frac{2 \times l}{\sqrt{I/A}} = \frac{2 \times l}{0,4} \tag{37}$$

The slenderness equals 25, 50 and 150 for the 5, 10 and 30 meters columns respectively. The coefficient n equals then for the 5 and 10 meters columns, when the limit is just reached :

$$n = \left(\frac{10,78}{25}\right)^2 = 0,186[-] \quad \& \quad n = \left(\frac{10,78}{50}\right)^2 = 0,0465[-] \tag{38}$$

This means that after 1/5 of the total the normal force capacity, the second order effect has to be taken into account for the 5 meters columns. This also answers the non necessity of changing the inclination for the column with high horizontal loads for which the normal forces are small at the failure.

Subsections in the following treat first the set of case defined in the table 25 for the columns of 5 and 10 meters. The last test operated concerns a column of 30 meters high that fail by buckling. Finally a discussion of the results obtained for the different cases and a comparison are done.

7.4.1 Columns of 5 meters

The first set of columns consists of the 5 meters columns. Concerning the safety coefficient γ_{Rd} and γ_{sd}, the recommended value provided in the Eurocode 1992-1-2 [2] are chosen ($\gamma_{Rd} = 1{,}06$ and $\gamma_{sd} = 1{,}15$). The table 26 summarizes the load limits, the demand value of the load and γ_{Om} for each set of test and for the several analysis.

/	$\alpha_{cc} = 0{,}85$		$\alpha_{cc} = 1$		/			
q [kN]	q_{ud}	$q_{u\tilde{m}}$	q_{ud}	$q_{u\tilde{m}}$	q_{uk}	q_{um}	q_{demand}	γ_{Om}
5A1	28700	36000	33480	42020	49480	64750	24610	1,641
5A2	35330	43600	40055	49470	56410	71470	29810	1,546
5B1	28230	35430	32910	41325	48620	63550	24220	1,638
5B2	34670	42840	39310	48580	55400	70160	29290	1,545
5C1	26980	33890	31400	39460	462990	60300	23170	1,627
5C2	33135	41055	37540	46535	52920	66950	28070	1,542
5D1	9560	11860	10800	13420	15080	18700	8110	1,486
5D2	14910	18090	15620	18915	21240	25480	12360	1,398
5E1	2825	3535	2960	3700	3640	4155	2420	1,275
5E2	7540	9300	8100	9790	10120	11680	6360	1,303
5F1	270	341	273	345	320	356	233	1,214
5F2	1123	1406	1142	1427	1344	1494	960	1,214

TABLE 26 – Ultimate load limits, q_{demand} and γ_{Om} for the 5 meters column set of test.

We observe on the table 26 the decreasing of the capacity with the increasing of the horizontal loads. Also, the columns with higher percentage of reinforcement have naturally a higher capacity and especially more for the columns subjected to higher moment. This last comment is especially marked for the column 5F1 and 5F2 that are essentially subjected to moment. Indeed, increasing the steel reinforcement from 0,2 to 1% increases the capacity of the section by a factor around 4 for the columns 5F and only by a factor 1,2 for the columns 5A.

Concerning the ECOV approach, the global safety factor γ_{Om} has to be calculated. The table 26 summarizes also the γ_{Om} factor for each set of test. We observe in the table 26 that the safety coefficient γ_{Om} is less important for the column 5D, 5E and 5F that are more subjected to bending moment. Indeed, in a flexural behaviour, the concrete properties are less important than in a more or less pure compression behaviour. It is especially true for the column 5F with only bending moment where the difference between the modified mean and the mean load limit is barely visible. Moreover the global factor γ_{Om} is equal to 1,214 where for the GRF approach γ_O equals 1,2.

The last comment concerns the value of the demand load q_{demand} that is still obtained by imposing 1 to the first relation of the GRF approach.

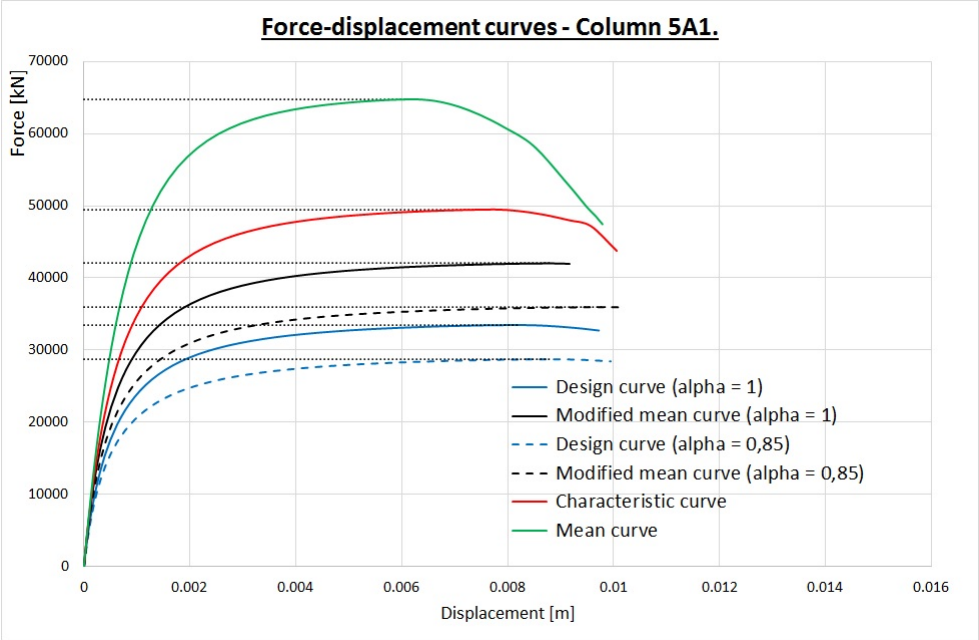

FIGURE 30 – Force-displacement curves for the columns 5A1.

Column 5A1				
Approach		LM	RM	χ
GRF $\underline{\alpha_{cc} = 0,85}$	$\gamma_{sd} q_{demand} \leq \frac{q_{u\tilde{m}}}{\gamma_O \gamma_{Rd}}$	28300	28300	**1,0000**
	$q\left[\gamma_{Rd} E(\gamma_{sd} q_{demand})\right] \leq \frac{q_{u\tilde{m}}}{\gamma_O}$	28800	30000	0,9600
	$q\left[\gamma_{Rd} \gamma_{sd} E(q_{demand})\right] \leq \frac{q_{u\tilde{m}}}{\gamma_O}$	26350	30000	0,8784
	$q_{demand} \leq \frac{q_{u\tilde{m}}}{\gamma_{O'}}$	24610	28350	0,8682
PSF $\underline{\alpha_{cc} = 0,85}$	$\gamma_{sd} q_{demand} \leq q_{ud}$	28300	28700	**0,9860**
	$q\left[\gamma_{sd} E(q_{demand})\right] \leq q_{ud}$	25270	28700	0,8804
GRF $\underline{\alpha_{cc} = 1}$	$\gamma_{sd} q_{demand} \leq \frac{q_{u\tilde{m}}}{\gamma_O \gamma_{Rd}}$	28300	33030	**0,8568**
	$q\left[\gamma_{Rd} E(\gamma_{sd} q_{demand})\right] \leq \frac{q_{u\tilde{m}}}{\gamma_O}$	28970	35015	0,8273
	$q\left[\gamma_{Rd} \gamma_{sd} E(q_{demand})\right] \leq \frac{q_{u\tilde{m}}}{\gamma_O}$	27015	35015	0,7715
	$q_{demand} \leq \frac{q_{u\tilde{m}}}{\gamma_{O'}}$	24610	33085	0,7439
PSF $\underline{\alpha_{cc} = 1}$	$\gamma_{sd} q_{demand} \leq q_{ud}$	28300	33480	**0,8454**
	$q\left[\gamma_{sd} E(q_{demand})\right] \leq q_{ud}$	25740	33480	0,7688
ECOV	$\gamma_{sd} q_{demand} \leq \frac{q_{um}}{\gamma_O \gamma_{Rd}}$	28300	37215	**0,7605**
	$q\left[\gamma_{Rd} E(\gamma_{sd} q_{demand})\right] \leq \frac{q_{um}}{\gamma_O}$	29430	39450	0,7460
	$q\left[\gamma_{Rd} \gamma_{sd} E(q_{demand})\right] \leq \frac{q_{um}}{\gamma_O}$	28510	39450	0,7228

TABLE 27 – χ factor for the different approaches for the column 5A1.

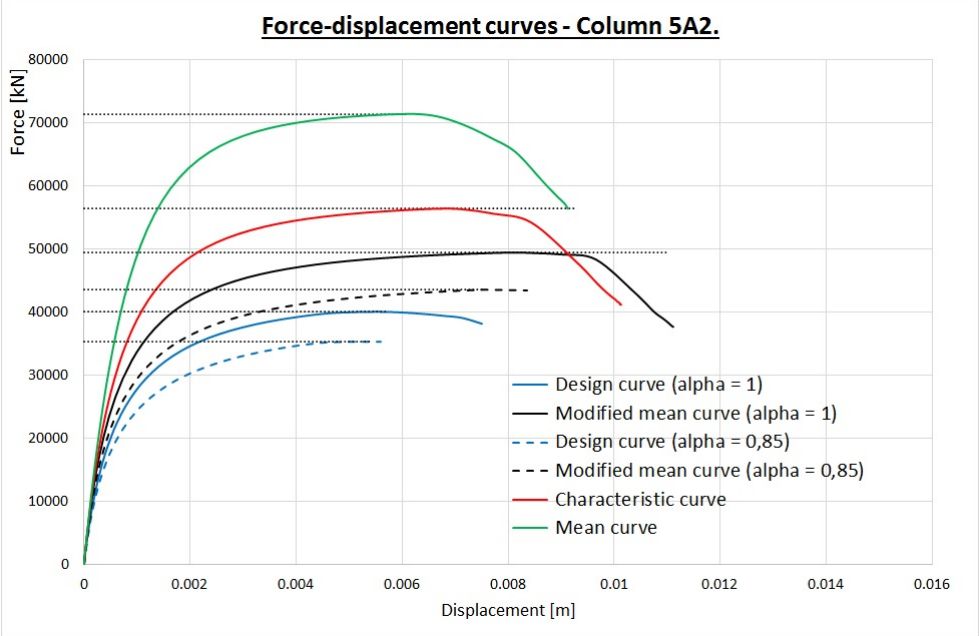

FIGURE 31 – Force-displacement curves for the columns 5A2.

Column 5A2				
Approach		LM	RM	χ
GRF $\underline{\alpha_{cc} = 0,85}$	$\gamma_{sd} q_{demand} \leq \frac{q_{u\tilde{m}}}{\gamma_O \gamma_{Rd}}$	34280	34280	**1,0000**
	$q\left[\gamma_{Rd} E(\gamma_{sd} q_{demand})\right] \leq \frac{q_{u\tilde{m}}}{\gamma_O}$	34800	36340	0,9576
	$q\left[\gamma_{Rd} \gamma_{sd} E(q_{demand})\right] \leq \frac{q_{u\tilde{m}}}{\gamma_O}$	31930	36340	0,8788
	$q_{demand} \leq \frac{q_{u\tilde{m}}}{\gamma_{O'}}$	29810	34330	0,8682
PSF $\underline{\alpha_{cc} = 0,85}$	$\gamma_{sd} q_{demand} \leq q_{ud}$	34280	35330	**0,9703**
	$q\left[\gamma_{sd} E(q_{demand})\right] \leq q_{ud}$	30870	35330	0,8738
GRF $\underline{\alpha_{cc} = 1}$	$\gamma_{sd} q_{demand} \leq \frac{q_{u\tilde{m}}}{\gamma_O \gamma_{Rd}}$	34280	38890	**0,8814**
	$q\left[\gamma_{Rd} E(\gamma_{sd} q_{demand})\right] \leq \frac{q_{u\tilde{m}}}{\gamma_O}$	35120	41230	0,8518
	$q\left[\gamma_{Rd} \gamma_{sd} E(q_{demand})\right] \leq \frac{q_{u\tilde{m}}}{\gamma_O}$	32540	41230	0,7893
	$q_{demand} \leq \frac{q_{u\tilde{m}}}{\gamma_{O'}}$	29810	38950	0,7652
PSF $\underline{\alpha_{cc} = 1}$	$\gamma_{sd} q_{demand} \leq q_{ud}$	34280	40060	**0,8558**
	$q\left[\gamma_{sd} E(q_{demand})\right] \leq q_{ud}$	31230	40060	0,7798
ECOV	$\gamma_{sd} q_{demand} \leq \frac{q_{um}}{\gamma_O \gamma_{Rd}}$	34280	43600	**0,7862**
	$q\left[\gamma_{Rd} E(\gamma_{sd} q_{demand})\right] \leq \frac{q_{um}}{\gamma_O}$	35590	46220	0,7700
	$q\left[\gamma_{Rd} \gamma_{sd} E(q_{demand})\right] \leq \frac{q_{um}}{\gamma_O}$	34360	46220	0,7435

TABLE 28 – χ factor for the different approaches for the column 5A2.

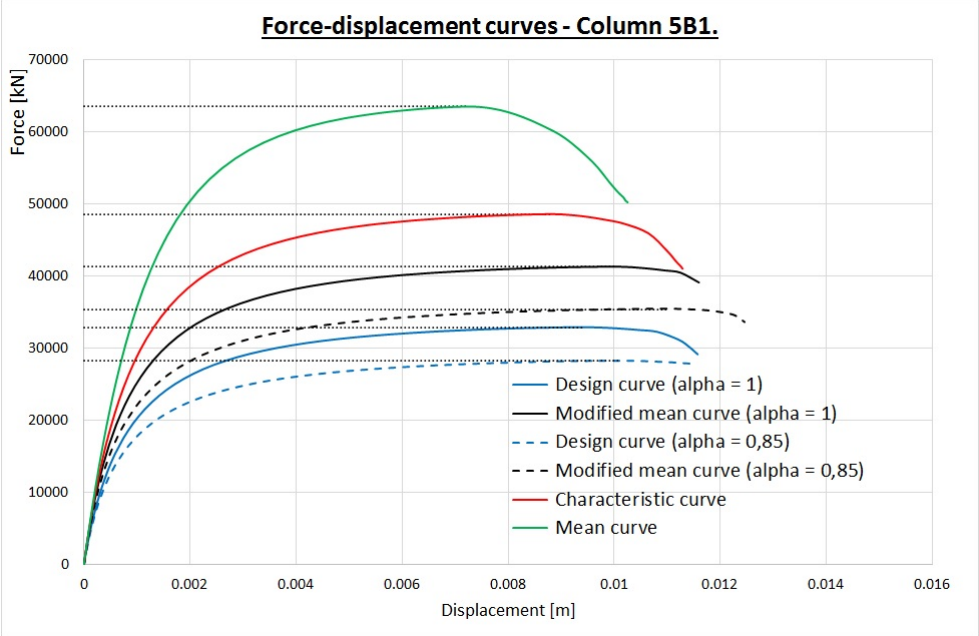

FIGURE 32 – Force-displacement curves for the columns 5B1.

Column 5B1				
Approach		LM	RM	χ
GRF $\underline{\alpha_{cc} = 0,85}$	$\gamma_{sd} q_{demand} \leq \frac{q_{u\tilde{m}}}{\gamma_O \gamma_{Rd}}$	27850	27850	**1,0000**
	$q\left[\gamma_{Rd} E(\gamma_{sd} q_{demand})\right] \leq \frac{q_{u\tilde{m}}}{\gamma_O}$	28340	29520	0,9598
	$q\left[\gamma_{Rd} \gamma_{sd} E(q_{demand})\right] \leq \frac{q_{u\tilde{m}}}{\gamma_O}$	25980	29520	0,8799
	$q_{demand} \leq \frac{q_{u\tilde{m}}}{\gamma_{O'}}$	24220	27900	0,8682
PSF $\underline{\alpha_{cc} = 0,85}$	$\gamma_{sd} q_{demand} \leq q_{ud}$	27850	28230	**0,9867**
	$q\left[\gamma_{sd} E(q_{demand})\right] \leq q_{ud}$	24910	28230	0,8825
GRF $\underline{\alpha_{cc} = 1}$	$\gamma_{sd} q_{demand} \leq \frac{q_{u\tilde{m}}}{\gamma_O \gamma_{Rd}}$	27850	32490	**0,8573**
	$q\left[\gamma_{Rd} E(\gamma_{sd} q_{demand})\right] \leq \frac{q_{u\tilde{m}}}{\gamma_O}$	28500	34440	0,8276
	$q\left[\gamma_{Rd} \gamma_{sd} E(q_{demand})\right] \leq \frac{q_{u\tilde{m}}}{\gamma_O}$	26690	34440	0,7751
	$q_{demand} \leq \frac{q_{u\tilde{m}}}{\gamma_{O'}}$	24220	32540	0,7443
PSF $\underline{\alpha_{cc} = 1}$	$\gamma_{sd} q_{demand} \leq q_{ud}$	27850	32910	**0,8463**
	$q\left[\gamma_{sd} E(q_{demand})\right] \leq q_{ud}$	25380	32910	0,7712
ECOV	$\gamma_{sd} q_{demand} \leq \frac{q_{um}}{\gamma_O \gamma_{Rd}}$	27850	36600	**0,7609**
	$q\left[\gamma_{Rd} E(\gamma_{sd} q_{demand})\right] \leq \frac{q_{um}}{\gamma_O}$	28950	38800	0,7462
	$q\left[\gamma_{Rd} \gamma_{sd} E(q_{demand})\right] \leq \frac{q_{um}}{\gamma_O}$	28100	38800	0,7243

TABLE 29 – χ factor for the different approaches for the column 5B1.

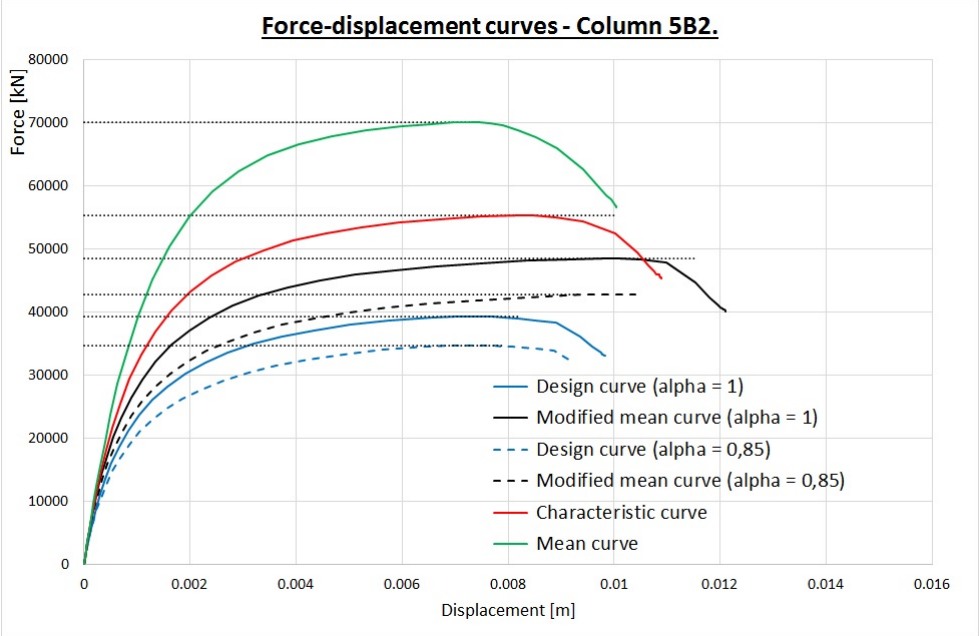

FIGURE 33 – Force-displacement curves for the columns 5B2.

Column 5B2				
Approach		LM	RM	χ
GRF $\alpha_{cc} = 0,85$	$\gamma_{sd} q_{demand} \leq \frac{q_{u\tilde{m}}}{\gamma_O \gamma_{Rd}}$	33680	33680	**1,0000**
	$q\left[\gamma_{Rd} E(\gamma_{sd} q_{demand})\right] \leq \frac{q_{u\tilde{m}}}{\gamma_O}$	34180	35700	0,9574
	$q\left[\gamma_{Rd} \gamma_{sd} E(q_{demand})\right] \leq \frac{q_{u\tilde{m}}}{\gamma_O}$	31410	35700	0,8798
	$q_{demand} \leq \frac{q_{u\tilde{m}}}{\gamma_{O'}}$	29290	33730	0,8682
PSF $\alpha_{cc} = 0,85$	$\gamma_{sd} q_{demand} \leq q_{ud}$	33680	34670	**0,9715**
	$q\left[\gamma_{sd} E(q_{demand})\right] \leq q_{ud}$	30360	34670	0,8756
GRF $\alpha_{cc} = 1$	$\gamma_{sd} q_{demand} \leq \frac{q_{u\tilde{m}}}{\gamma_O \gamma_{Rd}}$	33680	38190	**0,8819**
	$q\left[\gamma_{Rd} E(\gamma_{sd} q_{demand})\right] \leq \frac{q_{u\tilde{m}}}{\gamma_O}$	34490	40480	0,8519
	$q\left[\gamma_{Rd} \gamma_{sd} E(q_{demand})\right] \leq \frac{q_{u\tilde{m}}}{\gamma_O}$	32030	40480	0,7911
	$q_{demand} \leq \frac{q_{u\tilde{m}}}{\gamma_{O'}}$	29290	38250	0,7656
PSF $\alpha_{cc} = 1$	$\gamma_{sd} q_{demand} \leq q_{ud}$	33680	39310	**0,8568**
	$q\left[\gamma_{sd} E(q_{demand})\right] \leq q_{ud}$	30730	39310	0,7818
ECOV	$\gamma_{sd} q_{demand} \leq \frac{q_{um}}{\gamma_O \gamma_{Rd}}$	33680	42830	**0,7864**
	$q\left[\gamma_{Rd} E(\gamma_{sd} q_{demand})\right] \leq \frac{q_{um}}{\gamma_O}$	35180	45400	0,7750
	$q\left[\gamma_{Rd} \gamma_{sd} E(q_{demand})\right] \leq \frac{q_{um}}{\gamma_O}$	33800	45400	0,7446

TABLE 30 – χ factor for the different approaches for the column 5B2.

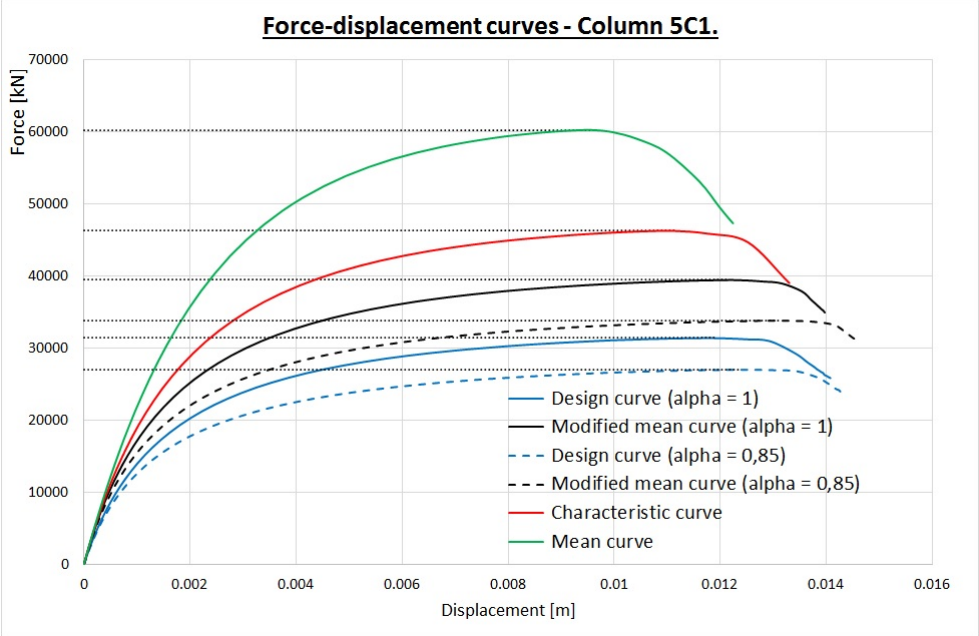

FIGURE 34 – Force-displacement curves for the columns 5C1.

Column 5C1				
Approach		LM	RM	χ
GRF $\underline{\alpha_{cc} = 0,85}$	$\gamma_{sd} q_{demand} \leq \frac{q_{u\tilde{m}}}{\gamma_O \gamma_{Rd}}$	26640	26640	**1,0000**
	$q\left[\gamma_{Rd} E(\gamma_{sd} q_{demand})\right] \leq \frac{q_{u\tilde{m}}}{\gamma_O}$	27100	28240	0,9596
	$q\left[\gamma_{Rd} \gamma_{sd} E(q_{demand})\right] \leq \frac{q_{u\tilde{m}}}{\gamma_O}$	24980	28240	0,8844
	$q_{demand} \leq \frac{q_{u\tilde{m}}}{\gamma_{O'}}$	23170	26685	0,8682
PSF $\underline{\alpha_{cc} = 0,85}$	$\gamma_{sd} q_{demand} \leq q_{ud}$	26640	26980	**0,9876**
	$q\left[\gamma_{sd} E(q_{demand})\right] \leq q_{ud}$	23930	26980	0,8871
GRF $\underline{\alpha_{cc} = 1}$	$\gamma_{sd} q_{demand} \leq \frac{q_{u\tilde{m}}}{\gamma_O \gamma_{Rd}}$	26640	31030	**0,8587**
	$q\left[\gamma_{Rd} E(\gamma_{sd} q_{demand})\right] \leq \frac{q_{u\tilde{m}}}{\gamma_O}$	27410	32890	0,8335
	$q\left[\gamma_{Rd} \gamma_{sd} E(q_{demand})\right] \leq \frac{q_{u\tilde{m}}}{\gamma_O}$	25510	32890	0,7757
	$q_{demand} \leq \frac{q_{u\tilde{m}}}{\gamma_{O'}}$	23170	31070	0,7456
PSF $\underline{\alpha_{cc} = 1}$	$\gamma_{sd} q_{demand} \leq q_{ud}$	26640	31400	**0,8485**
	$q\left[\gamma_{sd} E(q_{demand})\right] \leq q_{ud}$	24360	31400	0,7757
ECOV	$\gamma_{sd} q_{demand} \leq \frac{q_{um}}{\gamma_O \gamma_{Rd}}$	26640	34950	**0,7622**
	$q\left[\gamma_{Rd} E(\gamma_{sd} q_{demand})\right] \leq \frac{q_{um}}{\gamma_O}$	27850	37050	0,7518
	$q\left[\gamma_{Rd} \gamma_{sd} E(q_{demand})\right] \leq \frac{q_{um}}{\gamma_O}$	26830	37050	0,7241

TABLE 31 – χ factor for the different approaches for the column 5C1.

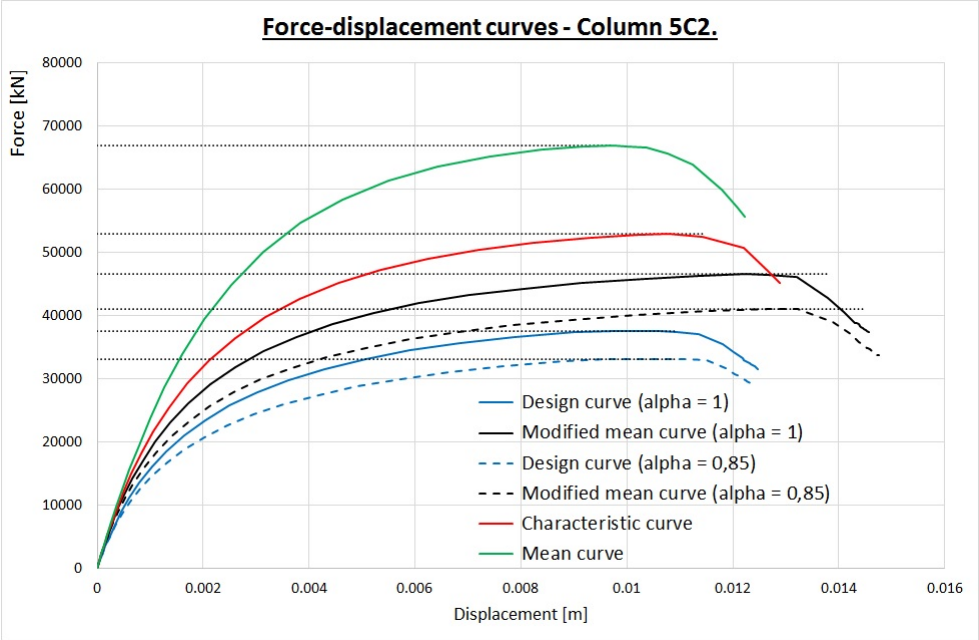

FIGURE 35 – Force-displacement curves for the columns 5C2.

Column 5C2				
Approach		LM	RM	χ
GRF $\underline{\alpha_{cc} = 0,85}$	$\gamma_{sd} q_{demand} \leq \frac{q_{u\tilde{m}}}{\gamma_O \gamma_{Rd}}$	32280	32280	**1,0000**
	$q\left[\gamma_{Rd} E(\gamma_{sd} q_{demand})\right] \leq \frac{q_{u\tilde{m}}}{\gamma_O}$	32870	34210	0,9608
	$q\left[\gamma_{Rd}\gamma_{sd} E(q_{demand})\right] \leq \frac{q_{u\tilde{m}}}{\gamma_O}$	30240	34210	0,8838
	$q_{demand} \leq \frac{q_{u\tilde{m}}}{\gamma_{O'}}$	28070	32330	0,8682
PSF $\underline{\alpha_{cc} = 0,85}$	$\gamma_{sd} q_{demand} \leq q_{ud}$	32280	33130	**0,9741**
	$q\left[\gamma_{sd} E(q_{demand})\right] \leq q_{ud}$	29200	33130	0,8813
GRF $\underline{\alpha_{cc} = 1}$	$\gamma_{sd} q_{demand} \leq \frac{q_{u\tilde{m}}}{\gamma_O \gamma_{Rd}}$	32280	36580	**0,8822**
	$q\left[\gamma_{Rd} E(\gamma_{sd} q_{demand})\right] \leq \frac{q_{u\tilde{m}}}{\gamma_O}$	33030	38780	0,8518
	$q\left[\gamma_{Rd}\gamma_{sd} E(q_{demand})\right] \leq \frac{q_{u\tilde{m}}}{\gamma_O}$	31000	38780	0,7995
	$q_{demand} \leq \frac{q_{u\tilde{m}}}{\gamma_{O'}}$	28070	36640	0,7660
PSF $\underline{\alpha_{cc} = 1}$	$\gamma_{sd} q_{demand} \leq q_{ud}$	32280	37540	**0,8598**
	$q\left[\gamma_{sd} E(q_{demand})\right] \leq q_{ud}$	29560	37540	0,7874
ECOV	$\gamma_{sd} q_{demand} \leq \frac{q_{um}}{\gamma_O \gamma_{Rd}}$	32280	40950	**0,7882**
	$q\left[\gamma_{Rd} E(\gamma_{sd} q_{demand})\right] \leq \frac{q_{um}}{\gamma_O}$	33690	43410	0,7762
	$q\left[\gamma_{Rd}\gamma_{sd} E(q_{demand})\right] \leq \frac{q_{um}}{\gamma_O}$	32400	43410	0,7463

TABLE 32 – χ factor for the different approaches for the column 5C2.

The figures 30, 31, 32, 33, 34 and 35 and the tables 27, 28, 29, 30, 31 and 32 summarize the force-displacement curves (vertical force and horizontal displacement at the top of the column) and the results for the column subjected essentially to normal forces and with different eccentricities. We observe the same behaviour independently of the reinforcement steel and the eccentricities. Differences are however noticed on the load limit and on the displacement capacity. The shape of the curves presents some kind of ductility, but the reason of this displacement increase is the second order moment resulting of the analysis.

Concerning the results for theses tests on the column essentially under compression, the same order of magnitude is observed for each configurations. Indeed, each configurations and each approaches present a higher χ value for the relation with the safety factor placed on the load. Moreover, the more restrictive approach is the GRF then the PSF with a small margin and finally the ECOV.

As said, there is a small difference between the GRF and the PSF approaches. The difference is about 1,3% for the column with only 0,2% of steel reinforcement and reaches 3 % when the steel accounts for 1% whatever the initial eccentricities.

Additionally, we notice a difference of around 12 to 15 % between the approaches (GRF and PSF) with $\alpha_{cc} = 0{,}85$ and with $\alpha_{cc} = 1$ which is logical because the failure occurs by compression of the concrete.

Finally, a major difference between the GRF and the ECOV approach is noticed. 21 to 24% of additional margin on the load can be account for the resistance of the columns with the ECOV approach.

The figures 36, 37, 38, 39, 40 and 41 and the tables 33, 34, 35, 36, 37 and 38 summarize the force-displacement curves and results for the columns subjected to both bending moment and normal forces or only bending moment. In the figures, the force corresponds to the vertical forces except for the column 5F1 and 5F2 for which it is the horizontal loads. The displacement is for all the model the horizontal top displacement of the column. We do not observe the same behaviour on each configurations. Some of them presents a high ductility and some not.

Still the relation with the safety factor on the loads presents the less safety margin on the verification. The GRF approach has also an higher value of the χ factor compared to the other approaches, but this decreases with the increase of the horizontal loads.

For small horizontal loads (5D1 and 5D2), the same remarks as the columns essentially in compression can be done with less percentage of difference.

For moderate horizontal loads (5E1 and 5E2), different behaviours are noticed. The column 5E1 presents a high ductility and the column 5E2 not. This difference is only due to the different section properties.

Concerning the columns 5F1 and 5F2 that are only subjected to horizontal loads, the structure presents a high ductility. The difference between the different approaches becomes less important. Indeed, the difference between the GRF and the PSF approaches is only around 1%. There is also no more major difference between the GRF and the PSF approaches regarding on the α_{cc} value. Moreover, the ECOV approach presents less than 5% of difference with the GRF approach.

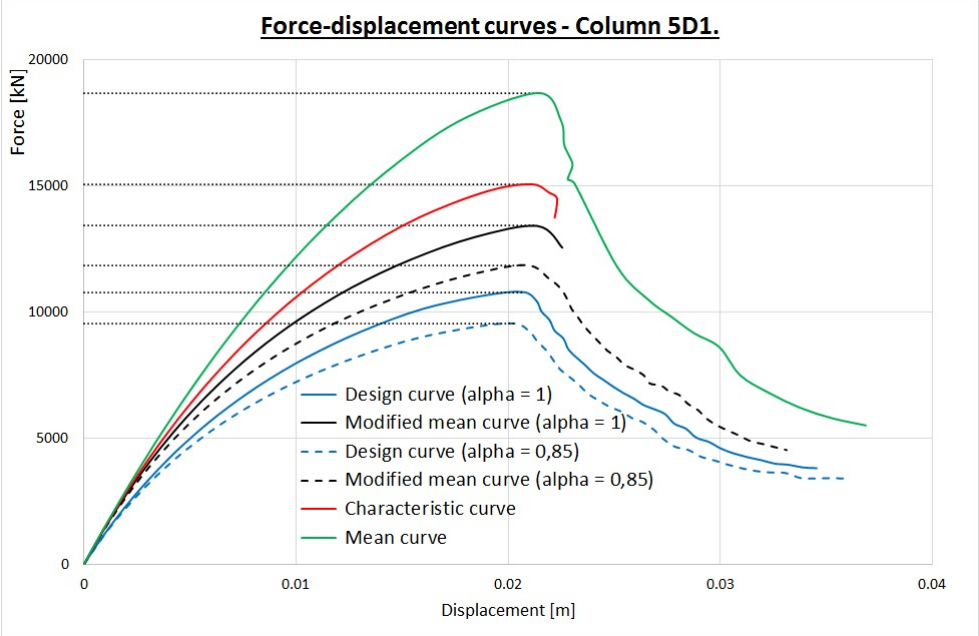

FIGURE 36 – Force-displacement curves for the columns 5D1.

Column 5D1				
Approach		LM	RM	χ
GRF $\alpha_{cc} = 0,85$	$\gamma_{sd} q_{demand} \leq \frac{q_{u\tilde{m}}}{\gamma_O \gamma_{Rd}}$	9325	9325	**1,0000**
	$q\left[\gamma_{Rd} E(\gamma_{sd} q_{demand})\right] \leq \frac{q_{u\tilde{m}}}{\gamma_O}$	9615	9890	0,9728
	$q\left[\gamma_{Rd} \gamma_{sd} E(q_{demand})\right] \leq \frac{q_{u\tilde{m}}}{\gamma_O}$	8830	9890	0,8933
	$q_{demand} \leq \frac{q_{u\tilde{m}}}{\gamma_{O'}}$	8110	9340	0,8682
PSF $\alpha_{cc} = 0,85$	$\gamma_{sd} q_{demand} \leq q_{ud}$	9325	9560	**0,9752**
	$q\left[\gamma_{sd} E(q_{demand})\right] \leq q_{ud}$	8630	9560	0,9026
GRF $\alpha_{cc} = 1$	$\gamma_{sd} q_{demand} \leq \frac{q_{u\tilde{m}}}{\gamma_O \gamma_{Rd}}$	9325	10550	**0,8837**
	$q\left[\gamma_{Rd} E(\gamma_{sd} q_{demand})\right] \leq \frac{q_{u\tilde{m}}}{\gamma_O}$	9680	11185	0,8655
	$q\left[\gamma_{Rd} \gamma_{sd} E(q_{demand})\right] \leq \frac{q_{u\tilde{m}}}{\gamma_O}$	9205	11185	0,8229
	$q_{demand} \leq \frac{q_{u\tilde{m}}}{\gamma_{O'}}$	8110	10570	0,7672
PSF $\alpha_{cc} = 1$	$\gamma_{sd} q_{demand} \leq q_{ud}$	9325	10800	**0,8637**
	$q\left[\gamma_{sd} E(q_{demand})\right] \leq q_{ud}$	8745	10800	0,8101
ECOV	$\gamma_{sd} q_{demand} \leq \frac{q_{um}}{\gamma_O \gamma_{Rd}}$	9325	11870	**0,7856**
	$q\left[\gamma_{Rd} E(\gamma_{sd} q_{demand})\right] \leq \frac{q_{um}}{\gamma_O}$	9770	12580	0,7767
	$q\left[\gamma_{Rd} \gamma_{sd} E(q_{demand})\right] \leq \frac{q_{um}}{\gamma_O}$	9570	12580	0,7606

TABLE 33 – χ factor for the different approaches for the column 5D1.

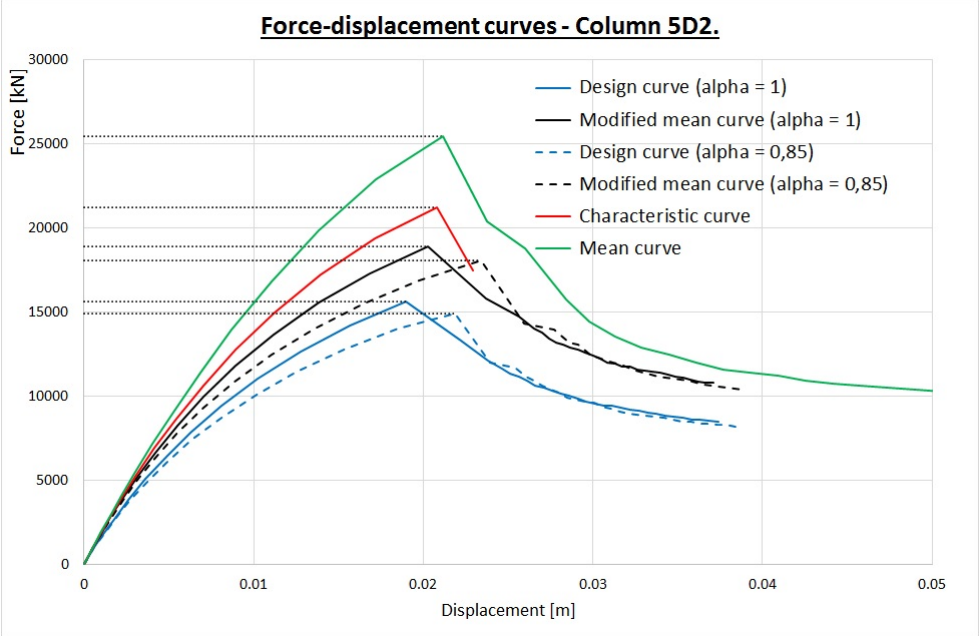

FIGURE 37 – Force-displacement curves for the columns 5D2.

Column 5D2				
Approach		LM	RM	χ
GRF $\alpha_{cc} = 0,85$	$\gamma_{sd} q_{demand} \leq \frac{q_{u\tilde{m}}}{\gamma_O \gamma_{Rd}}$	14220	14220	**1,0000**
	$q\left[\gamma_{Rd} E(\gamma_{sd} q_{demand})\right] \leq \frac{q_{u\tilde{m}}}{\gamma_O}$	14650	15070	0,9720
	$q\left[\gamma_{Rd} \gamma_{sd} E(q_{demand})\right] \leq \frac{q_{u\tilde{m}}}{\gamma_O}$	13860	15070	0,9195
	$q_{demand} \leq \frac{q_{u\tilde{m}}}{\gamma_{O'}}$	12360	14240	0,8682
PSF $\alpha_{cc} = 0,85$	$\gamma_{sd} q_{demand} \leq q_{ud}$	14220	14910	**0,9536**
	$q\left[\gamma_{sd} E(q_{demand})\right] \leq q_{ud}$	13290	14910	0,8911
GRF $\alpha_{cc} = 1$	$\gamma_{sd} q_{demand} \leq \frac{q_{u\tilde{m}}}{\gamma_O \gamma_{Rd}}$	14220	14870	**0,9562**
	$q\left[\gamma_{Rd} E(\gamma_{sd} q_{demand})\right] \leq \frac{q_{u\tilde{m}}}{\gamma_O}$	14720	15760	0,9341
	$q\left[\gamma_{Rd} \gamma_{sd} E(q_{demand})\right] \leq \frac{q_{u\tilde{m}}}{\gamma_O}$	14060	15760	0,8917
	$q_{demand} \leq \frac{q_{u\tilde{m}}}{\gamma_{O'}}$	12360	14890	0,8302
PSF $\alpha_{cc} = 1$	$\gamma_{sd} q_{demand} \leq q_{ud}$	14220	15620	**0,9105**
	$q\left[\gamma_{sd} E(q_{demand})\right] \leq q_{ud}$	13400	15620	0,8583
ECOV	$\gamma_{sd} q_{demand} \leq \frac{q_{um}}{\gamma_O \gamma_{Rd}}$	14220	17190	**0,8273**
	$q\left[\gamma_{Rd} E(\gamma_{sd} q_{demand})\right] \leq \frac{q_{um}}{\gamma_O}$	14880	18220	0,8168
	$q\left[\gamma_{Rd} \gamma_{sd} E(q_{demand})\right] \leq \frac{q_{um}}{\gamma_O}$	14570	18220	0,7995

TABLE 34 – χ factor for the different approaches for the column 5D2.

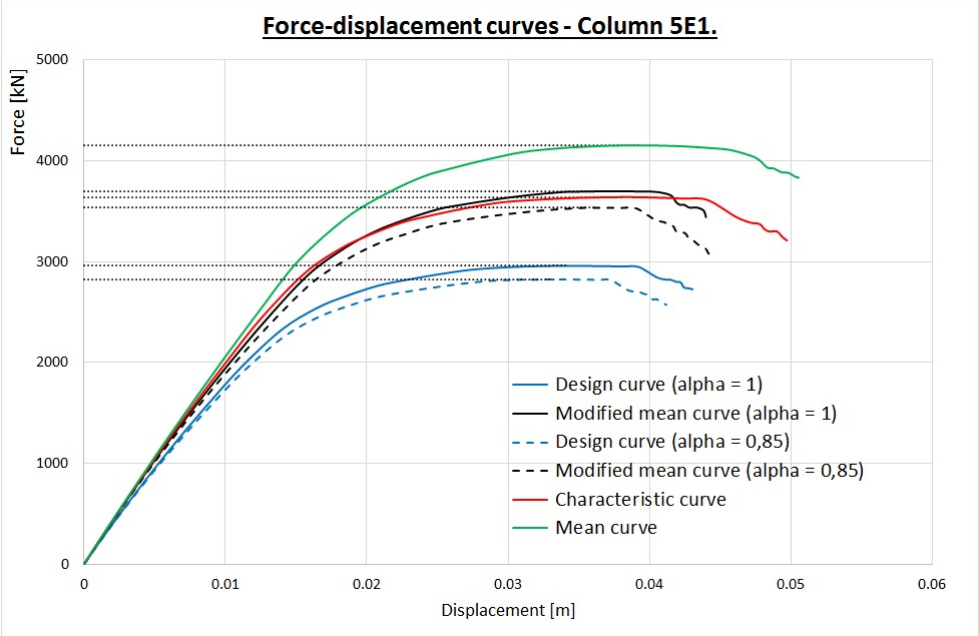

FIGURE 38 – Force-displacement curves for the columns 5E1.

Column 5E1				
Approach		LM	RM	χ
GRF $\alpha_{cc} = 0,85$	$\gamma_{sd} q_{demand} \leq \frac{q_{u\tilde{m}}}{\gamma_O \gamma_{Rd}}$	2780	2780	**1,0000**
	$q\left[\gamma_{Rd} E(\gamma_{sd} q_{demand})\right] \leq \frac{q_{u\tilde{m}}}{\gamma_O}$	2870	2950	0,9739
	$q\left[\gamma_{Rd} \gamma_{sd} E(q_{demand})\right] \leq \frac{q_{u\tilde{m}}}{\gamma_O}$	2810	2950	0,9548
	$q_{demand} \leq \frac{q_{u\tilde{m}}}{\gamma_{O'}}$	2420	2780	0,8682
PSF $\alpha_{cc} = 0,85$	$\gamma_{sd} q_{demand} \leq q_{ud}$	2780	2825	**0,9836**
	$q\left[\gamma_{sd} E(q_{demand})\right] \leq q_{ud}$	2555	2825	0,9046
GRF $\alpha_{cc} = 1$	$\gamma_{sd} q_{demand} \leq \frac{q_{u\tilde{m}}}{\gamma_O \gamma_{Rd}}$	2780	2910	**0,9554**
	$q\left[\gamma_{Rd} E(\gamma_{sd} q_{demand})\right] \leq \frac{q_{u\tilde{m}}}{\gamma_O}$	2920	3080	0,9460
	$q\left[\gamma_{Rd} \gamma_{sd} E(q_{demand})\right] \leq \frac{q_{u\tilde{m}}}{\gamma_O}$	2840	3080	0,9212
	$q_{demand} \leq \frac{q_{u\tilde{m}}}{\gamma_{O'}}$	2420	2910	0,8295
PSF $\alpha_{cc} = 1$	$\gamma_{sd} q_{demand} \leq q_{ud}$	2780	2960	**0,9392**
	$q\left[\gamma_{sd} E(q_{demand})\right] \leq q_{ud}$	2590	2960	0,8744
ECOV	$\gamma_{sd} q_{demand} \leq \frac{q_{um}}{\gamma_O \gamma_{Rd}}$	2780	3070	**0,9041**
	$q\left[\gamma_{Rd} E(\gamma_{sd} q_{demand})\right] \leq \frac{q_{um}}{\gamma_O}$	2930	3260	0,8989
	$q\left[\gamma_{Rd} \gamma_{sd} E(q_{demand})\right] \leq \frac{q_{um}}{\gamma_O}$	2890	3260	0,8867

TABLE 35 – χ factor for the different approaches for the column 5E1.

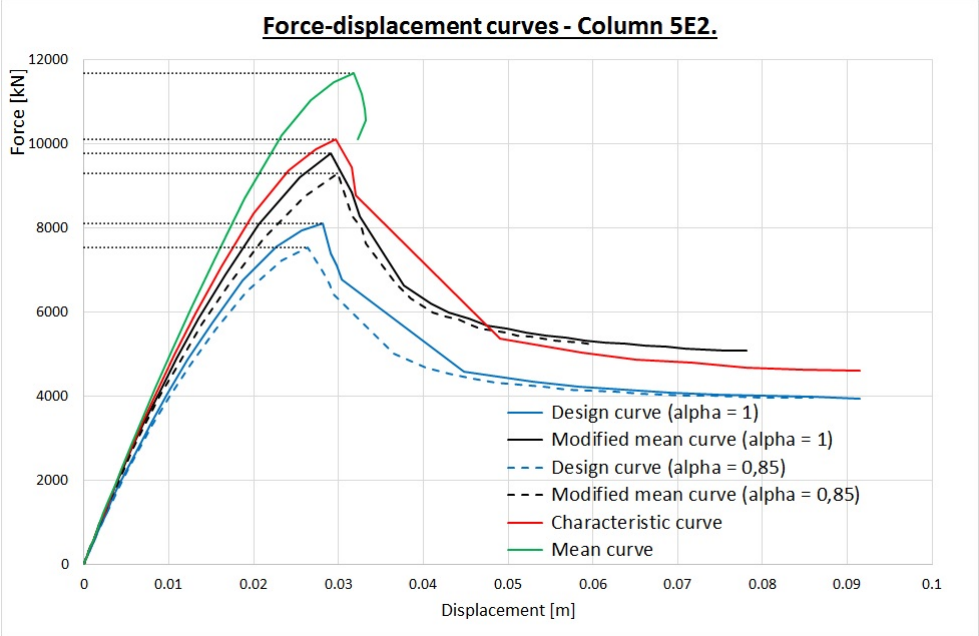

FIGURE 39 – Force-displacement curves for the columns 5E2.

Column 5E2				
Approach		LM	RM	χ
GRF $\underline{\alpha_{cc} = 0,85}$	$\gamma_{sd} q_{demand} \leq \frac{q_{u\tilde{m}}}{\gamma_O \gamma_{Rd}}$	7310	7310	**1,0000**
	$q\left[\gamma_{Rd} E(\gamma_{sd} q_{demand})\right] \leq \frac{q_{u\tilde{m}}}{\gamma_O}$	7620	7750	0,9839
	$q\left[\gamma_{Rd} \gamma_{sd} E(q_{demand})\right] \leq \frac{q_{u\tilde{m}}}{\gamma_O}$	7340	7750	0,9467
	$q_{demand} \leq \frac{q_{u\tilde{m}}}{\gamma_{O'}}$	6360	7320	0,8682
PSF $\underline{\alpha_{cc} = 0,85}$	$\gamma_{sd} q_{demand} \leq q_{ud}$	7310	7540	**0,9695**
	$q\left[\gamma_{sd} E(q_{demand})\right] \leq q_{ud}$	6900	7540	0,9145
GRF $\underline{\alpha_{cc} = 1}$	$\gamma_{sd} q_{demand} \leq \frac{q_{u\tilde{m}}}{\gamma_O \gamma_{Rd}}$	7310	7690	**0,9501**
	$q\left[\gamma_{Rd} E(\gamma_{sd} q_{demand})\right] \leq \frac{q_{u\tilde{m}}}{\gamma_O}$	7640	8160	0,9362
	$q\left[\gamma_{Rd} \gamma_{sd} E(q_{demand})\right] \leq \frac{q_{u\tilde{m}}}{\gamma_O}$	7400	8160	0,9075
	$q_{demand} \leq \frac{q_{u\tilde{m}}}{\gamma_{O'}}$	6360	7710	0,8249
PSF $\underline{\alpha_{cc} = 1}$	$\gamma_{sd} q_{demand} \leq q_{ud}$	7310	8100	**0,9024**
	$q\left[\gamma_{sd} E(q_{demand})\right] \leq q_{ud}$	6990	8100	0,8624
ECOV	$\gamma_{sd} q_{demand} \leq \frac{q_{um}}{\gamma_O \gamma_{Rd}}$	7310	8460	**0,8645**
	$q\left[\gamma_{Rd} E(\gamma_{sd} q_{demand})\right] \leq \frac{q_{um}}{\gamma_O}$	7710	8960	0,8596
	$q\left[\gamma_{Rd} \gamma_{sd} E(q_{demand})\right] \leq \frac{q_{um}}{\gamma_O}$	7590	8960	0,8464

TABLE 36 – χ factor for the different approaches for the column 5E2.

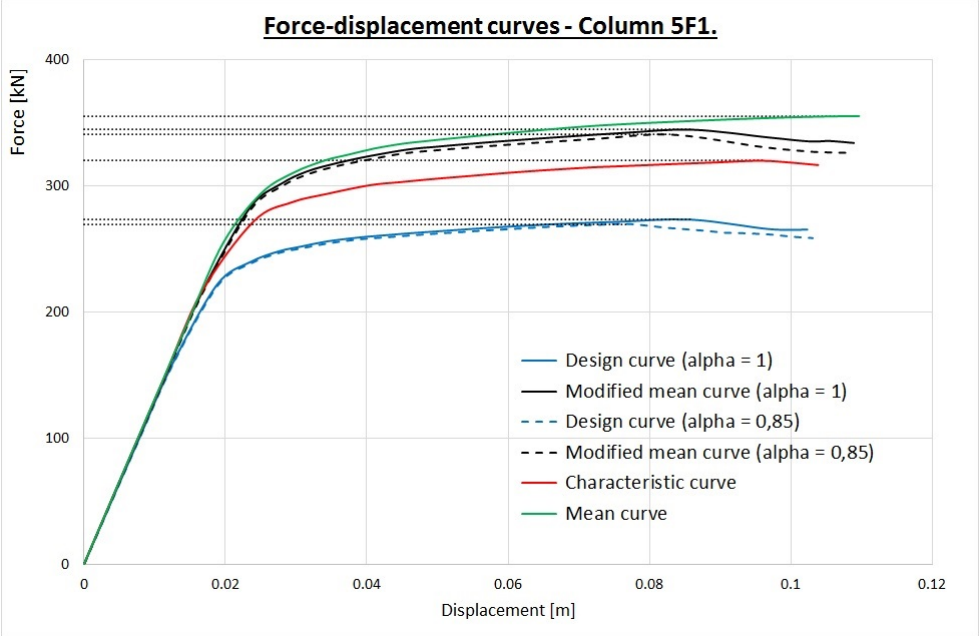

FIGURE 40 – Force-displacement curves for the column of 5F1.

Column 5F1				
Approach		LM	RM	χ
GRF $\underline{\alpha_{cc} = 0,85}$	$\gamma_{sd} q_{demand} \leq \frac{q_{u\tilde{m}}}{\gamma_O \gamma_{Rd}}$	268	268	**1,0000**
	$q\left[\gamma_{Rd} E(\gamma_{sd} q_{demand})\right] \leq \frac{q_{u\tilde{m}}}{\gamma_O}$	281	284	0,9891
	$q\left[\gamma_{Rd}\gamma_{sd} E(q_{demand})\right] \leq \frac{q_{u\tilde{m}}}{\gamma_O}$	273	284	0,9601
	$q_{demand} \leq \frac{q_{u\tilde{m}}}{\gamma_{O'}}$	233	269	0,8682
PSF $\underline{\alpha_{cc} = 0,85}$	$\gamma_{sd} q_{demand} \leq q_{ud}$	268	270	**0,9944**
	$q\left[\gamma_{sd} E(q_{demand})\right] \leq q_{ud}$	242	270	0,8987
GRF $\underline{\alpha_{cc} = 1}$	$\gamma_{sd} q_{demand} \leq \frac{q_{u\tilde{m}}}{\gamma_O \gamma_{Rd}}$	268	271	**0,9896**
	$q\left[\gamma_{Rd} E(\gamma_{sd} q_{demand})\right] \leq \frac{q_{u\tilde{m}}}{\gamma_O}$	281	287	0,9791
	$q\left[\gamma_{Rd}\gamma_{sd} E(q_{demand})\right] \leq \frac{q_{u\tilde{m}}}{\gamma_O}$	273	287	0,9515
	$q_{demand} \leq \frac{q_{u\tilde{m}}}{\gamma_{O'}}$	233	272	0,8591
PSF $\underline{\alpha_{cc} = 1}$	$\gamma_{sd} q_{demand} \leq q_{ud}$	268	273	**0,9810**
	$q\left[\gamma_{sd} E(q_{demand})\right] \leq q_{ud}$	243	273	0,8887
ECOV	$\gamma_{sd} q_{demand} \leq \frac{q_{um}}{\gamma_O \gamma_{Rd}}$	268	276	**0,9706**
	$q\left[\gamma_{Rd} E(\gamma_{sd} q_{demand})\right] \leq \frac{q_{um}}{\gamma_O}$	278	293	0,9477
	$q\left[\gamma_{Rd}\gamma_{sd} E(q_{demand})\right] \leq \frac{q_{um}}{\gamma_O}$	271	293	0,9262

TABLE 37 – χ factor for the different approaches for the column of 5F1.

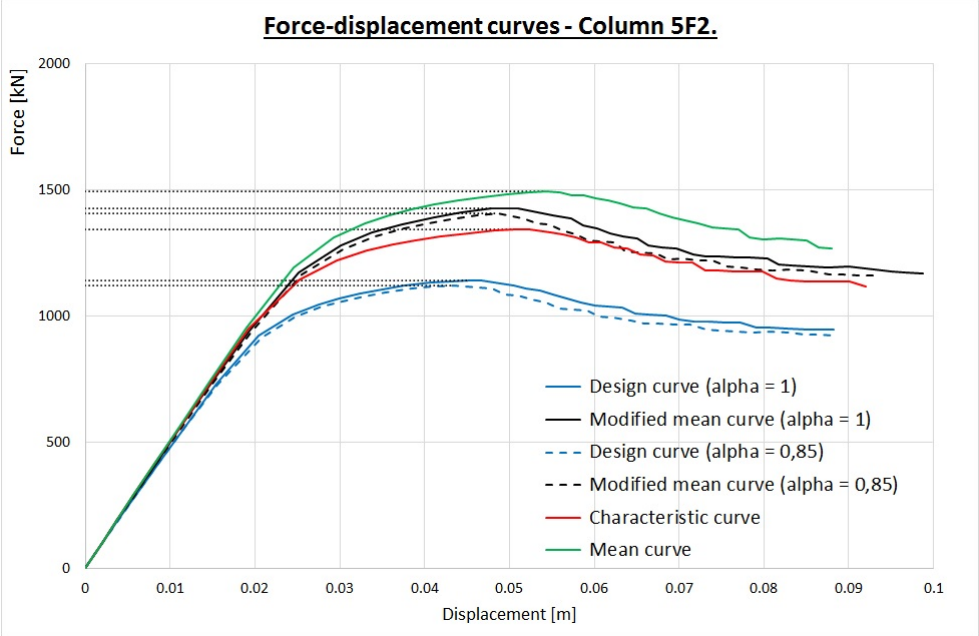

FIGURE 41 – Force-displacement curves for the column of 5F2.

Column 5F2				
Approach		LM	RM	χ
GRF $\alpha_{cc} = 0,85$	$\gamma_{sd} q_{demand} \leq \frac{q_{u\tilde{m}}}{\gamma_O \gamma_{Rd}}$	1110	1110	**1,0000**
	$q\left[\gamma_{Rd} E(\gamma_{sd} q_{demand})\right] \leq \frac{q_{u\tilde{m}}}{\gamma_O}$	1160	1170	0,9898
	$q\left[\gamma_{Rd} \gamma_{sd} E(q_{demand})\right] \leq \frac{q_{u\tilde{m}}}{\gamma_O}$	1130	1170	0,9629
	$q_{demand} \leq \frac{q_{u\tilde{m}}}{\gamma_{O'}}$	960	1110	0,8682
PSF $\alpha_{cc} = 0,85$	$\gamma_{sd} q_{demand} \leq q_{ud}$	1110	1120	**0,9847**
	$q\left[\gamma_{sd} E(q_{demand})\right] \leq q_{ud}$	1020	1120	0,9073
GRF $\alpha_{cc} = 1$	$\gamma_{sd} q_{demand} \leq \frac{q_{u\tilde{m}}}{\gamma_O \gamma_{Rd}}$	1110	1120	**0,9855**
	$q\left[\gamma_{Rd} E(\gamma_{sd} q_{demand})\right] \leq \frac{q_{u\tilde{m}}}{\gamma_O}$	1160	1190	0,9765
	$q\left[\gamma_{Rd} \gamma_{sd} E(q_{demand})\right] \leq \frac{q_{u\tilde{m}}}{\gamma_O}$	1130	1190	0,9525
	$q_{demand} \leq \frac{q_{u\tilde{m}}}{\gamma_{O'}}$	960	1120	0,8556
PSF $\alpha_{cc} = 1$	$\gamma_{sd} q_{demand} \leq q_{ud}$	1110	1140	**0,9682**
	$q\left[\gamma_{sd} E(q_{demand})\right] \leq q_{ud}$	1020	1140	0,8957
ECOV	$\gamma_{sd} q_{demand} \leq \frac{q_{um}}{\gamma_O \gamma_{Rd}}$	1110	1160	**0,9531**
	$q\left[\gamma_{Rd} E(\gamma_{sd} q_{demand})\right] \leq \frac{q_{um}}{\gamma_O}$	1160	1230	0,9466
	$q\left[\gamma_{Rd} \gamma_{sd} E(q_{demand})\right] \leq \frac{q_{um}}{\gamma_O}$	1140	1230	0,9293

TABLE 38 – χ factor for the different approaches for the column of 5F2.

The reason of the different behaviour obtained in the analysis comes from the failure types and can be observed on the MN interaction plan. The figure 42 illustrates than MN plan for both types of section with all tests performed. A comparison between the envelope obtained from Cinelu and manually is also done.

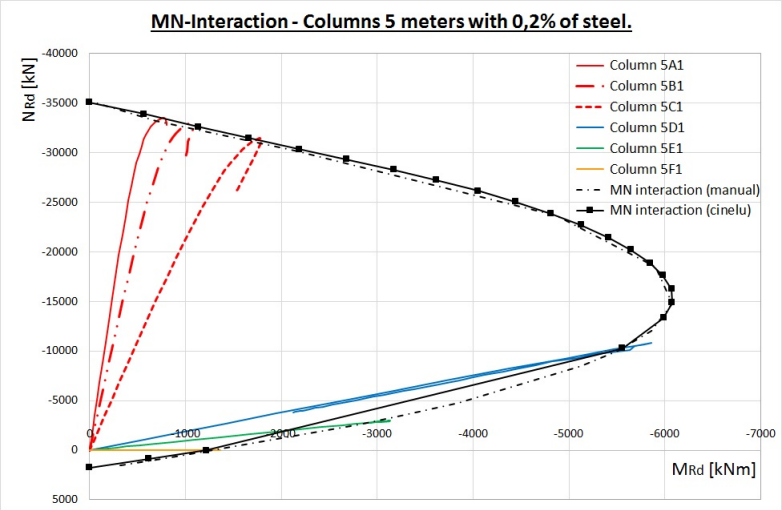

(a) Column with 0,2 % of steel reinforcement.

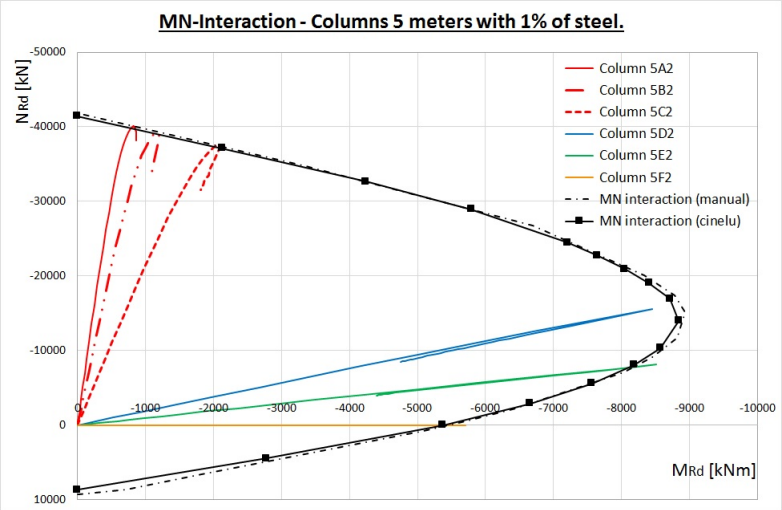

(b) Column with 1 % of steel reinforcement.

FIGURE 42 – Comparison of the MN interaction from Cinelu and manually with MN curves from tests on the 5 meters columns.

The difference on the behaviour comes on the failure zones that the columns reach in figure 42. Indeed, the column 5A, 5B and 5C fails by compression in the concrete ($\epsilon_{c1} = 0,0021$) where 5D, 5E and 5F by failure of the concrete in bending ($\epsilon_{cu2} = 0,0035$). Still in the column 5D, 5E and 5F, different behaviours are observed. To understand these differences, a deeper comprehension of the MN interaction curve has to be done. The peak of the moment on the envelope corresponds to the failure of the concrete in one side and the beginning of the plasticity in the other side. This means that the columns that failed around the peak of moment cannot account for high ductility because the plasticity begins. Moreover in a circular column, the

reinforcement bars are not all situated at the bottom. This explains the more brittle behaviour for the column 5D1, 5D2 and 5E2. More we decrease the compression, higher strain in the steel reinforcement can be possible and so ductility (column 5E1, 5F1 and 5F2).

A difference between the two envelopes for the column with 0,2% of steel is observed for quite small normal forces and moderate moments. The error, on the envelope provided by Cinelu, is simply due to the lack of point computed by the program and then miss that part by interpolation. This part is important because the result obtained for the column 5E1 reaches the failure around there. For the other type of section (with 1% of steel), the envelopes obtained manually and from Cinelu match well. A small difference is however obtained in the tensile zone due to the bilinear approximation for the steel reinforcement material law. The program Cinelu has some difficulties to reach that point and seems to use a steel material law without hardening.

Some differences are observed in the results regarding on the value of α_{cc} (0,85 or 1). Indeed, depending on the case, the difference is not constant. The difference is higher when no lateral loads are applied on the structure (so few bending moment in the column). In contrary, when the bending moment increases in the column, the difference becomes less important by reaching nearly no influence when only moment are present.

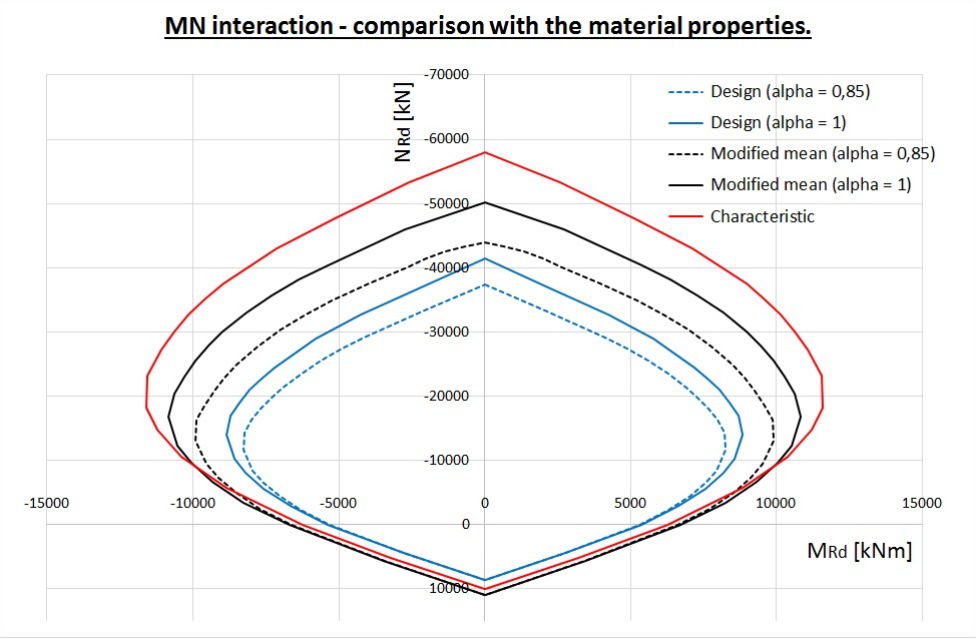

FIGURE 43 – Comparison of the MN envelop for the different material properties $\rho_s = 1\%$(Cinelu).

In figure 43, the different interaction curves for the different material properties are illustrated for the column with 1% of steel. We clearly see that for small compression forces, the influence of the concrete properties are quite small. In contrast, the influence of the steel reinforcement properties is in that zone quite marked. This explains the decrease of the difference between the GRF and PSF approaches regarding on the α_{cc} value (concrete) with the increase of moment in the columns.

7.4.2 Columns of 10 meters

The second set of tests involve columns of 10 meters high. As for the 5 meters columns, the safety factor γ_{Rd} and γ_{sd} are taken as 1,06 and 1,15 respectively. The table 39 summarizes the load limits, the demand value of the load and γ_{Om} for each set of test and for the several analysis made.

/	$\alpha_{cc} = 0{,}85$		$\alpha_{cc} = 1$		/			
q [kN]	q_{ud}	$q_{u\tilde{m}}$	q_{ud}	$q_{u\tilde{m}}$	q_{uk}	q_{um}	q_{demand}	γ_{Om}
10A1	25880	32470	30300	379450	44880	59080	22200	1,659
10A2	32140	38972	36500	44510	51280	65300	26640	1,561
10B1	25390	31730	29670	37020	43790	57330	21690	1,643
10B2	31290	38250	35520	43510	49890	63430	26150	1,556
10C1	23930	29970	27810	34860	40850	52990	20490	1,615
10C2	29280	35920	33170	40770	46540	58780	24560	1,539
10D1	2310	2850	2400	2960	2880	3220	1950	1,230
10D2	6690	8230	7110	8590	8750	9930	5620	1,264
10E1	833	1039	846	1056	990	1096	710	1,206
10E2	3110	3835	3210	3970	3830	4280	2620	1,220

TABLE 39 – Ultimate load limits, q_{demand} and γ_{Om} for the 10 meters column set of test.

We observe on the table 39 the decreasing of the capacity with the increasing of the horizontal loads as for the 5 meters columns. We can also notice by comparing the load limit for the 5 and 10 meters columns (table 26 and 39) that obviously the capacity decreases with the high because of the moment generated. This remark is especially more true for the column with more horizontal loads.

Concerning the ECOV approach, the global safety factor γ_{Om} has to be also calculated. The table 39 summarizes the γ_{Om} factor for each configurations. Again, the safety factor γ_{Om} decreases with the increase of the horizontal loads as for the 5 meters columns.

As previously, the value of q_{demand} is obtained by imposing a unit value for the first relation of the GRF approach.

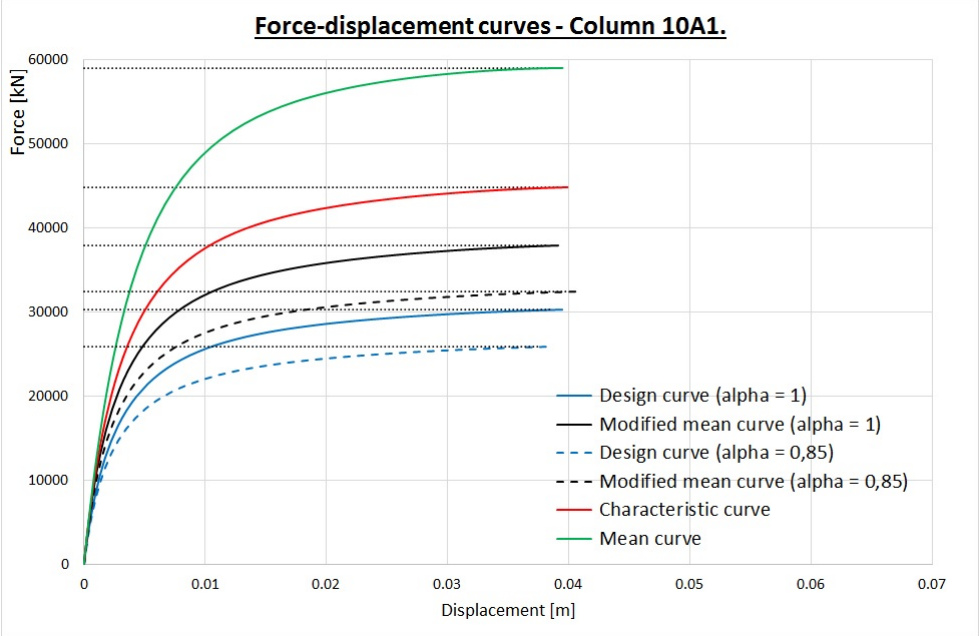

FIGURE 44 – Force-displacement curves for the columns 10A1.

Column 10A1				
Approach		LM	RM	χ
GRF $\underline{\alpha_{cc} = 0,85}$	$\gamma_{sd} q_{demand} \leq \frac{q_{u\tilde{m}}}{\gamma_O \gamma_{Rd}}$	25530	25530	**1,0000**
	$q\left[\gamma_{Rd} E(\gamma_{sd} q_{demand})\right] \leq \frac{q_{u\tilde{m}}}{\gamma_O}$	25960	27060	0,9594
	$q\left[\gamma_{Rd} \gamma_{sd} E(q_{demand})\right] \leq \frac{q_{u\tilde{m}}}{\gamma_O}$	23710	27060	0,8764
	$q_{demand} \leq \frac{q_{u\tilde{m}}}{\gamma_{O'}}$	22200	25570	0,8682
PSF $\underline{\alpha_{cc} = 0,85}$	$\gamma_{sd} q_{demand} \leq q_{ud}$	25530	25880	**0,9864**
	$q\left[\gamma_{sd} E(q_{demand})\right] \leq q_{ud}$	22770	25880	0,8800
GRF $\underline{\alpha_{cc} = 1}$	$\gamma_{sd} q_{demand} \leq \frac{q_{u\tilde{m}}}{\gamma_O \gamma_{Rd}}$	25530	29830	**0,8558**
	$q\left[\gamma_{Rd} E(\gamma_{sd} q_{demand})\right] \leq \frac{q_{u\tilde{m}}}{\gamma_O}$	26080	31620	0,8247
	$q\left[\gamma_{Rd} \gamma_{sd} E(q_{demand})\right] \leq \frac{q_{u\tilde{m}}}{\gamma_O}$	24420	31620	0,7723
	$q_{demand} \leq \frac{q_{u\tilde{m}}}{\gamma_{O'}}$	22200	29880	0,7430
PSF $\underline{\alpha_{cc} = 1}$	$\gamma_{sd} q_{demand} \leq q_{ud}$	25530	30300	**0,8424**
	$q\left[\gamma_{sd} E(q_{demand})\right] \leq q_{ud}$	23180	30300	0,7648
ECOV	$\gamma_{sd} q_{demand} \leq \frac{q_{um}}{\gamma_O \gamma_{Rd}}$	25530	33590	**0,7600**
	$q\left[\gamma_{Rd} E(\gamma_{sd} q_{demand})\right] \leq \frac{q_{um}}{\gamma_O}$	26600	35600	0,7471
	$q\left[\gamma_{Rd} \gamma_{sd} E(q_{demand})\right] \leq \frac{q_{um}}{\gamma_O}$	25450	35600	0,7149

TABLE 40 – χ factor for the different approaches for the column 10A1.

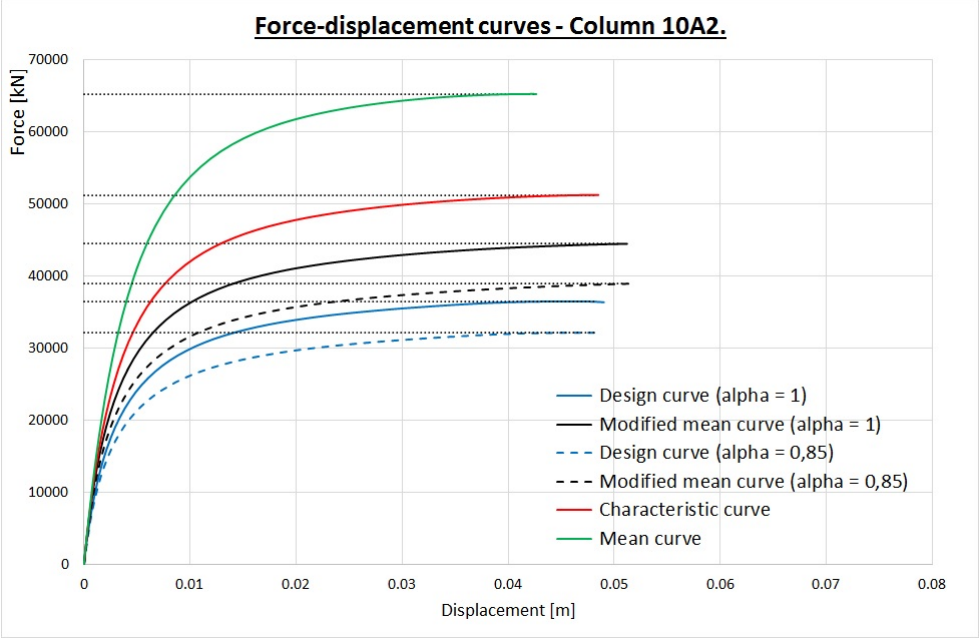

FIGURE 45 – Force-displacement curves for the columns 10A2.

Column 10A2				
Approach		LM	RM	χ
GRF $\alpha_{cc} = 0,85$	$\gamma_{sd} q_{demand} \leq \frac{q_{u\tilde{m}}}{\gamma_O \gamma_{Rd}}$	30640	30640	**1,0000**
	$q\left[\gamma_{Rd} E(\gamma_{sd} q_{demand})\right] \leq \frac{q_{u\tilde{m}}}{\gamma_O}$	31030	32480	0,9555
	$q\left[\gamma_{Rd} \gamma_{sd} E(q_{demand})\right] \leq \frac{q_{u\tilde{m}}}{\gamma_O}$	28410	32480	0,8747
	$q_{demand} \leq \frac{q_{u\tilde{m}}}{\gamma_{O'}}$	26640	30690	0,8682
PSF $\alpha_{cc} = 0,85$	$\gamma_{sd} q_{demand} \leq q_{ud}$	30640	32140	**0,9532**
	$q\left[\gamma_{sd} E(q_{demand})\right] \leq q_{ud}$	27440	32140	0,8536
GRF $\alpha_{cc} = 1$	$\gamma_{sd} q_{demand} \leq \frac{q_{u\tilde{m}}}{\gamma_O \gamma_{Rd}}$	30640	34990	**0,8757**
	$q\left[\gamma_{Rd} E(\gamma_{sd} q_{demand})\right] \leq \frac{q_{u\tilde{m}}}{\gamma_O}$	31280	37090	0,8434
	$q\left[\gamma_{Rd} \gamma_{sd} E(q_{demand})\right] \leq \frac{q_{u\tilde{m}}}{\gamma_O}$	29130	37090	0,7854
	$q_{demand} \leq \frac{q_{u\tilde{m}}}{\gamma_{O'}}$	26640	35040	0,7602
PSF $\alpha_{cc} = 1$	$\gamma_{sd} q_{demand} \leq q_{ud}$	30640	36500	**0,8394**
	$q\left[\gamma_{sd} E(q_{demand})\right] \leq q_{ud}$	27840	36500	0,7626
ECOV	$\gamma_{sd} q_{demand} \leq \frac{q_{um}}{\gamma_O \gamma_{Rd}}$	30640	39470	**0,7763**
	$q\left[\gamma_{Rd} E(\gamma_{sd} q_{demand})\right] \leq \frac{q_{um}}{\gamma_O}$	31910	41830	0,7628
	$q\left[\gamma_{Rd} \gamma_{sd} E(q_{demand})\right] \leq \frac{q_{um}}{\gamma_O}$	30410	41830	0,7270

TABLE 41 – χ factor for the different approaches for the column 10A2.

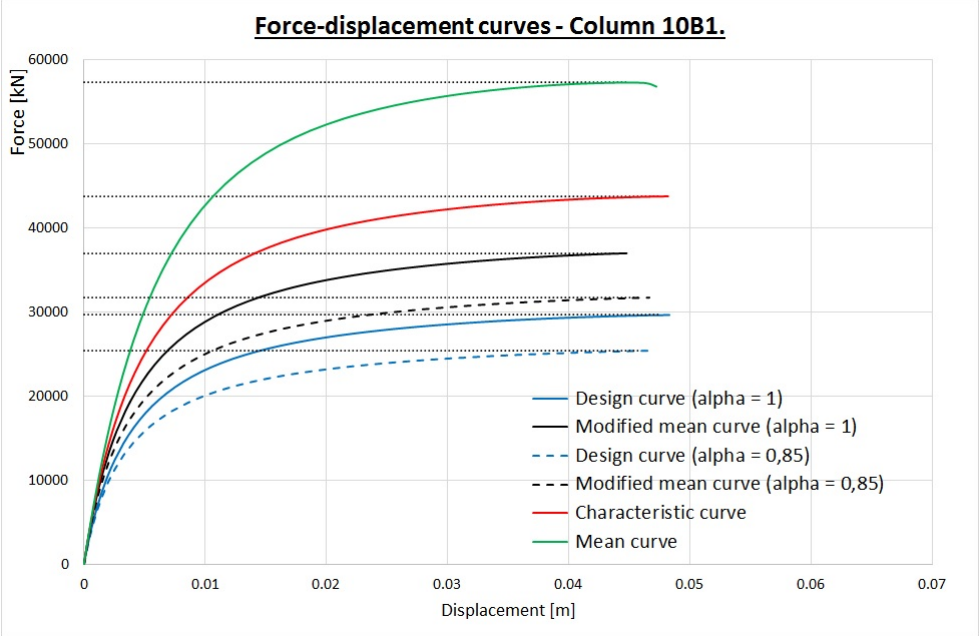

FIGURE 46 – Force-displacement curves for the columns 10B1.

Column 10B1				
Approach		LM	RM	χ
GRF $\alpha_{cc} = 0,85$	$\gamma_{sd} q_{demand} \leq \frac{q_{u\tilde{m}}}{\gamma_O \gamma_{Rd}}$	24950	24950	**1,0000**
	$q\left[\gamma_{Rd} E(\gamma_{sd} q_{demand})\right] \leq \frac{q_{u\tilde{m}}}{\gamma_O}$	25380	26450	0,9598
	$q\left[\gamma_{Rd} \gamma_{sd} E(q_{demand})\right] \leq \frac{q_{u\tilde{m}}}{\gamma_O}$	23230	26450	0,8785
	$q_{demand} \leq \frac{q_{u\tilde{m}}}{\gamma_{O'}}$	21690	24990	0,8682
PSF $\alpha_{cc} = 0,85$	$\gamma_{sd} q_{demand} \leq q_{ud}$	24950	25390	**0,9826**
	$q\left[\gamma_{sd} E(q_{demand})\right] \leq q_{ud}$	22300	25390	0,8784
GRF $\alpha_{cc} = 1$	$\gamma_{sd} q_{demand} \leq \frac{q_{u\tilde{m}}}{\gamma_O \gamma_{Rd}}$	24950	29100	**0,8572**
	$q\left[\gamma_{Rd} E(\gamma_{sd} q_{demand})\right] \leq \frac{q_{u\tilde{m}}}{\gamma_O}$	25500	30850	0,8264
	$q\left[\gamma_{Rd} \gamma_{sd} E(q_{demand})\right] \leq \frac{q_{u\tilde{m}}}{\gamma_O}$	23940	30850	0,7759
	$q_{demand} \leq \frac{q_{u\tilde{m}}}{\gamma_{O'}}$	21690	29150	0,7442
PSF $\alpha_{cc} = 1$	$\gamma_{sd} q_{demand} \leq q_{ud}$	24950	29670	**0,8409**
	$q\left[\gamma_{sd} E(q_{demand})\right] \leq q_{ud}$	22700	29670	0,7651
ECOV	$\gamma_{sd} q_{demand} \leq \frac{q_{um}}{\gamma_O \gamma_{Rd}}$	24950	32930	**0,7577**
	$q\left[\gamma_{Rd} E(\gamma_{sd} q_{demand})\right] \leq \frac{q_{um}}{\gamma_O}$	25990	34900	0,7446
	$q\left[\gamma_{Rd} \gamma_{sd} E(q_{demand})\right] \leq \frac{q_{um}}{\gamma_O}$	24920	34900	0,7141

TABLE 42 – χ factor for the different approaches for the column 10B1.

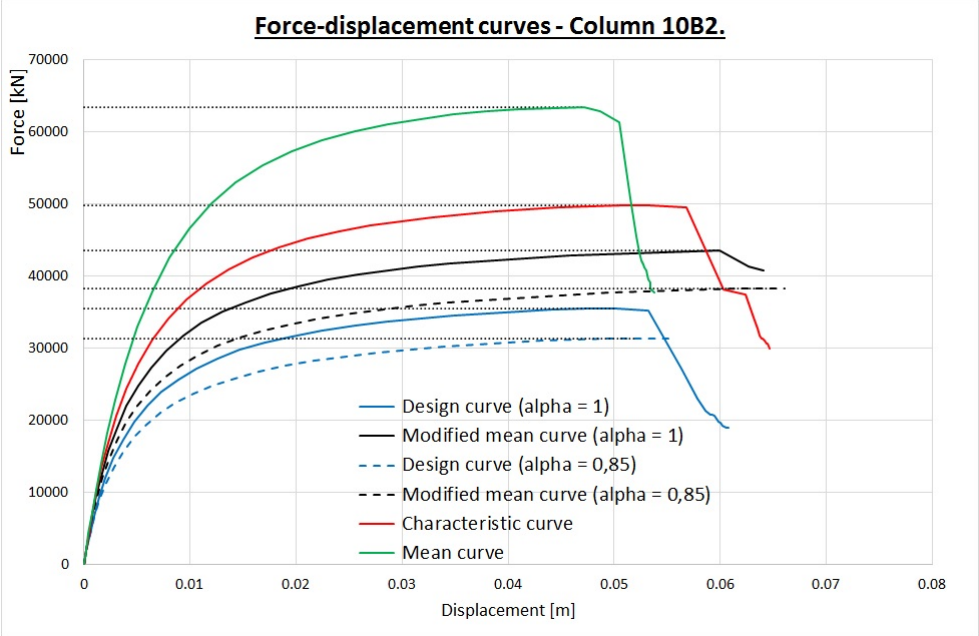

FIGURE 47 – Force-displacement curves for the columns 10B2.

Column 10B2				
Approach		LM	RM	χ
GRF $\underline{\alpha_{cc} = 0,85}$	$\gamma_{sd} q_{demand} \leq \frac{q_{u\tilde{m}}}{\gamma_O \gamma_{Rd}}$	30070	30070	**1,0000**
	$q\left[\gamma_{Rd} E(\gamma_{sd} q_{demand})\right] \leq \frac{q_{u\tilde{m}}}{\gamma_O}$	30580	31880	0,9594
	$q\left[\gamma_{Rd}\gamma_{sd} E(q_{demand})\right] \leq \frac{q_{u\tilde{m}}}{\gamma_O}$	27930	31880	0,8761
	$q_{demand} \leq \frac{q_{u\tilde{m}}}{\gamma_{O'}}$	26150	30120	0,8682
PSF $\underline{\alpha_{cc} = 0,85}$	$\gamma_{sd} q_{demand} \leq q_{ud}$	30070	31290	**0,9611**
	$q\left[\gamma_{sd} E(q_{demand})\right] \leq q_{ud}$	26970	31290	0,8620
GRF $\underline{\alpha_{cc} = 1}$	$\gamma_{sd} q_{demand} \leq \frac{q_{u\tilde{m}}}{\gamma_O \gamma_{Rd}}$	30070	34210	**0,8792**
	$q\left[\gamma_{Rd} E(\gamma_{sd} q_{demand})\right] \leq \frac{q_{u\tilde{m}}}{\gamma_O}$	30700	36260	0,8466
	$q\left[\gamma_{Rd}\gamma_{sd} E(q_{demand})\right] \leq \frac{q_{u\tilde{m}}}{\gamma_O}$	28720	36260	0,7921
	$q_{demand} \leq \frac{q_{u\tilde{m}}}{\gamma_{O'}}$	26150	34260	0,7633
PSF $\underline{\alpha_{cc} = 1}$	$\gamma_{sd} q_{demand} \leq q_{ud}$	30070	35520	**0,8467**
	$q\left[\gamma_{sd} E(q_{demand})\right] \leq q_{ud}$	27360	35520	0,7704
ECOV	$\gamma_{sd} q_{demand} \leq \frac{q_{um}}{\gamma_O \gamma_{Rd}}$	30070	38450	**0,7821**
	$q\left[\gamma_{Rd} E(\gamma_{sd} q_{demand})\right] \leq \frac{q_{um}}{\gamma_O}$	31240	40760	0,7664
	$q\left[\gamma_{Rd}\gamma_{sd} E(q_{demand})\right] \leq \frac{q_{um}}{\gamma_O}$	29890	40760	0,7334

TABLE 43 – χ factor for the different approaches for the column 10B2.

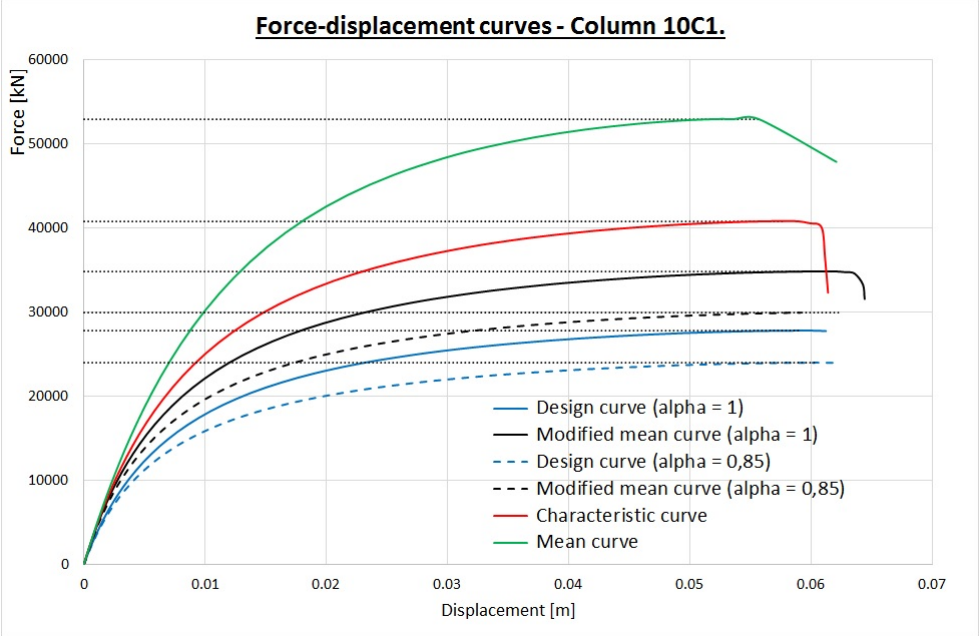

FIGURE 48 – Force-displacement curves for the columns 10C1.

Column 10C1				
Approach		LM	RM	χ
GRF $\underline{\alpha_{cc} = 0,85}$	$\gamma_{sd} q_{demand} \leq \frac{q_{u\tilde{m}}}{\gamma_O \gamma_{Rd}}$	23560	23560	**1,0000**
	$q\left[\gamma_{Rd} E(\gamma_{sd} q_{demand})\right] \leq \frac{q_{u\tilde{m}}}{\gamma_O}$	23960	24970	0,9596
	$q\left[\gamma_{Rd} \gamma_{sd} E(q_{demand})\right] \leq \frac{q_{u\tilde{m}}}{\gamma_O}$	22100	24970	0,8848
	$q_{demand} \leq \frac{q_{u\tilde{m}}}{\gamma_{O'}}$	20490	23600	0,8682
PSF $\underline{\alpha_{cc} = 0,85}$	$\gamma_{sd} q_{demand} \leq q_{ud}$	23560	23930	**0,9844**
	$q\left[\gamma_{sd} E(q_{demand})\right] \leq q_{ud}$	21170	23930	0,8845
GRF $\underline{\alpha_{cc} = 1}$	$\gamma_{sd} q_{demand} \leq \frac{q_{u\tilde{m}}}{\gamma_O \gamma_{Rd}}$	23560	27410	**0,8597**
	$q\left[\gamma_{Rd} E(\gamma_{sd} q_{demand})\right] \leq \frac{q_{u\tilde{m}}}{\gamma_O}$	24210	29050	0,8332
	$q\left[\gamma_{Rd} \gamma_{sd} E(q_{demand})\right] \leq \frac{q_{u\tilde{m}}}{\gamma_O}$	22530	29050	0,7756
	$q_{demand} \leq \frac{q_{u\tilde{m}}}{\gamma_{O'}}$	20490	27450	0,7463
PSF $\underline{\alpha_{cc} = 1}$	$\gamma_{sd} q_{demand} \leq q_{ud}$	23560	27810	**0,8471**
	$q\left[\gamma_{sd} E(q_{demand})\right] \leq q_{ud}$	21530	27810	0,7740
ECOV	$\gamma_{sd} q_{demand} \leq \frac{q_{um}}{\gamma_O \gamma_{Rd}}$	23560	30950	**0,7612**
	$q\left[\gamma_{Rd} E(\gamma_{sd} q_{demand})\right] \leq \frac{q_{um}}{\gamma_O}$	24530	32810	0,7476
	$q\left[\gamma_{Rd} \gamma_{sd} E(q_{demand})\right] \leq \frac{q_{um}}{\gamma_O}$	23640	32810	0,7207

TABLE 44 – χ factor for the different approaches for the column 10C1.

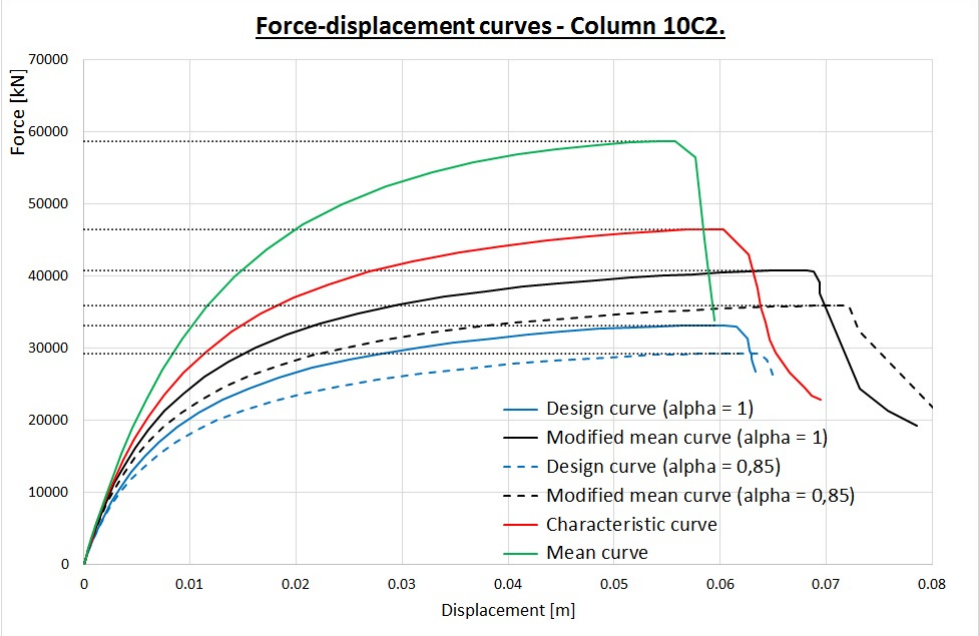

FIGURE 49 – Force-displacement curves for the columns 10C2.

Column 10C2				
Approach		LM	RM	χ
GRF $\underline{\alpha_{cc} = 0,85}$	$\gamma_{sd} q_{demand} \leq \frac{q_{u\tilde{m}}}{\gamma_O \gamma_{Rd}}$	28240	28240	**1,0000**
	$q\left[\gamma_{Rd} E(\gamma_{sd} q_{demand})\right] \leq \frac{q_{u\tilde{m}}}{\gamma_O}$	28750	29940	0,9604
	$q\left[\gamma_{Rd}\gamma_{sd} E(q_{demand})\right] \leq \frac{q_{u\tilde{m}}}{\gamma_O}$	26400	29940	0,8818
	$q_{demand} \leq \frac{q_{u\tilde{m}}}{\gamma_{O'}}$	24560	28290	0,8682
PSF $\underline{\alpha_{cc} = 0,85}$	$\gamma_{sd} q_{demand} \leq q_{ud}$	28240	29280	**0,9646**
	$q\left[\gamma_{sd} E(q_{demand})\right] \leq q_{ud}$	25460	29280	0,8698
GRF $\underline{\alpha_{cc} = 1}$	$\gamma_{sd} q_{demand} \leq \frac{q_{u\tilde{m}}}{\gamma_O \gamma_{Rd}}$	28240	32050	**0,8810**
	$q\left[\gamma_{Rd} E(\gamma_{sd} q_{demand})\right] \leq \frac{q_{u\tilde{m}}}{\gamma_O}$	28870	33980	0,8496
	$q\left[\gamma_{Rd}\gamma_{sd} E(q_{demand})\right] \leq \frac{q_{u\tilde{m}}}{\gamma_O}$	27130	33980	0,7986
	$q_{demand} \leq \frac{q_{u\tilde{m}}}{\gamma_{O'}}$	24560	32100	0,7649
PSF $\underline{\alpha_{cc} = 1}$	$\gamma_{sd} q_{demand} \leq q_{ud}$	28240	33170	**0,8515**
	$q\left[\gamma_{sd} E(q_{demand})\right] \leq q_{ud}$	25810	33170	0,7782
ECOV	$\gamma_{sd} q_{demand} \leq \frac{q_{um}}{\gamma_O \gamma_{Rd}}$	28240	36060	**0,7832**
	$q\left[\gamma_{Rd} E(\gamma_{sd} q_{demand})\right] \leq \frac{q_{um}}{\gamma_O}$	29350	38220	0,7678
	$q\left[\gamma_{Rd}\gamma_{sd} E(q_{demand})\right] \leq \frac{q_{um}}{\gamma_O}$	28210	38220	0,7380

TABLE 45 – χ factor for the different approaches for the column 10C2.

The figures 44, 45, 46, 47, 48 and 49 and the tables 40, 41, 42, 43, 44 and 45 illustrate and summarize the force-displacement curves (vertical force and horizontal displacement at the top of the column) and the results for the 10 meters columns subjected essentially to compression. As for the 5 meters columns, the 10 meters columns essentially subjected to normal forces present the same behaviour. Kind of ductility is present and is due to the second order effect of the high columns.

On the results for these configurations, the same order of magnitude is observed. For each approaches, the relation with the safety factor placed on the load presents the higher value of the coefficient χ. Again, the GRF approach seems to be the most restrictive approach followed closely by the PSF and finally the ECOV approach.

Here again, the difference between the GRF and the PSF approach is quite small independently of the eccentricities. Indeed, for the column with 0,2% of reinforcement steel, the difference is only of 1 to 2% and reaches 4 to 5% for the column with 1% of reinforcement.

The same remark as for the 5 meters columns can be done here concerning the influence of the α_{cc} value. There is a difference of about 13 to 15% between the approaches with $\alpha_{cc} = 0{,}85$ and 1.

Again, a major difference is present between the ECOV and the GRF approach. The difference is about 21 to 24%. It means that the ECOV approach allows the structure to carry more loads.

The figures 50, 51, 52 and 53 and the tables 46, 47, 48 and 49 illustrate and summarize the force-displacement curves (vertical force and horizontal displacement at the top of the column) and the results for the 10 meters columns subjected to normal forces and horizontal loads. The behaviour is quite different for each configurations. The column 10D1 and 10E1 present a good ductility, in contrast the column 10D2 do not. In the middle, the column 10E2 presents a small ductility before a brittle failure.

The relations with the safety factor on the loads present the less safety margin on the verification. The GRF is still the most restrictive approach, followed closely by the PSF and the ECOV especially with the increase of the horizontal loads.

The difference between the GRF and the PSF approach is constant and varies around 2 to 3%.

As for the 5 meters columns, the difference between the GRF and the PSF approaches regarding on the value of α_{cc} becomes less important with the increase of the horizontal loads. Also this increase of horizontal loads leads to a decrease of the gap between the GRF and the ECOV approach.

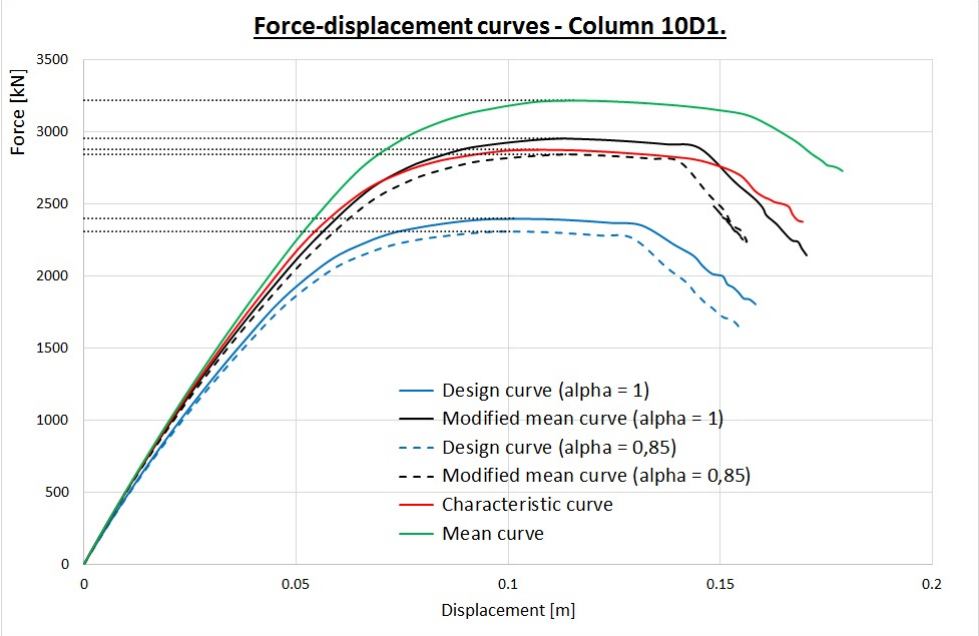

FIGURE 50 – Force-displacement curves for the columns 10D1.

Column 10D1				
Approach		LM	RM	χ
GRF $\underline{\alpha_{cc} = 0,85}$	$\gamma_{sd} q_{demand} \leq \frac{q_{u\tilde{m}}}{\gamma_O \gamma_{Rd}}$	2240	2240	**1,0000**
	$q\left[\gamma_{Rd} E(\gamma_{sd} q_{demand})\right] \leq \frac{q_{u\tilde{m}}}{\gamma_O}$	2330	2370	0,9802
	$q\left[\gamma_{Rd} \gamma_{sd} E(q_{demand})\right] \leq \frac{q_{u\tilde{m}}}{\gamma_O}$	2250	2370	0,9500
	$q_{demand} \leq \frac{q_{u\tilde{m}}}{\gamma_{O'}}$	1950	2240	0,8682
PSF $\underline{\alpha_{cc} = 0,85}$	$\gamma_{sd} q_{demand} \leq q_{ud}$	2240	2310	**0,9681**
	$q\left[\gamma_{sd} E(q_{demand})\right] \leq q_{ud}$	2100	2310	0,9065
GRF $\underline{\alpha_{cc} = 1}$	$\gamma_{sd} q_{demand} \leq \frac{q_{u\tilde{m}}}{\gamma_O \gamma_{Rd}}$	2240	2320	**0,9635**
	$q\left[\gamma_{Rd} E(\gamma_{sd} q_{demand})\right] \leq \frac{q_{u\tilde{m}}}{\gamma_O}$	2330	2460	0,9452
	$q\left[\gamma_{Rd} \gamma_{sd} E(q_{demand})\right] \leq \frac{q_{u\tilde{m}}}{\gamma_O}$	2280	2460	0,9266
	$q_{demand} \leq \frac{q_{u\tilde{m}}}{\gamma_{O'}}$	1950	2330	0,8365
PSF $\underline{\alpha_{cc} = 1}$	$\gamma_{sd} q_{demand} \leq q_{ud}$	2240	2400	**0,9335**
	$q\left[\gamma_{sd} E(q_{demand})\right] \leq q_{ud}$	2120	2400	0,8848
ECOV	$\gamma_{sd} q_{demand} \leq \frac{q_{um}}{\gamma_O \gamma_{Rd}}$	2240	2470	**0,9065**
	$q\left[\gamma_{Rd} E(\gamma_{sd} q_{demand})\right] \leq \frac{q_{um}}{\gamma_O}$	2350	2620	0,8989
	$q\left[\gamma_{Rd} \gamma_{sd} E(q_{demand})\right] \leq \frac{q_{um}}{\gamma_O}$	2300	2620	0,8788

TABLE 46 – χ factor for the different approaches for the column 10D1.

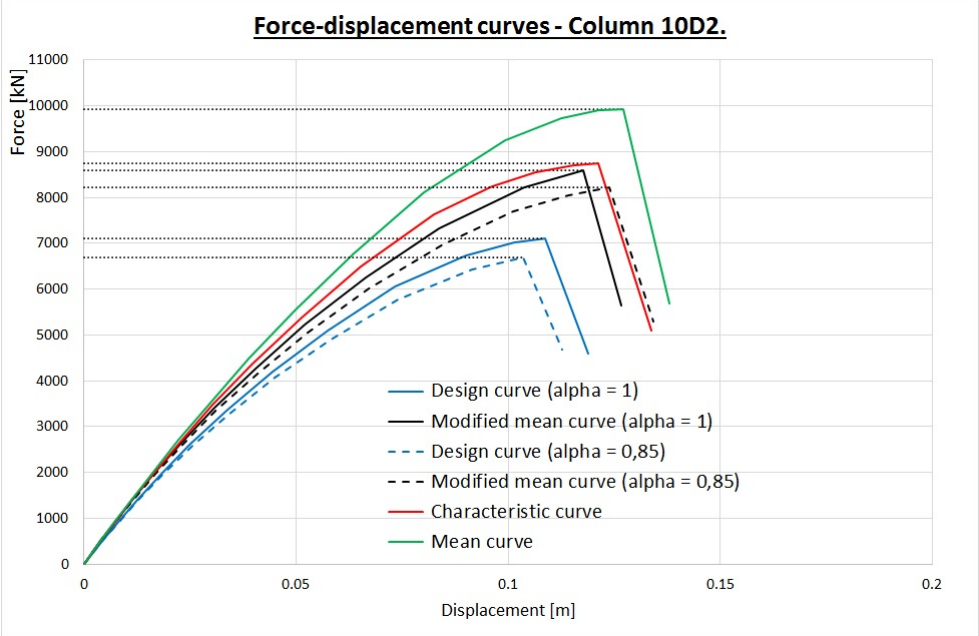

FIGURE 51 – Force-displacement curves for the columns 10D2.

Column 10D2				
Approach		LM	RM	χ
GRF $\underline{\alpha_{cc} = 0,85}$	$\gamma_{sd} q_{demand} \leq \frac{q_{u\tilde{m}}}{\gamma_O \gamma_{Rd}}$	6470	6470	**1,0000**
	$q\left[\gamma_{Rd} E(\gamma_{sd} q_{demand})\right] \leq \frac{q_{u\tilde{m}}}{\gamma_O}$	6720	6860	0,9804
	$q\left[\gamma_{Rd} \gamma_{sd} E(q_{demand})\right] \leq \frac{q_{u\tilde{m}}}{\gamma_O}$	6430	6860	0,9383
	$q_{demand} \leq \frac{q_{u\tilde{m}}}{\gamma_{O'}}$	5620	6480	0,8682
PSF $\underline{\alpha_{cc} = 0,85}$	$\gamma_{sd} q_{demand} \leq q_{ud}$	6470	6690	**0,9666**
	$q\left[\gamma_{sd} E(q_{demand})\right] \leq q_{ud}$	6080	6690	0,9082
GRF $\underline{\alpha_{cc} = 1}$	$\gamma_{sd} q_{demand} \leq \frac{q_{u\tilde{m}}}{\gamma_O \gamma_{Rd}}$	6470	6750	**0,9578**
	$q\left[\gamma_{Rd} E(\gamma_{sd} q_{demand})\right] \leq \frac{q_{u\tilde{m}}}{\gamma_O}$	6730	7160	0,9398
	$q\left[\gamma_{Rd} \gamma_{sd} E(q_{demand})\right] \leq \frac{q_{u\tilde{m}}}{\gamma_O}$	6490	7160	0,9070
	$q_{demand} \leq \frac{q_{u\tilde{m}}}{\gamma_{O'}}$	5620	6760	0,8316
PSF $\underline{\alpha_{cc} = 1}$	$\gamma_{sd} q_{demand} \leq q_{ud}$	6470	7110	**0,9102**
	$q\left[\gamma_{sd} E(q_{demand})\right] \leq q_{ud}$	6170	7110	0,8677
ECOV	$\gamma_{sd} q_{demand} \leq \frac{q_{um}}{\gamma_O \gamma_{Rd}}$	6470	7420	**0,8720**
	$q\left[\gamma_{Rd} E(\gamma_{sd} q_{demand})\right] \leq \frac{q_{um}}{\gamma_O}$	6790	7860	0,8638
	$q\left[\gamma_{Rd} \gamma_{sd} E(q_{demand})\right] \leq \frac{q_{um}}{\gamma_O}$	6620	7860	0,8420

TABLE 47 – χ factor for the different approaches for the column 10D2.

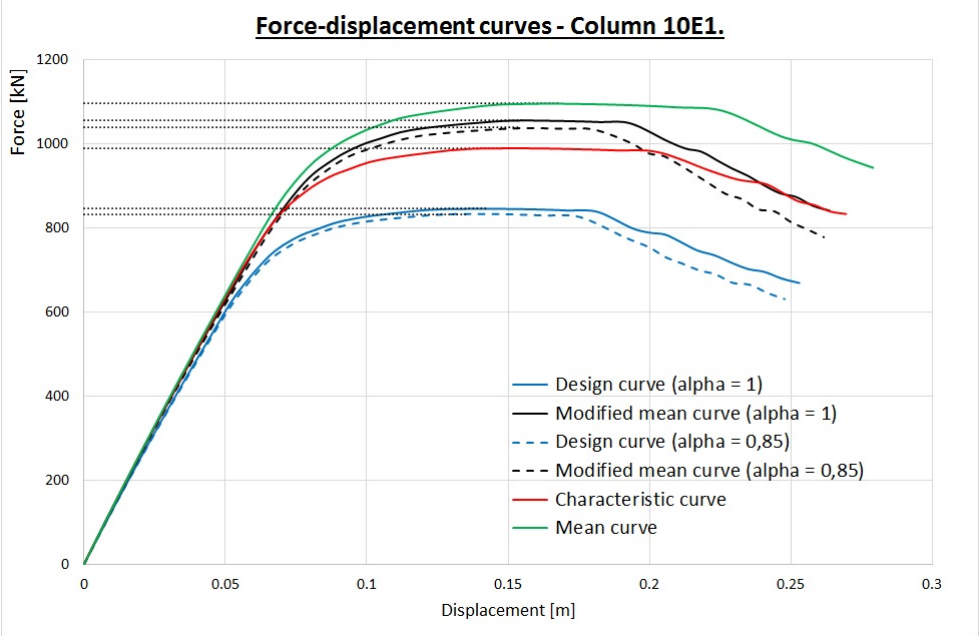

FIGURE 52 – Force-displacement curves for the columns 10E1.

Column 10E1				
Approach		LM	RM	χ
GRF $\underline{\alpha_{cc} = 0,85}$	$\gamma_{sd} q_{demand} \leq \frac{q_{u\tilde{m}}}{\gamma_O \gamma_{Rd}}$	817	817	**1,0000**
	$q\left[\gamma_{Rd} E(\gamma_{sd} q_{demand})\right] \leq \frac{q_{u\tilde{m}}}{\gamma_O}$	851	866	0,9830
	$q\left[\gamma_{Rd} \gamma_{sd} E(q_{demand})\right] \leq \frac{q_{u\tilde{m}}}{\gamma_O}$	837	866	0,9666
	$q_{demand} \leq \frac{q_{u\tilde{m}}}{\gamma_{O'}}$	710	818	0,8682
PSF $\underline{\alpha_{cc} = 0,85}$	$\gamma_{sd} q_{demand} \leq q_{ud}$	817	833	**0,9806**
	$q\left[\gamma_{sd} E(q_{demand})\right] \leq q_{ud}$	758	833	0,9098
GRF $\underline{\alpha_{cc} = 1}$	$\gamma_{sd} q_{demand} \leq \frac{q_{u\tilde{m}}}{\gamma_O \gamma_{Rd}}$	817	831	**0,9836**
	$q\left[\gamma_{Rd} E(\gamma_{sd} q_{demand})\right] \leq \frac{q_{u\tilde{m}}}{\gamma_O}$	853	880	0,9684
	$q\left[\gamma_{Rd} \gamma_{sd} E(q_{demand})\right] \leq \frac{q_{u\tilde{m}}}{\gamma_O}$	837	880	0,9513
	$q_{demand} \leq \frac{q_{u\tilde{m}}}{\gamma_{O'}}$	710	832	0,8540
PSF $\underline{\alpha_{cc} = 1}$	$\gamma_{sd} q_{demand} \leq q_{ud}$	817	846	**0,9655**
	$q\left[\gamma_{sd} E(q_{demand})\right] \leq q_{ud}$	763	846	0,9022
ECOV	$\gamma_{sd} q_{demand} \leq \frac{q_{um}}{\gamma_O \gamma_{Rd}}$	817	858	**0,9527**
	$q\left[\gamma_{Rd} E(\gamma_{sd} q_{demand})\right] \leq \frac{q_{um}}{\gamma_O}$	861	909	0,9471
	$q\left[\gamma_{Rd} \gamma_{sd} E(q_{demand})\right] \leq \frac{q_{um}}{\gamma_O}$	850	909	0,9347

TABLE 48 – χ factor for the different approaches for the column 10E1.

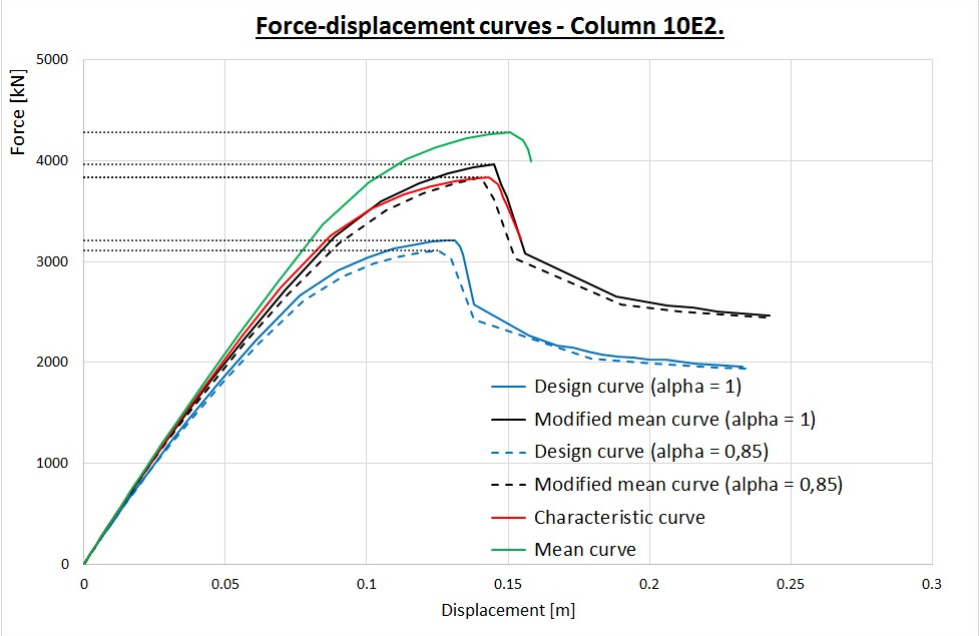

FIGURE 53 – Force-displacement curves for the columns 10E2.

Column 10E2				
Approach		LM	RM	χ
GRF $\alpha_{cc} = 0,85$	$\gamma_{sd} q_{demand} \leq \frac{q_{u\tilde{m}}}{\gamma_O \gamma_{Rd}}$	3010	3010	**1,0000**
	$q\left[\gamma_{Rd} E(\gamma_{sd} q_{demand})\right] \leq \frac{q_{u\tilde{m}}}{\gamma_O}$	3160	3200	0,9882
	$q\left[\gamma_{Rd} \gamma_{sd} E(q_{demand})\right] \leq \frac{q_{u\tilde{m}}}{\gamma_O}$	3060	3200	0,9589
	$q_{demand} \leq \frac{q_{u\tilde{m}}}{\gamma_{O'}}$	2620	3020	0,8682
PSF $\alpha_{cc} = 0,85$	$\gamma_{sd} q_{demand} \leq q_{ud}$	3010	3110	**0,9693**
	$q\left[\gamma_{sd} E(q_{demand})\right] \leq q_{ud}$	2820	3110	0,9079
GRF $\alpha_{cc} = 1$	$\gamma_{sd} q_{demand} \leq \frac{q_{u\tilde{m}}}{\gamma_O \gamma_{Rd}}$	3010	3120	**0,9660**
	$q\left[\gamma_{Rd} E(\gamma_{sd} q_{demand})\right] \leq \frac{q_{u\tilde{m}}}{\gamma_O}$	3160	3310	0,9558
	$q\left[\gamma_{Rd} \gamma_{sd} E(q_{demand})\right] \leq \frac{q_{u\tilde{m}}}{\gamma_O}$	3080	3310	0,9321
	$q_{demand} \leq \frac{q_{u\tilde{m}}}{\gamma_{O'}}$	2620	3130	0,8387
PSF $\alpha_{cc} = 1$	$\gamma_{sd} q_{demand} \leq q_{ud}$	3010	3210	**0,9383**
	$q\left[\gamma_{sd} E(q_{demand})\right] \leq q_{ud}$	2840	3210	0,8853
ECOV	$\gamma_{sd} q_{demand} \leq \frac{q_{um}}{\gamma_O \gamma_{Rd}}$	3010	3290	**0,9154**
	$q\left[\gamma_{Rd} E(\gamma_{sd} q_{demand})\right] \leq \frac{q_{um}}{\gamma_O}$	3170	3490	0,9092
	$q\left[\gamma_{Rd} \gamma_{sd} E(q_{demand})\right] \leq \frac{q_{um}}{\gamma_O}$	3130	3490	0,8961

TABLE 49 – χ factor for the different approaches for the column 10E2.

The reason of the different behaviour obtained in the analysis comes from the failure types and can be observed on the MN interaction plan. The figure 54 illustrates than MN plan for both types of section with all configurations performed with again both envelopes calculated manually and thanks to Cinelu.

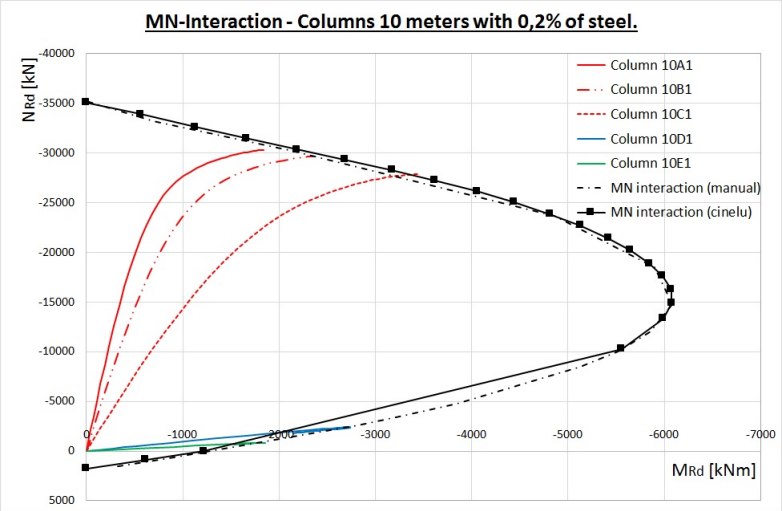

(a) Column with 0,2 % of steel reinforcement.

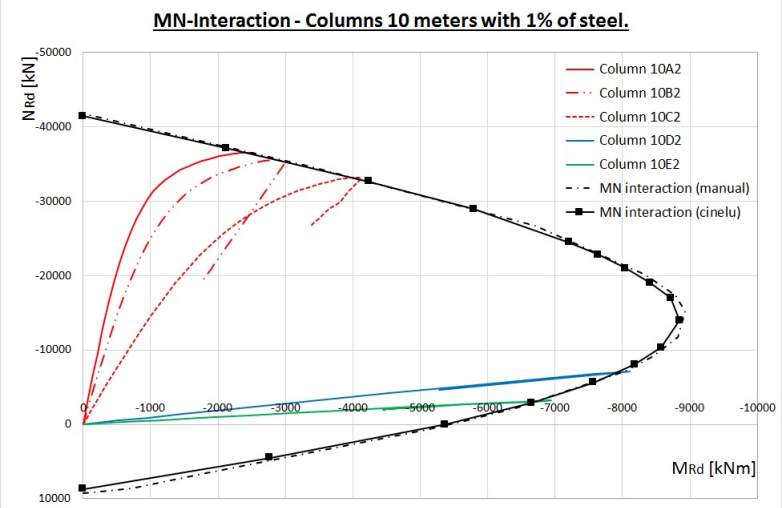

(b) Column with 1 % of steel reinforcement.

FIGURE 54 – Comparison of the MN interaction from Cinelu and manually with MN curves from tests on the 10 meters columns.

The difference of the behaviour comes again from the failure types and the zone that the structure reaches in figure 54. The configurations 10A, 10B and 10C as for the 5 meters columns fail by compression in the concrete. In contrast, the columns 10D and 10E fail by concrete failure ($\epsilon_c = 0{,}0035$). Depending on the zones reached in figure 54, some ductility are observed. The columns 10D1 and 10E1 closed to a simple bending state present high ductility. As the peak of moment is reached, the ductility disappears slowly. This explains why the column 10E2 presents a few ductility and the column 10D2 almost not.

7.4.3 Columns of 30 meters

The last step in the column section is the modelling of one slender column. Columns of 30 meters are then modelled. A slender column is investigated in order to obtain a failure by buckling and not a failure of the section obtained in the previous configurations. Two columns are investigated, one column with 0,2% of steel reinforcement and the second with 1%. Only one load configuration is studied, vertical load and the horizontal load for the initial imperfections with a basic inclination θ_0 of 1/200.

As said, we want to obtain a failure by buckling and no more of the section. The buckling load can be then calculated. Indeed, theoretically the buckling load for a column is simply :

$$P_{cr} = \frac{\pi^2 EI}{L_{fl}^2} \tag{39}$$

where EI corresponds to the total rigidity of the section where I accounts for the inertia of the section and E for the Young modulus. These parameters depends on the reference material chosen (steel or concrete). L_{fl} is the buckling length of the element. A cantilever column is here modelled, so L_{fl} is equal to 2 times the length of the element.

Two sections are studied here, so two inertias have to be obtained. For the design analysis, the young modulus of the concrete changes ($E_{cm}/1{,}2$) and the young modulus of the steel reinforcement stays constant. In final four rigidities are then necessary and obtained with the concrete as the reference material. The table 50 below summarizes the procedure and the results of the critical loads obtained :

/		$E_{cd} = E_{cm}/1{,}2$	E_{cm}
Section 1	E [kN/m^2]	$25{,}83 \times 10^6$	31×10^6
	I_y [m^4]	0,327	0,326
	P_{cr-1} [kN]	23160	27710
Section 2	E [kN/m^2]	$25{,}83 \times 10^6$	31×10^6
	I_y [m^4]	0,356	0,349
	P_{cr-2} [kN]	25210	29660

TABLE 50 – Critical load procedure and results.

The different load limits, the value of q_{demand} and γ_{Om} for the analysis proceeded are contained in the table 51. We clearly see an increase of the capacity for the section with more reinforcement. We also observe that the load capacity are quite lower than the buckling load calculated previously for each cases.

/	$\alpha_{cc} = 0{,}85$		$\alpha_{cc} = 1$		/			
q [kN]	q_{ud}	$q_{u\tilde{m}}$	q_{ud}	$q_{u\tilde{m}}$	q_{uk}	q_{um}	q_{demand}	γ_{Om}
$\rho_s = 0{,}2\%$	11300	13900	12430	15250	16740	19090	9500	1,274
$\rho_s = 1\%$	12890	15470	14050	16870	18380	20800	10580	1,256

TABLE 51 – Ultimate load limits, q_{demand} and γ_{Om} for the 30 meters columns configurations.

The table 52 contains the ratio between the load limit obtained in the table 51 and the critical load calculated previously. We observed on that table that the ratio varies from 0,4 to 0,7. The difference between these loads comes from the theory behind the buckling load which is an elastic critical load. So the cracking, the plasticity are not included in that load. In the definition of the load, the length and the Young modulus are constant all along the non linear loading. In contrast, the inertia of the section changes. Indeed, the cracks induced by a rotation of the section decrease the inertia of the section during the loading of the structure. So an other view to the ratio calculated on the table 52 can be the percentage of the remaining inertia of the section at the failure.

/	$\alpha_{cc} = 0{,}85$		$\alpha_{cc} = 1$		/	
/	q_{ud}/P_{cr-i}	$q_{u\tilde{m}}/P_{cr-i}$	q_{ud}/P_{cr-i}	$q_{u\tilde{m}}/P_{cr-i}$	q_{uk}/P_{cr-i}	q_{um}/P_{cr-i}
$\rho_s = 0{,}2\%$	0,488	0,502	0,537	0,550	0,604	0,689
$\rho_s = 1\%$	0,511	0,522	0,557	0,569	0,620	0,701

TABLE 52 – Ratio between the load limit obtained numerically and the critical load P_{cr}.

The figures 55 and 56 and the tables 53 and 54 illustrate and contain the forces-displacement curves (vertical force and horizontal displacement at the top of the column) and the results of the 30 meters columns tests for both reinforcement ratio.

Concerning the results, more or less the same remarks as for previous columns (5 and 10 meters) can be done here. The safety coefficients have to be placed on the load to obtain the most restrictive verification. 3 to 5% of difference exists between the GRF and the PSF approach. Around 9% of difference separates the results from the GRF and the PSF regarding of the value of α_{cc}. Finally, the ECOV approach have about 22% of additional margin compared to the GRF approach.

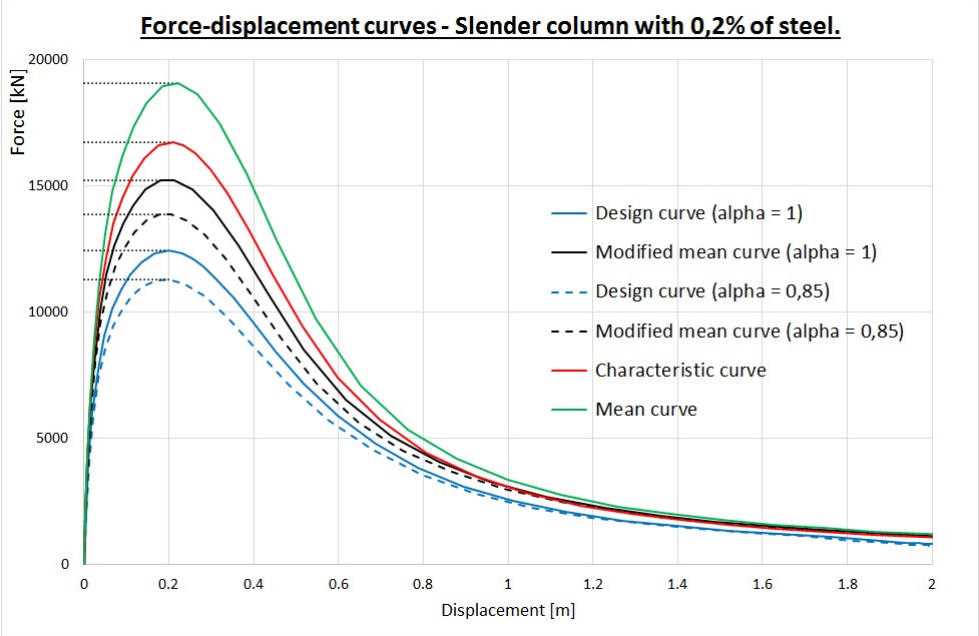

FIGURE 55 – Force-displacement curves for the 30 meters column investigated ($\rho_s = 0,2\%$).

Column of 30 meters - $\rho_s = 0,2\%$				
Approach		LM	RM	χ
GRF $\underline{\alpha_{cc} = 0,85}$	$\gamma_{sd} q_{demand} \leq \frac{q_{u\tilde{m}}}{\gamma_O \gamma_{Rd}}$	10920	10920	**1,0000**
	$q\left[\gamma_{Rd} E(\gamma_{sd} q_{demand})\right] \leq \frac{q_{u\tilde{m}}}{\gamma_O}$	11110	11580	0,9591
	$q\left[\gamma_{Rd}\gamma_{sd} E(q_{demand})\right] \leq \frac{q_{u\tilde{m}}}{\gamma_O}$	10190	11580	0,8797
	$q_{demand} \leq \frac{q_{u\tilde{m}}}{\gamma_{O'}}$	9500	10940	0,8682
PSF $\underline{\alpha_{cc} = 0,85}$	$\gamma_{sd} q_{demand} \leq q_{ud}$	10920	11300	**0,9667**
	$q\left[\gamma_{sd} E(q_{demand})\right] \leq q_{ud}$	9830	11300	0,8700
GRF $\underline{\alpha_{cc} = 1}$	$\gamma_{sd} q_{demand} \leq \frac{q_{u\tilde{m}}}{\gamma_O \gamma_{Rd}}$	10920	11990	**0,9114**
	$q\left[\gamma_{Rd} E(\gamma_{sd} q_{demand})\right] \leq \frac{q_{u\tilde{m}}}{\gamma_O}$	11190	12710	0,8806
	$q\left[\gamma_{Rd}\gamma_{sd} E(q_{demand})\right] \leq \frac{q_{u\tilde{m}}}{\gamma_O}$	10380	12710	0,8169
	$q_{demand} \leq \frac{q_{u\tilde{m}}}{\gamma_{O'}}$	9500	12010	0,7913
PSF $\underline{\alpha_{cc} = 1}$	$\gamma_{sd} q_{demand} \leq q_{ud}$	10920	12440	**0,8785**
	$q\left[\gamma_{sd} E(q_{demand})\right] \leq q_{ud}$	9960	12440	0,8014
ECOV	$\gamma_{sd} q_{demand} \leq \frac{q_{um}}{\gamma_O \gamma_{Rd}}$	10920	14130	**0,7729**
	$q\left[\gamma_{Rd} E(\gamma_{sd} q_{demand})\right] \leq \frac{q_{um}}{\gamma_O}$	11320	14980	0,7555
	$q\left[\gamma_{Rd}\gamma_{sd} E(q_{demand})\right] \leq \frac{q_{um}}{\gamma_O}$	10630	14980	0,7093

TABLE 53 – χ factor for the different approaches for the 30 meters column analysis ($\rho_s = 0,2\%$).

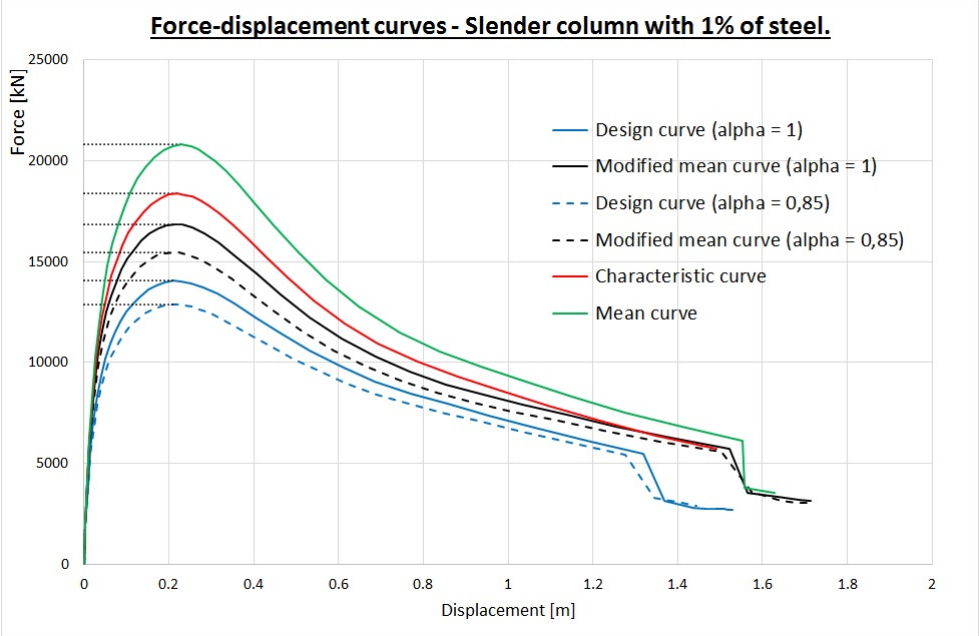

FIGURE 56 – Force-displacement curves for the 30 meters column investigated ($\rho_s = 1\%$).

Column of 30 meters - $\rho_s = 1\%$				
Approach		LM	RM	χ
GRF $\underline{\alpha_{cc} = 0,85}$	$\gamma_{sd} q_{demand} \leq \frac{q_{u\tilde{m}}}{\gamma_O \gamma_{Rd}}$	12160	12160	**1,0000**
	$q\left[\gamma_{Rd} E(\gamma_{sd} q_{demand})\right] \leq \frac{q_{u\tilde{m}}}{\gamma_O}$	12410	12890	0,9623
	$q\left[\gamma_{Rd} \gamma_{sd} E(q_{demand})\right] \leq \frac{q_{u\tilde{m}}}{\gamma_O}$	11400	12890	0,8838
	$q_{demand} \leq \frac{q_{u\tilde{m}}}{\gamma_{O'}}$	10580	12180	0,8682
PSF $\underline{\alpha_{cc} = 0,85}$	$\gamma_{sd} q_{demand} \leq q_{ud}$	12160	12890	**0,9440**
	$q\left[\gamma_{sd} E(q_{demand})\right] \leq q_{ud}$	10980	12890	0,8524
GRF $\underline{\alpha_{cc} = 1}$	$\gamma_{sd} q_{demand} \leq \frac{q_{u\tilde{m}}}{\gamma_O \gamma_{Rd}}$	12160	13260	**0,9170**
	$q\left[\gamma_{Rd} E(\gamma_{sd} q_{demand})\right] \leq \frac{q_{u\tilde{m}}}{\gamma_O}$	12450	14060	0,8852
	$q\left[\gamma_{Rd} \gamma_{sd} E(q_{demand})\right] \leq \frac{q_{u\tilde{m}}}{\gamma_O}$	11540	14060	0,8205
	$q_{demand} \leq \frac{q_{u\tilde{m}}}{\gamma_{O'}}$	10580	13290	0,7961
PSF $\underline{\alpha_{cc} = 1}$	$\gamma_{sd} q_{demand} \leq q_{ud}$	12160	14050	**0,8660**
	$q\left[\gamma_{sd} E(q_{demand})\right] \leq q_{ud}$	11080	14050	0,7889
ECOV	$\gamma_{sd} q_{demand} \leq \frac{q_{um}}{\gamma_O \gamma_{Rd}}$	12160	15620	**0,7788**
	$q\left[\gamma_{Rd} E(\gamma_{sd} q_{demand})\right] \leq \frac{q_{um}}{\gamma_O}$	12500	16560	0,7551
	$q\left[\gamma_{Rd} \gamma_{sd} E(q_{demand})\right] \leq \frac{q_{um}}{\gamma_O}$	11850	16560	0,7157

TABLE 54 – χ factor for the different approaches for the 30 meters column analysis ($\rho_s = 1\%$).

The figure 57 (a) and (b) illustrates the MN interaction envelope and the MN path for both section respectively.

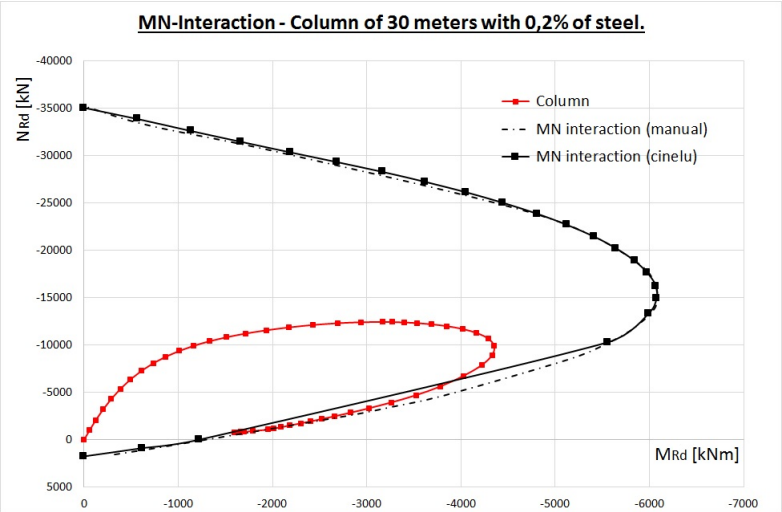

(a) Column with 0,2 % of steel reinforcement.

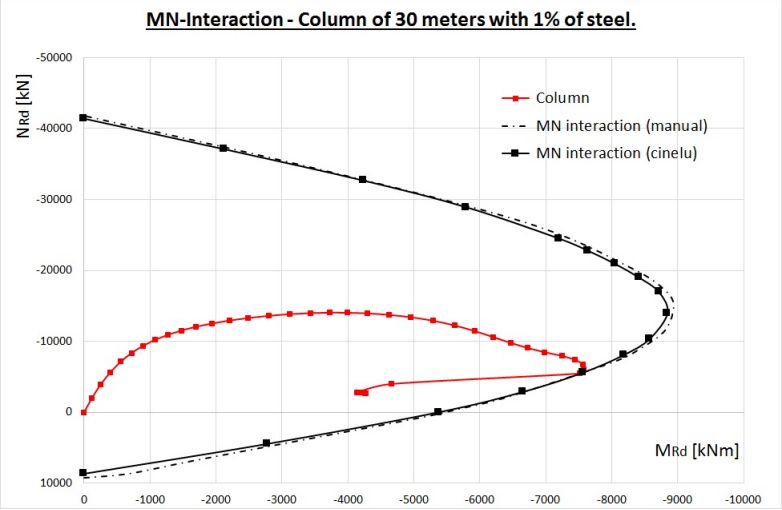

(b) Column with 1 % of steel reinforcement.

FIGURE 57 – Comparison of the MN interaction from Cinelu and manually with MN curves from tests on the 30 meters columns.

We observe again the importance of the part neglected by the program Cinelu for moderate normal force (section with 0,2% of steel). We also clearly see the high importance of the second order effect. This importance is marked by the fact that the bending moment increases much higher than the normal forces. The load limit is reached before the failure of the section that happen when the curve reaches the MN envelope.

7.4.4 Discussion of the results and comparison

In the introduction of the column models, a brief part concerning the slenderness factor is mentioned. In that part, we said that for the column of 5 meters, after 1/5 of the normal force capacity of the section, the second order effect has to be calculated. For the 10 meters columns, this is 4,6 % of the normal force capacity which is barely nothing and appears directly. We can compare these facts with the MN path obtained in figure 42 and 54. On these figures, we clearly observe non linearity for the column subjected essentially to normal forces for which the second order effect matters. In contrast, for the columns subjected to horizontal loads, this effect seems to be less important. This explains why the initial inclination does not vary for these columns with high bending moment.

For this kind of structure (column), the safety factor should be applied on the load and not on the displacement. Indeed, this leads to a more restrictive verification because the structure's behaviour is overproportional (as seen in figure 4).

Again a good correlation between the GRF and the PSF approaches is seen for the different columns modelled. The higher difference accounts for 5 %.

When the structure is more subjected to moment than normal forces, the influence of the α_{cc} value is barely visible. Indeed, this fact can be seen on the results obtained for the previous model or also in figure 43.

We observe also that the height does not give a clear difference between the relation or the approach. Indeed, the same conclusion can be made for each case. However, on the structure behaviour, we clearly observe a increase of the second order effect with the high.

No major difference in the relations or in the approaches are noticed between the column of 10 m and 30 meters for which the failure differ. The 10 meters column fails in the section where the 30 meters column by buckling and then in the section.

Finally, as said separately for the different columns height, we observe a tendency of decrease of the difference between the different approaches when the bending moment increases in the structure. This is explained amongst other by the higher importance of the steel in the failure of the structure. With the same idea, the gain of the ECOV approach decreases with the increase of the bending moment. Indeed, when normal forces are the main internal forces in the structure, the gain can reach 20 - 25 % and 10 % compared to the GRF approach with $\alpha_{cc} = 0{,}85$ and 1 respectively. In contrast, when bending moments are introduced in the structure, this gain drops to 5 - 10 % and 3 - 5 % compared to the GRF approach with $\alpha_{cc} = 0{,}85$ and 1 respectively.

To conclude, the importance of the approach is higher when the normal forces is high. In that case, using the ECOV approach seems to be the more clever way to design the structure. However, a remark and an attention has to be done on the fact that the ECOV approach does not include the α_{cc} value into the analysis. So when α_{cc} is not equal to 1, a criticism of this approach has to be done. Then concerning the structure more subjected to bending moments, the choice of the approach has no more an huge importance. So using a simple approach like the PSF is according to me the right choice because no further computation on the resistance are necessary and the verification is less restrictive than the GRF approach.

7.5 Frame models

The next model consists of one 2D reinforced concrete frame for what the complexity of the structure increases a bit. A more or less usual type of frame is modelled with quite common section dimensions for a normal building.

First, the global geometry of the frame is presented, then the results for a beam and a column failure are given. Finally a brief discussion and comparison of the results are done.

7.5.1 Geometry

The first important step is to define the geometry of the frame used for the test. A 2D frame is here investigated with the assumption of an effective bracing in the other direction that stabilises the frame in that direction. In the 2D frame modelled here, the horizontal load are carried by the frame itself (no bracing in his plan). An illustration of that frame is presented in figure 58.

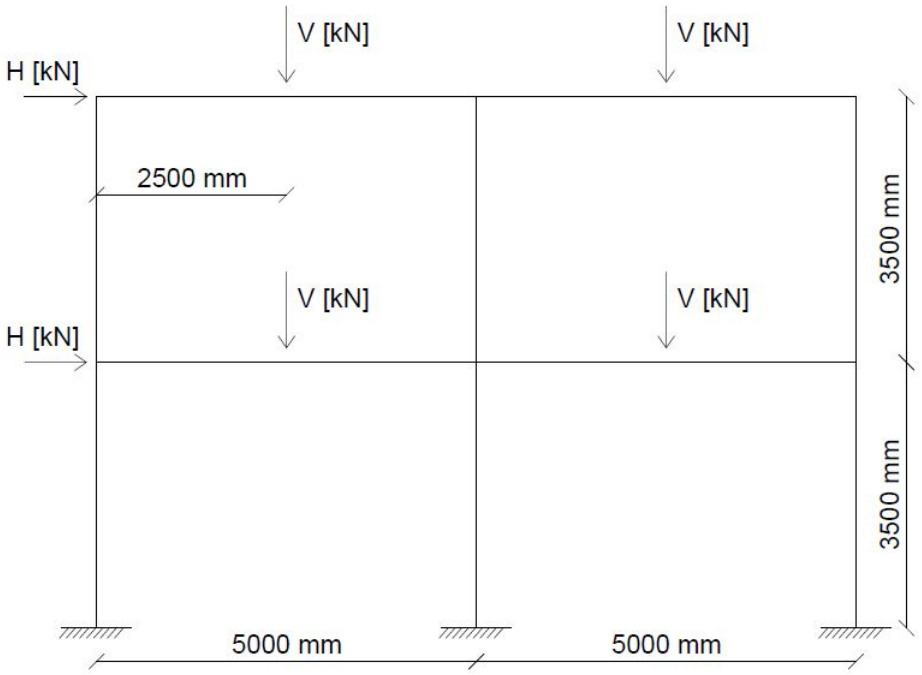

FIGURE 58 – Illustration of the frame structure model investigated.

The frame is composed of two stages and two bays. The high of one stage is equal to 3,5 meters and the columns are placed each 5 meters. The value of the vertical and horizontal loads (V and H) are variables in order to obtain different types of failure. Additional to these loads, the dead load of each elements is taken into account. The geometrical imperfections are here not taken into account for simplicity. The figure 59 shows the section properties for the columns and the beams of the frame structure. Beams of 250x400 mm of section are used with 8 reinforcement bars of 16 mm of diameter. For the columns, section of 250x250 mm is used with 4 bars of 16 mm of diameter.

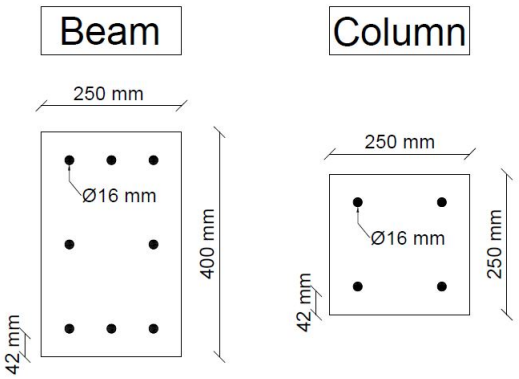

FIGURE 59 – Illustration of the section properties for the beams and columns of the frame structure model.

The value of the loads determines the failure obtained in the analysis. The table 55 summarizes the combination of the vertical and the horizontal loads used. In order to obtain a failure of the column first, the horizontal loads have to be higher. The same idea is done for the beam failure but with an higher value for the vertical loads at the midspan of the beam.

/	V [kN]	H [kN]
Beam failure	1	0,5
Column failure	0,5	1

TABLE 55 – Summary of the vertical and horizontal loads used for both failure types.

7.5.2 Beam failure

The first type of frame modelled presents a failure first in the beam. The table 56 contains the load limits for the different analysis and γ_{Om} for the ECOV approach. The load limits represent here the vertical force V on the frame.

$\alpha_{cc} = 0{,}85$		$\alpha_{cc} = 1$		/		
q_{ud} [kN]	$q_{u\tilde{m}}$[kN]	q_{ud} [kN]	$q_{u\tilde{m}}$ [kN]	q_{uk} [kN]	q_{um} [kN]	γ_{Om}
53,3	62,3	57,8	66,3	68,8	80,2	1,326

TABLE 56 – Ultimate load limits for the frame model - Beam failure.

The figure 60 and the table 57 illustrates and summarizes the results of the several analysis made. The displacement corresponds here to the horizontal displacement of the top floor. The behaviour of the structure is almost elastic until the failure. The failure appears first in the top beam at the mid support. Cause of the hyperstaticity of the frame, the convergence of the numerical model is a big issue and the discretisation of the element has to be refined at the connections zones.

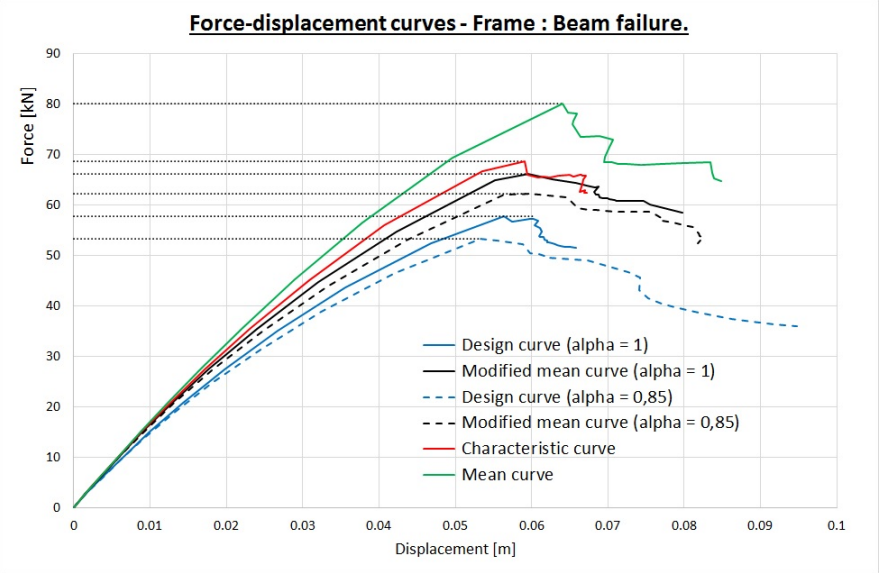

FIGURE 60 – Force-displacement curves for the frame - Beam failure.

Frame - Beam failure				
Approach		LM	RM	χ
GRF $\underline{\alpha_{cc} = 0,85}$	$\gamma_{sd} q_{demand} \leq \frac{q_{u\tilde{m}}}{\gamma_O \gamma_{Rd}}$	49,0	49,0	**1,0000**
	$q\left[\gamma_{Rd} E(\gamma_{sd} q_{demand})\right] \leq \frac{q_{u\tilde{m}}}{\gamma_O}$	51,0	51,9	0,9832
	$q\left[\gamma_{Rd} \gamma_{sd} E(q_{demand})\right] \leq \frac{q_{u\tilde{m}}}{\gamma_O}$	49,0	51,9	0,9433
	$q_{demand} \leq \frac{q_{u\tilde{m}}}{\gamma_{O'}}$	42,6	49,0	0,8682
PSF $\underline{\alpha_{cc} = 0,85}$	$\gamma_{sd} q_{demand} \leq q_{ud}$	49,0	53,3	**0,9190**
	$q\left[\gamma_{sd} E(q_{demand})\right] \leq q_{ud}$	46,8	53,3	0,8784
GRF $\underline{\alpha_{cc} = 1}$	$\gamma_{sd} q_{demand} \leq \frac{q_{u\tilde{m}}}{\gamma_O \gamma_{Rd}}$	49,0	52,1	**0,9396**
	$q\left[\gamma_{Rd} E(\gamma_{sd} q_{demand})\right] \leq \frac{q_{u\tilde{m}}}{\gamma_O}$	51,1	55,2	0,9255
	$q\left[\gamma_{Rd} \gamma_{sd} E(q_{demand})\right] \leq \frac{q_{u\tilde{m}}}{\gamma_O}$	49,4	55,2	0,8941
	$q_{demand} \leq \frac{q_{u\tilde{m}}}{\gamma_{O'}}$	42,6	52,2	0,8158
PSF $\underline{\alpha_{cc} = 1}$	$\gamma_{sd} q_{demand} \leq q_{ud}$	49,0	57,8	**0,8474**
	$q\left[\gamma_{sd} E(q_{demand})\right] \leq q_{ud}$	46,8	57,8	0,8107
ECOV	$\gamma_{sd} q_{demand} \leq \frac{q_{um}}{\gamma_O \gamma_{Rd}}$	49,0	57,0	**0,8589**
	$q\left[\gamma_{Rd} E(\gamma_{sd} q_{demand})\right] \leq \frac{q_{um}}{\gamma_O}$	51,4	60,4	0,8508
	$q\left[\gamma_{Rd} \gamma_{sd} E(q_{demand})\right] \leq \frac{q_{um}}{\gamma_O}$	50,4	60,4	0,8339

TABLE 57 – χ factor for the different approaches for the frame model with failure on the beam.

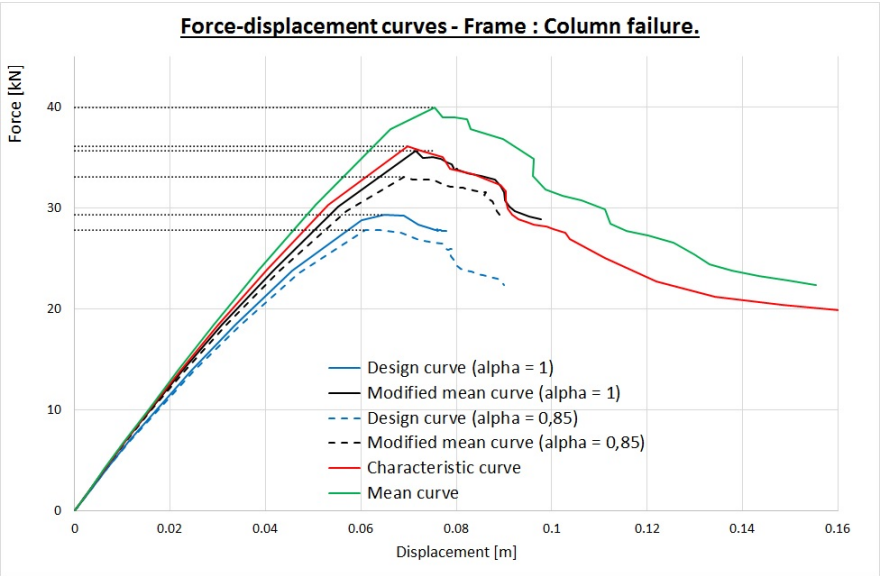

FIGURE 61 – Force-displacement curves for the frame - Column failure.

Frame - Column failure				
Approach		LM	RM	χ
GRF $\alpha_{cc} = 0,85$	$\gamma_{sd} q_{demand} \leq \frac{q_{u\tilde{m}}}{\gamma_O \gamma_{Rd}}$	26,0	26,0	**1,0000**
	$q\left[\gamma_{Rd} E(\gamma_{sd} q_{demand})\right] \leq \frac{q_{u\tilde{m}}}{\gamma_O}$	27,3	27,6	0,9883
	$q\left[\gamma_{Rd} \gamma_{sd} E(q_{demand})\right] \leq \frac{q_{u\tilde{m}}}{\gamma_O}$	26,6	27,6	0,9621
	$q_{demand} \leq \frac{q_{u\tilde{m}}}{\gamma_{O'}}$	22,6	26,1	0,8682
PSF $\alpha_{cc} = 0,85$	$\gamma_{sd} q_{demand} \leq q_{ud}$	26,0	27,9	**0,9344**
	$q\left[\gamma_{sd} E(q_{demand})\right] \leq q_{ud}$	24,2	27,9	0,8676
GRF $\alpha_{cc} = 1$	$\gamma_{sd} q_{demand} \leq \frac{q_{u\tilde{m}}}{\gamma_O \gamma_{Rd}}$	26,0	28,1	**0,9281**
	$q\left[\gamma_{Rd} E(\gamma_{sd} q_{demand})\right] \leq \frac{q_{u\tilde{m}}}{\gamma_O}$	27,3	29,7	0,9186
	$q\left[\gamma_{Rd} \gamma_{sd} E(q_{demand})\right] \leq \frac{q_{u\tilde{m}}}{\gamma_O}$	26,7	29,7	0,8982
	$q_{demand} \leq \frac{q_{u\tilde{m}}}{\gamma_{O'}}$	22,6	28,1	0,8057
PSF $\alpha_{cc} = 1$	$\gamma_{sd} q_{demand} \leq q_{ud}$	26,0	29,3	**0,8880**
	$q\left[\gamma_{sd} E(q_{demand})\right] \leq q_{ud}$	25,1	29,3	0,8572
ECOV	$\gamma_{sd} q_{demand} \leq \frac{q_{um}}{\gamma_O \gamma_{Rd}}$	26,0	31,3	**0,8316**
	$q\left[\gamma_{Rd} E(\gamma_{sd} q_{demand})\right] \leq \frac{q_{um}}{\gamma_O}$	27,4	33,2	0,8267
	$q\left[\gamma_{Rd} \gamma_{sd} E(q_{demand})\right] \leq \frac{q_{um}}{\gamma_O}$	27,1	33,2	0,8162

TABLE 58 – χ factor for the different approaches for the frame model with failure on the column.

7.5.3 Column failure

The second type of frame modelled presents a failure first in the column. The table 59 contains the load limit for the different analysis and γ_{Om} for the ECOV approach. The load limits represent here the horizontal force H on the frame.

$\alpha_{cc} = 0{,}85$		$\alpha_{cc} = 1$		/		
q_{ud} [kN]	$q_{u\tilde{m}}$[kN]	q_{ud} [kN]	$q_{u\tilde{m}}$ [kN]	q_{uk} [kN]	q_{um} [kN]	γ_{Om}
27,9	33,1	29,3	35,7	36,1	39,9	1,204

TABLE 59 – Ultimate load limits for the frame model - Column failure.

The figure 61 and the table 58 illustrates and summarizes the results of the several analysis made. The displacement corresponds here again to the horizontal displacement of the top floor. The behaviour of the structure is here again almost elastic until the failure. The failure appears first in the middle column.

7.5.4 Discussion of the results and comparison

First of all, an attention on the convergence issue of the non linear analysis is made. Indeed, the structure is hyperstatic and contains a lot of integration point in one section (almost 500 points).

The results obtained on the table 57 and 58 are here discussed and analysed. Still in the frame model, the more restrictive approach seems to be the GRF and again when the safety factor are placed on the load. Then the PSF and the ECOV follow with 6-8 % and 14-16 % of extra margin respectively. The GRF and PSF approaches are no more well correlated in this case (6-8 % of difference). As previously, there is a difference for the GRF and PSF approaches with the value of α_{cc} (around 6-7 %).

The choice of the approach seems here complicated. Indeed, the less restrictive approach is the ECOV approach but this approach requires two non linear analysis and the convergence for more complicated structure can be an issue. The right choice according to me is the PSF approach that is simple to implement, less restrictive than the GRF approach and without any further computation on the resistance load.

7.6 Beam models with catenary effect

An other types of structure is modelled in order to obtain a different behaviour. Indeed, all previous structures present an overproportional behaviour, and the case of an underproportional behaviour has not been yet investigated. This type of behaviour can be obtained when the catenary effect plays a role. This caterany effect is activated when for example a column is removed accidentally or intentionally in a frame structure. Tension in the beam elements are then introduced and activate that catenary effect for then transmitting the load to the neighboured frames or elements.

This principle is here investigated with a simplified structure. Indeed, one simple supported beam with a force at mid-span is modelled. The support condition are similar in both side. Indeed, in order to be able to activate the tension in the beam, the lateral displacement has to be blocked. The section's dimensions of the beam is the same as for the frame structure. An illustration of the model and the different reinforced section is presented in figure 62.

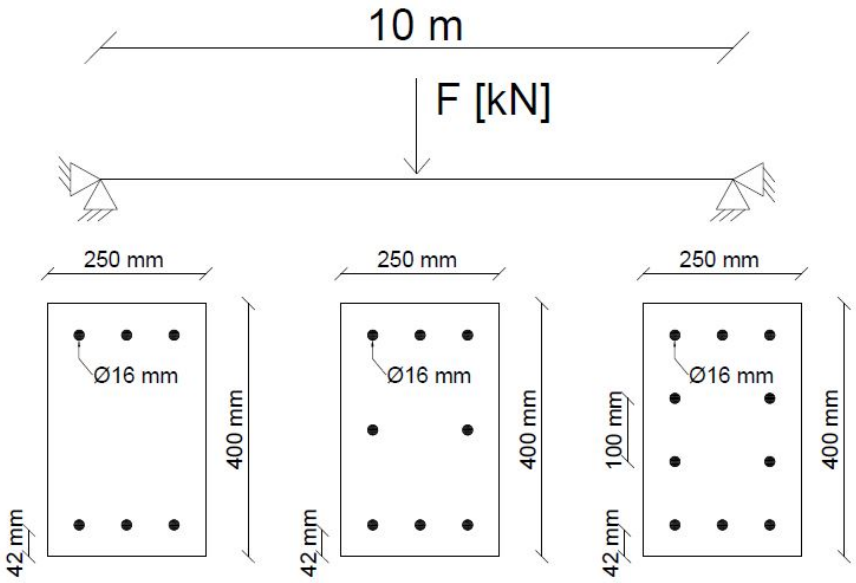

FIGURE 62 – Illustration of the model studied with the different case investigated.

The force-displacement curve studied for this case corresponds to the vertical force and the vertical displacement at mid-span. The failure of the structure is imposed by a fixed displacement. Otherwise the failure would be controlled by the ability of the software to reach the ultimate strain of the steel in a certain iteration step. Moreover, the mid-span can reach a vertical displacement above 0,4 meter which represents a ratio of L/25. This displacement capacity is higher to the natural design of beams that corresponds to L/200 or even L/300 that corresponds to the serviceability limit states. In contrast, the ratio L/25 can be related to a case of extreme failure. Indeed, the design of common element is not made thanks to this benefit, but when the concept of robustness is addressed, the catenary effect can help. The displacement limit is taken as 0,4 meter in order to fix a failure characteristic with only this catenary effect acting.

Three types of beams with different reinforcement amount are modelled (1,2%, 1,6% and 2%). In fact, that is the reinforcement that provides the increasing of the capacity of the beam and also the concave curve shape. The next sections treat separately each type of beams modelled. An additional point for the beam with 1,6 % of reinforcement is done with a change of the failure criteria. The last section discusses the results and compare the three types of beams investigated here.

7.6.1 Beam with ρ_s = 1,2 %

The first beam investigated is with 1,2 % of reinforcement ratio (this corresponds to 6 bars of 16 mm of diameter). The table 60 contains the load limits for the case with 1,2 % and the global resistance factor γ_{Om}.

α_{cc} = 0,85		α_{cc} = 1		/		
q_{ud} [kN]	$q_{u\tilde{m}}$[kN]	q_{ud} [kN]	$q_{u\tilde{m}}$ [kN]	q_{uk} [kN]	q_{um} [kN]	γ_{Om}
65,2	78,1	65,3	78,1	72,4	78,2	1,154

TABLE 60 – Ultimate load limits for the catenary test analysis (ρ_s = 1,2%).

We observe that the value of α_{cc} has no influence on the load limit. Moreover because at the imposed failure, only the reinforcement governs, the mean and the modified mean analysis give similar load limit. We see this observation on the figure 63 that illustrates the different analysis. The table 62 shows the results for the different approaches. The value of q_{demand} equals 53,4 kN and is obtained as previously by imposing the first relation of the GRF approach to 1.

7.6.2 Beam with ρ_s = 1,6 %

The second beam modelled presents 1,6 % of reinforcement which corresponds to 8 bars of 16 mm of diameter. For this type of beam two verifications are done with a change in the failure criteria. Indeed, the position of the criteria guides the results and the tendency of the relations. For example, the first part of the behaviour shows a failure by flexure studied in the previous model. With the failure criteria at 0,4 meter, the first part does not directly influence the results obtained. That's why an additional failure criteria at 0,34 meter is introduced.

Failure criteria at 0,4 meters The table 61 contains the load limits for the different analysis and the global resistance factor γ_{Om} at 0,4 m for the failure criteria.

α_{cc} = 0,85		α_{cc} = 1		/		
q_{ud} [kN]	$q_{u\tilde{m}}$[kN]	q_{ud} [kN]	$q_{u\tilde{m}}$ [kN]	q_{uk} [kN]	q_{um} [kN]	γ_{Om}
91,4	109,3	91,1	109,3	101,4	109,4	1,150

TABLE 61 – Ultimate load limits for the catenary test (ρ_s = 1,6% and failure criteria = 0,4 m).

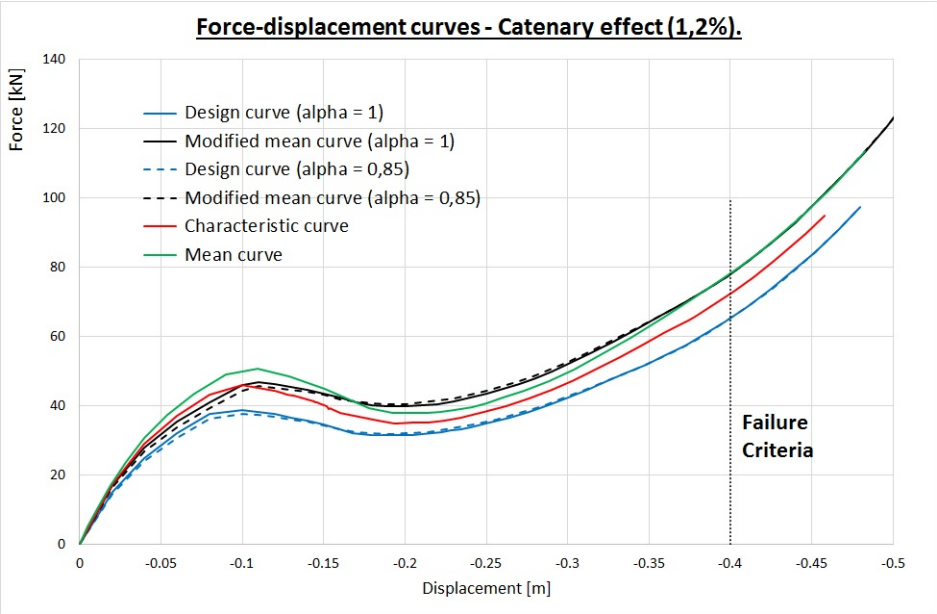

FIGURE 63 – Force-displacement curves for the catenary test investigated ($\rho_s = 1{,}2\%$).

Beam - Catenary effect ($\rho_s = 1{,}2\%$)				
Approach		LM	RM	χ
GRF $\underline{\alpha_{cc} = 0,85}$	$\gamma_{sd} q_{demand} \leq \frac{q_{u\tilde{m}}}{\gamma_O \gamma_{Rd}}$	61,4	61,4	1,0000
	$q\left[\gamma_{Rd} E(\gamma_{sd} q_{demand})\right] \leq \frac{q_{u\tilde{m}}}{\gamma_O}$	66,2	65,1	1,0170
	$q\left[\gamma_{Rd} \gamma_{sd} E(q_{demand})\right] \leq \frac{q_{u\tilde{m}}}{\gamma_O}$	69,1	65,1	**1,0620**
	$q_{demand} \leq \frac{q_{u\tilde{m}}}{\gamma_{O'}}$	53,4	61,5	0,8682
PSF $\underline{\alpha_{cc} = 0,85}$	$\gamma_{sd} q_{demand} \leq q_{ud}$	61,4	65,2	0,9414
	$q\left[\gamma_{sd} E(q_{demand})\right] \leq q_{ud}$	68,0	65,2	**1,0425**
GRF $\underline{\alpha_{cc} = 1}$	$\gamma_{sd} q_{demand} \leq \frac{q_{u\tilde{m}}}{\gamma_O \gamma_{Rd}}$	61,4	61,4	1,0000
	$q\left[\gamma_{Rd} E(\gamma_{sd} q_{demand})\right] \leq \frac{q_{u\tilde{m}}}{\gamma_O}$	66,6	65,1	1,0229
	$q\left[\gamma_{Rd} \gamma_{sd} E(q_{demand})\right] \leq \frac{q_{u\tilde{m}}}{\gamma_O}$	70,2	65,1	**1,0785**
	$q_{demand} \leq \frac{q_{u\tilde{m}}}{\gamma_{O'}}$	53,4	61,5	0,8682
PSF $\underline{\alpha_{cc} = 1}$	$\gamma_{sd} q_{demand} \leq q_{ud}$	61,4	65,3	0,9407
	$q\left[\gamma_{sd} E(q_{demand})\right] \leq q_{ud}$	67,9	65,3	**1,0404**
ECOV	$\gamma_{sd} q_{demand} \leq \frac{q_{um}}{\gamma_O \gamma_{Rd}}$	61,4	63,9	0,9606
	$q\left[\gamma_{Rd} E(\gamma_{sd} q_{demand})\right] \leq \frac{q_{um}}{\gamma_O}$	67,5	67,8	0,9963
	$q\left[\gamma_{Rd} \gamma_{sd} E(q_{demand})\right] \leq \frac{q_{um}}{\gamma_O}$	73,2	67,8	**1,0805**

TABLE 62 – χ factor for the different approaches for the catenary test analysis ($\rho_s = 1{,}2\%$).

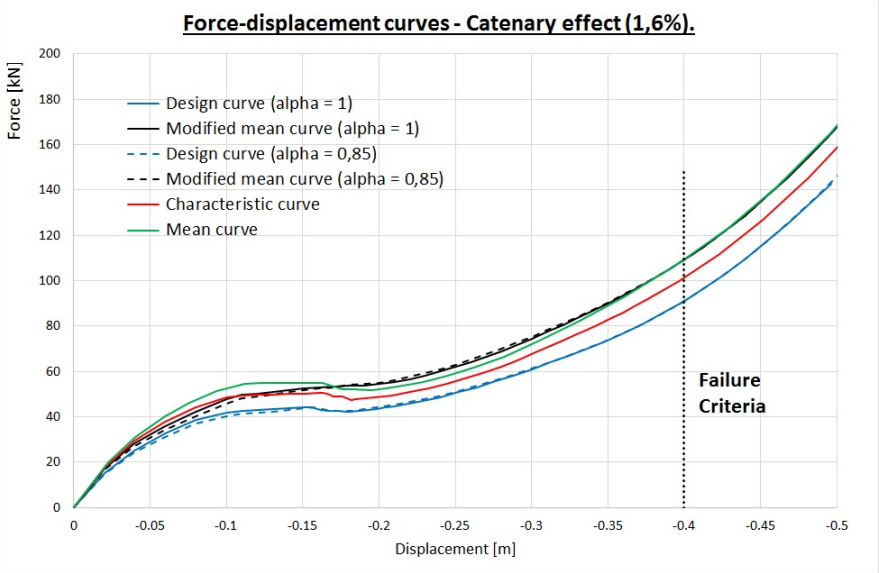

FIGURE 64 – Force-displacement curves for the catenary test investigated (ρ_s = 1,6%) and a failure criteria of 0,4 meter.

Beam - Catenary effect (ρ_s = 1,6%) - Failure criteria = 0,4m				
Approach		LM	RM	χ
GRF $\alpha_{cc} = 0,85$	$\gamma_{sd} q_{demand} \leq \frac{q_{u\tilde{m}}}{\gamma_O \gamma_{Rd}}$	85,9	85,9	1,0000
	$q\left[\gamma_{Rd} E(\gamma_{sd} q_{demand})\right] \leq \frac{q_{u\tilde{m}}}{\gamma_O}$	92,5	91,1	1,0153
	$q\left[\gamma_{Rd} \gamma_{sd} E(q_{demand})\right] \leq \frac{q_{u\tilde{m}}}{\gamma_O}$	94,8	91,1	**1,0404**
	$q_{demand} \leq \frac{q_{u\tilde{m}}}{\gamma_{O'}}$	74,7	86,1	0,8682
PSF $\alpha_{cc} = 0,85$	$\gamma_{sd} q_{demand} \leq q_{ud}$	85,9	91,4	0,9403
	$q\left[\gamma_{sd} E(q_{demand})\right] \leq q_{ud}$	93,8	91,4	**1,0264**
GRF $\alpha_{cc} = 1$	$\gamma_{sd} q_{demand} \leq \frac{q_{u\tilde{m}}}{\gamma_O \gamma_{Rd}}$	85,9	85,9	1,0003
	$q\left[\gamma_{Rd} E(\gamma_{sd} q_{demand})\right] \leq \frac{q_{u\tilde{m}}}{\gamma_O}$	92,7	91,0	1,0177
	$q\left[\gamma_{Rd} \gamma_{sd} E(q_{demand})\right] \leq \frac{q_{u\tilde{m}}}{\gamma_O}$	95,9	91,0	**1,0531**
	$q_{demand} \leq \frac{q_{u\tilde{m}}}{\gamma_{O'}}$	74,7	86,0	0,8685
PSF $\alpha_{cc} = 1$	$\gamma_{sd} q_{demand} \leq q_{ud}$	85,9	91,1	0,9433
	$q\left[\gamma_{sd} E(q_{demand})\right] \leq q_{ud}$	93,5	91,1	**1,0263**
ECOV	$\gamma_{sd} q_{demand} \leq \frac{q_{um}}{\gamma_O \gamma_{Rd}}$	85,9	89,8	0,9570
	$q\left[\gamma_{Rd} E(\gamma_{sd} q_{demand})\right] \leq \frac{q_{um}}{\gamma_O}$	93,3	95,2	0,9806
	$q\left[\gamma_{Rd} \gamma_{sd} E(q_{demand})\right] \leq \frac{q_{um}}{\gamma_O}$	99,3	95,2	**1,0433**

TABLE 63 – χ factor for the different approaches for the catenary test analysis (ρ_s = 1,6%) and a failure criteria of 0,4 meter.

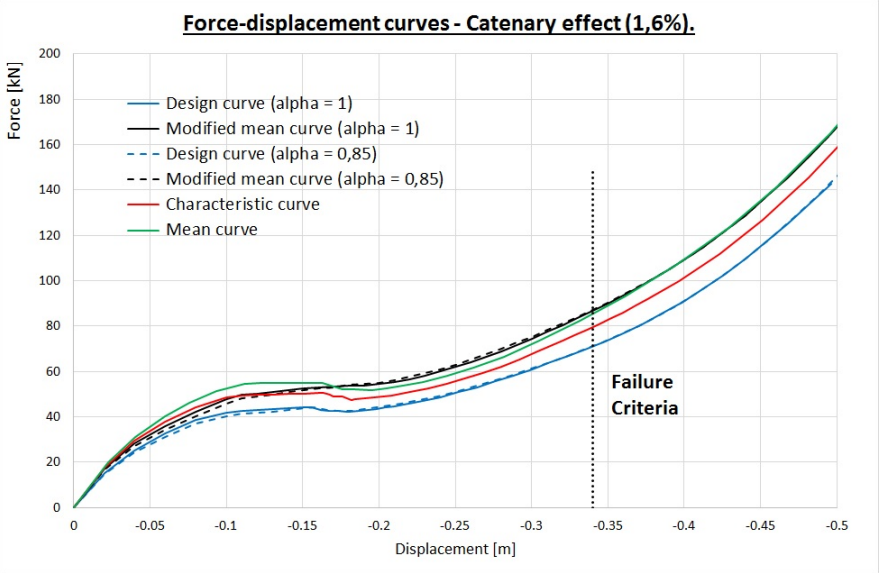

FIGURE 65 – Force-displacement curves for the catenary test investigated (ρ_s = 1,6%) and a failure criteria of 0,34 meter.

Beam - Catenary effect (ρ_s = 1,6%) - Failure criteria = 0,34m				
Approach		LM	RM	χ
GRF $\underline{\alpha_{cc} = 0,85}$	$\gamma_{sd} q_{demand} \leq \frac{q_{u\tilde{m}}}{\gamma_O \gamma_{Rd}}$	68,5	68,5	1,0000
	$q\left[\gamma_{Rd} E(\gamma_{sd} q_{demand})\right] \leq \frac{q_{u\tilde{m}}}{\gamma_O}$	72,7	72,6	**1,0017**
	$q\left[\gamma_{Rd} \gamma_{sd} E(q_{demand})\right] \leq \frac{q_{u\tilde{m}}}{\gamma_O}$	70,7	72,6	0,9741
	$q_{demand} \leq \frac{q_{u\tilde{m}}}{\gamma_{O'}}$	59,6	68,6	0,8682
PSF $\underline{\alpha_{cc} = 0,85}$	$\gamma_{sd} q_{demand} \leq q_{ud}$	68,5	71,1	0,9633
	$q\left[\gamma_{sd} E(q_{demand})\right] \leq q_{ud}$	69,9	71,1	**0,9833**
GRF $\underline{\alpha_{cc} = 1}$	$\gamma_{sd} q_{demand} \leq \frac{q_{u\tilde{m}}}{\gamma_O \gamma_{Rd}}$	68,5	68,3	1,0034
	$q\left[\gamma_{Rd} E(\gamma_{sd} q_{demand})\right] \leq \frac{q_{u\tilde{m}}}{\gamma_O}$	73,0	72,4	**1,0089**
	$q\left[\gamma_{Rd} \gamma_{sd} E(q_{demand})\right] \leq \frac{q_{u\tilde{m}}}{\gamma_O}$	71,5	72,4	0,9888
	$q_{demand} \leq \frac{q_{u\tilde{m}}}{\gamma_{O'}}$	59,6	68,4	0,8712
PSF $\underline{\alpha_{cc} = 1}$	$\gamma_{sd} q_{demand} \leq q_{ud}$	68,5	71,1	0,9636
	$q\left[\gamma_{sd} E(q_{demand})\right] \leq q_{ud}$	70,5	71,1	**0,9917**
ECOV	$\gamma_{sd} q_{demand} \leq \frac{q_{um}}{\gamma_O \gamma_{Rd}}$	68,5	70,6	0,9697
	$q\left[\gamma_{Rd} E(\gamma_{sd} q_{demand})\right] \leq \frac{q_{um}}{\gamma_O}$	73,6	74,9	0,9837
	$q\left[\gamma_{Rd} \gamma_{sd} E(q_{demand})\right] \leq \frac{q_{um}}{\gamma_O}$	74,3	74,9	**0,9925**

TABLE 64 – χ factor for the different approaches for the catenary test analysis (ρ_s = 1,6%) and a failure criteria of 0,34 meter.

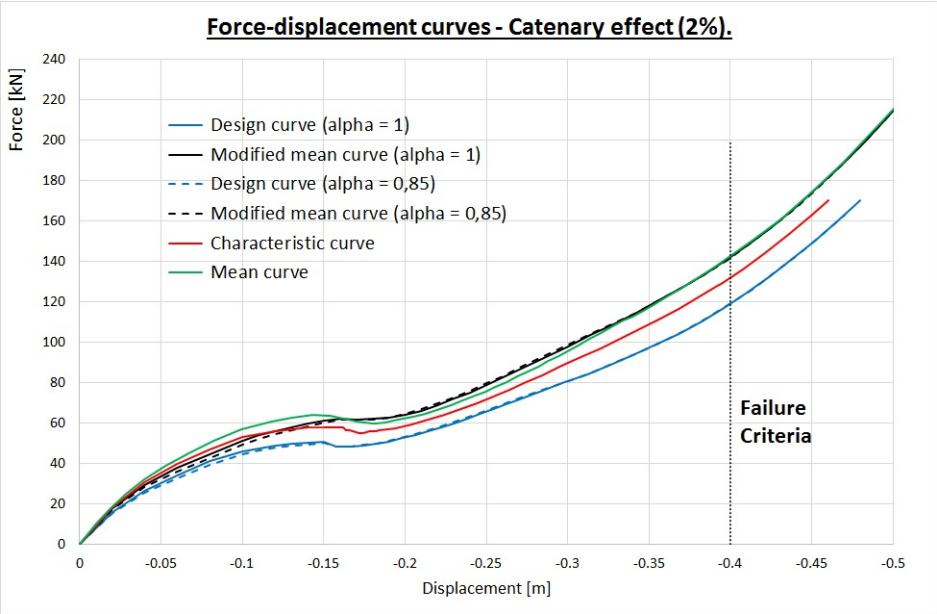

FIGURE 66 – Force-displacement curves for the catenary test investigated (beam with 2%).

Beam - Catenary effect ($\rho_s = 2\%$)				
Approach		LM	RM	χ
GRF $\alpha_{cc} = 0,85$	$\gamma_{sd} q_{demand} \leq \frac{q_{u\tilde{m}}}{\gamma_O \gamma_{Rd}}$	111,7	111,7	1,0000
	$q\left[\gamma_{Rd} E(\gamma_{sd} q_{demand})\right] \leq \frac{q_{u\tilde{m}}}{\gamma_O}$	119,9	118,4	1,0125
	$q\left[\gamma_{Rd} \gamma_{sd} E(q_{demand})\right] \leq \frac{q_{u\tilde{m}}}{\gamma_O}$	122,6	118,4	**1,0354**
	$q_{demand} \leq \frac{q_{u\tilde{m}}}{\gamma_{O'}}$	97,2	111,9	0,8682
PSF $\alpha_{cc} = 0,85$	$\gamma_{sd} q_{demand} \leq q_{ud}$	111,7	119,2	0,9374
	$q\left[\gamma_{sd} E(q_{demand})\right] \leq q_{ud}$	120,6	119,2	**1,0116**
GRF $\alpha_{cc} = 1$	$\gamma_{sd} q_{demand} \leq \frac{q_{u\tilde{m}}}{\gamma_O \gamma_{Rd}}$	111,7	111,8	0,9993
	$q\left[\gamma_{Rd} E(\gamma_{sd} q_{demand})\right] \leq \frac{q_{u\tilde{m}}}{\gamma_O}$	120,1	118,5	1,0133
	$q\left[\gamma_{Rd} \gamma_{sd} E(q_{demand})\right] \leq \frac{q_{u\tilde{m}}}{\gamma_O}$	123,6	118,5	**1,0431**
	$q_{demand} \leq \frac{q_{u\tilde{m}}}{\gamma_{O'}}$	97,2	112,0	0,8676
PSF $\alpha_{cc} = 1$	$\gamma_{sd} q_{demand} \leq q_{ud}$	111,7	119,3	0,9368
	$q\left[\gamma_{sd} E(q_{demand})\right] \leq q_{ud}$	120,6	119,3	**1,0115**
ECOV	$\gamma_{sd} q_{demand} \leq \frac{q_{um}}{\gamma_O \gamma_{Rd}}$	111,7	117,0	0,9545
	$q\left[\gamma_{Rd} E(\gamma_{sd} q_{demand})\right] \leq \frac{q_{um}}{\gamma_O}$	120,7	124,1	0,9725
	$q\left[\gamma_{Rd} \gamma_{sd} E(q_{demand})\right] \leq \frac{q_{um}}{\gamma_O}$	126,7	124,1	**1,0213**

TABLE 65 – χ factor for the different approaches for the catenary test analysis ($\rho_s = 2\%$).

The same remarks can be done here, indeed, the α_{cc} has no influence on the load limit and the modified mean and the mean analysis are similar. The figure 64 illustrates the different analysis and the table 63 the results. The value of q_{demand} is here equal to 74,7 kN.

Failure criteria at 0,34 meters The table 66 contains the load limits for the different analysis and the global resistance factor γ_{Om} at 0,34 m for the failure criteria.

α_{cc} = 0,85		α_{cc} = 1		/		
q_{ud} [kN]	$q_{u\tilde{m}}$[kN]	q_{ud} [kN]	$q_{u\tilde{m}}$ [kN]	q_{uk} [kN]	q_{um} [kN]	γ_{Om}
71,1	87,1	71,1	86,8	79,6	85,6	1,143

TABLE 66 – Ultimate load limits for the catenary test (ρ_s = 1,6% and failure criteria = 0,34 m).

The figure 65 illustrates the different analysis and the table 64 the results. The value of q_{demand} is here equal to 59,6 kN.

7.6.3 Beam with ρ_s = 2 %

The third type of beam modelled present 2 % of reinforcement which corresponds to 10 bars of 16 mm of diameter. The table 67 contains the load limits for the different analysis and the global resistance factor γ_{Om}.

α_{cc} = 0,85		α_{cc} = 1		/		
q_{ud} [kN]	$q_{u\tilde{m}}$[kN]	q_{ud} [kN]	$q_{u\tilde{m}}$ [kN]	q_{uk} [kN]	q_{um} [kN]	γ_{Om}
119,2	142,1	119,3	142,2	132,2	142,6	1,150

TABLE 67 – Ultimate load limits for the catenary test analysis (ρ_s = 2%).

The same remarks can be also done here. The figure 66 illustrates the different analysis and the table 65 the results. The value of q_{demand} is equal to 97,2 kN.

7.6.4 Discussion of the results and comparison

The difference between the three beams can be observed in figure 67 with the design force-displacement curve for each types. We clearly see the difference of capacity of the different types of beams. Moreover we observe a difference in the shape of the curves. Indeed, the beam with 1,2 % of reinforcement presents a negative slope after the flexural failure. We also notice some trouble for the other curve (1,6 and 2 % of reinforcement) but this is less marked.

In this section, a discussion on the results obtained and a comparison for the three types beams are done and first for the same failure criteria. The first remark concerns the change in the results for the different relation's approaches. Indeed,

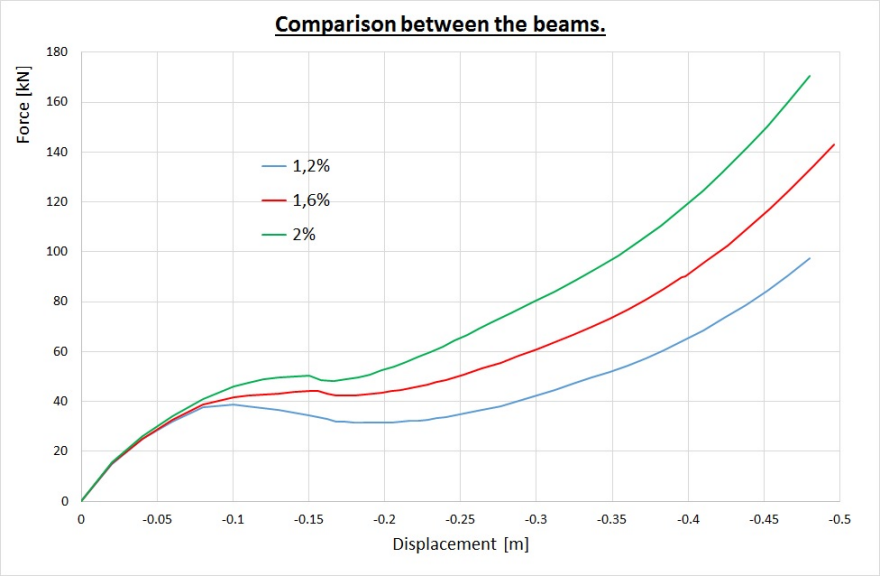

FIGURE 67 – Comparison between the different types of beam modelled (design analysis with α_{cc} = 1).

when the safety factor are imposed on the displacement instead of on the load, the verification becomes now more restrictive. In fact, this observation is explained by the underproportional behaviour observed for the catenary effect (as seen in figure 4). Depending on the percentage of the reinforcement, can vary from 4 to 7% and is more important for the beam with the less amount of reinforcement. The second remark concerns the independence of the α_{cc} value on the results for the GRF and the PSF approaches caused by the not influenced of the concrete in the failure. The third point concerns the nearly correlation between the GRF and the PSF approaches that have around 3 to 4% of difference for the χ factor. The fourth remark concerns the ECOV approach that presents a χ factor around 0,9600 when the safety factor are placed on the load (so 4% lower than the GRF approach), and is more or less equal to the GRF approach when the safety factor are placed on the displacement. As a conclusion for these results, we can say that it is more restrictive to use the GRF or the ECOV approaches compared to the PSF approach. We can gain 2 to 4 % of capacity if the PSF approach is chosen.

After this first comparison when the failure criteria remains constant, the discussion can be done on the position of the failure criteria. Indeed, the results are dependent of this criteria and for example if the criteria is placed on the flexural limit, the results will be similar as the previous model (cubes, columns and frames) for which the safety factor have to be placed on the load. In contrast, as explained for these beams, if the failure criteria is placed in the catenary effect range, then the situation is reversed and the safety coefficient are rather placed on the displacement. These facts are both either all the safety coefficient on the load either on the displacement and a mixed relation is always no effective. In fact, if the failure criteria is placed more close to the transition range (from flexural to catenary), then the mix relation can be effective. This is exactly what happened for the failure criteria

that is equal to 0,34 meter. Indeed, for this case, the relations with a mix in the position of the safety factor is the more restrictive relation for the GRF approach (see table 64). This effect is however with a small margin compare to the other relations. Also, we notice that this observation is not valid for the ECOV approach that present the more restrictive verification when the safety factor are both placed on the displacement.

The figure 68 illustrates the path in the MN plan of the beam with 1,6 % of reinforcement for the design analysis with $\alpha_{cc} = 1$.

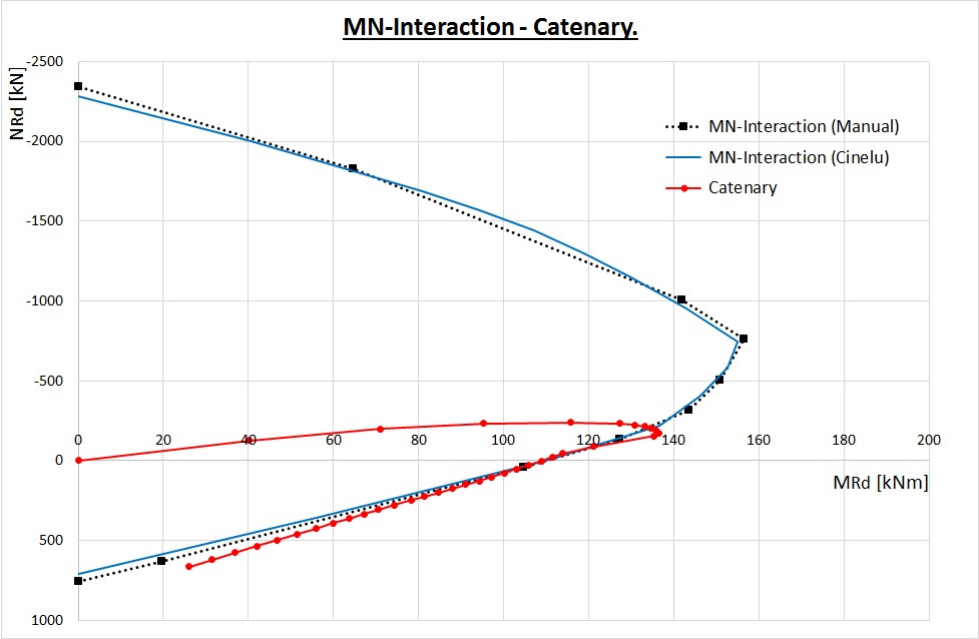

FIGURE 68 – MN-Interaction for the beam with 1,6 % of reinforcement and design analysis.

We observe that the MN path begins in the compression zone until the failure by flexure. The failure of the section at mid-span leads the structure to the catenary effect (both inclined members in tension). The beam then failed by excessive tension in the reinforcement. In figure 68, we can notice two points : First, the failure by flexure appears out of the MN-interaction envelope. Secondly, the catenary effect in figure 68 is represented by the inclined line that follows and diverge from the MN-interaction envelope. These problems are mostly due to the precision of the non linear analysis with the discretisation made.

8 Conclusion

Running a complete non linear analysis of concrete structure has some difficulties especially on the material properties choice and the position of the safety factor in the verification process.

Different approaches are investigated in this work and a focus on three coming from the main codes available is done (Eurocode 1992 [1][2] and the concrete model code [3]). A difference regarding the value of the coefficient α_{cc} is also done. There is not a clear answer on which approach should be used whatever the structure. Indeed, it depends on the type of structure and the investment the engineer is able to provide. Of course, each approach are not done with the same investment, some require only one analysis where others two analysis with an additional computation of the resistance value. The simplest approach is the partial safety factor (PSF) that requires one analysis with the design value for the material properties. Then the global resistance factor (GRF) appears to be similar but with some extra computation on the resistance load and uses other material properties. Finally, the estimation of the coefficient of variation (ECOV) requires two analysis with also a computation on the load resistance. Beside the investment, the notion of hyperstaticity has also an importance. In fact, more the structure becomes complex, more it is difficult to obtain a convergence and a good precision for the analysis.

However, a brief guideline can be expressed. For isostatic and simple hyperstatic structure, the ECOV approach is the best choice. It requires more work, but in return, the capacity of the structure is larger compared to the other approach. This fact is also more important for the structure with essentially normal forces. When the structure is more subjected to bending moment, the difference between the approaches becomes less important and so the advantage of the ECOV approach cannot justify the use of it. In this case, the PSF approach can be chosen especially because of its simple investment.

The second important point concerns the position of the safety coefficient in the different approaches relation studied. Thanks to the models on cubes, columns and frames the safety factor related to the uncertainties on the model of action γ_{sd} and resistance γ_{Rd} should be placed on the load. This conclusion is right for the structure presenting an overproportional behaviour as the cubes, columns and frames. Concerning the structure presenting an underproportional behaviour as for the catenary effect, this conclusion is reversed. The safety factor should be placed rather on the displacement. This becomes more complex when the verification is done near a transition of these both behaviour as it is done for the catenary effect with a failure criteria at 0,34 meter. In that case, a mix relation should be used. It means that the safety factors are placed on the load and on the displacement. This last point shows however a small impact on the results in our case.

9 Perspective

In this section, one perspective is introduced and briefly explained. This idea concerns the safety approach of the partial safety factor (PSF) for high strength concrete. This approach is based on partial safety factor that are calculated with constant value of the coefficient of variation for the concrete material (see the table 5 and equation 17). The coefficient of variation of a density of probability is the standard deviation over the mean value. Or the increase of the concrete strength increases by the fact the mean value without a big change in the standard deviation. Moreover, the difference between the mean and the characteristic strength of the concrete is constant and equals 8 MPa ($f_{cm} = f_{ck} + 8$) as seen in the table 68. In that case, the coefficient of variation of the concrete material should decrease with the increase of the strength. The evolution of that coefficient of variation is illustrated in figure 69 assuming a lognormal and a normal distribution of the concrete strength.

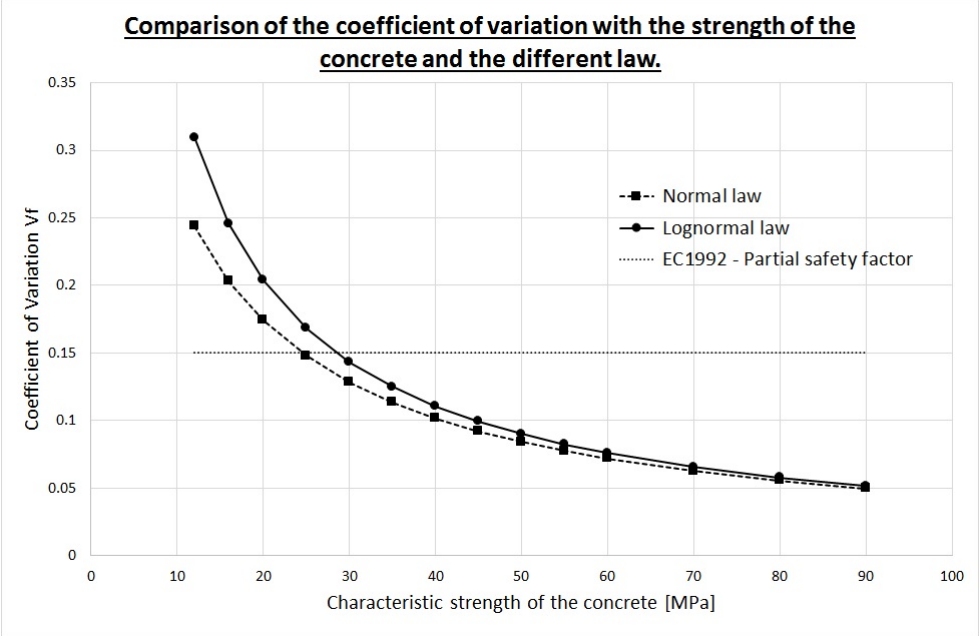

FIGURE 69 – Evolution of the coefficient of variation of the material with the concrete strength.

The decrease of the coefficient of variation leads to a decrease of the partial safety factor. The evolution of the partial safety factor γ_c using the equation 40 and 41 when the coefficient of variation varies with the strength is illustrated in the following figure 70.

$$\frac{f_{ck}}{f_{cd}} = \gamma_c = 1,15 \exp(3,04 V_R - 1,64 V_f) \tag{40}$$

with

$$V_R = \sqrt{V_m^2 + V_G^2 + V_f^2} \tag{41}$$

In this case, the coefficient of variation on the model and on the geometry is kept constant and equal both to 5 %.

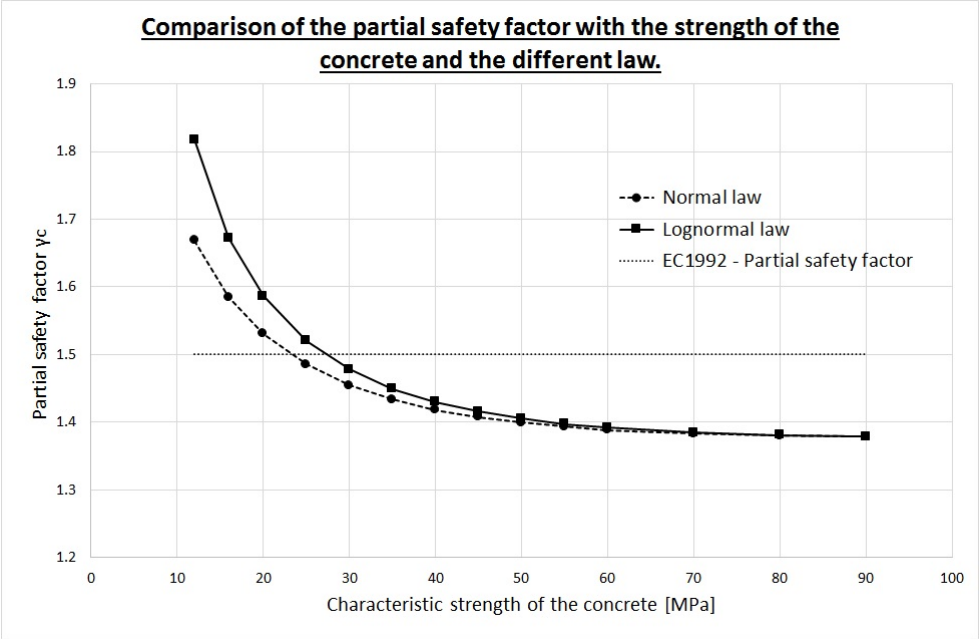

FIGURE 70 – Evolution of the partial safety factor γ_c with the concrete strength.

The question and remarks about this observation can be done for both low and high strength concrete. Indeed, for low strength concrete, the partial safety factor γ_c calculated thanks to the both probability law are higher than the recommended value from the Eurocode 1992 [1]. Note that, the coefficient 1,15 is also used in our study. The second remark concerns the high strength concrete for which it would be tempting to use a lower value of the partial safety factor. For example, from the class C50/60 a value of 1,4 for γ_c could be used if the we follow that logic.

10 Annex

In the annex, an typical example of the input *.dat* files used for running the software Finelg is presented. Also the table of the different concrete class properties from the Eurocode 1992-1-1 [1] is placed.

10.1 Concrete class properties

Resistance classes of the concrete																
f_{ck} [Mpa]	12	16	20	25	30	35	40	45	50	55	60	70	80	90		
$f_{ck,cube}$ [Mpa]	15	20	25	30	37	45	50	55	60	67	75	85	95	105		
f_{cm} [Mpa]	20	24	28	33	38	43	48	53	58	63	68	78	88	98		
f_{ctm} [Mpa]	1,6	1,9	2,2	2,6	2,9	3,2	3,5	3,8	4,1	4,2	4,4	4,6	4,8	5,0		
$f_{ctk,0.05}$ [Mpa]	1,1	1,3	1,5	1,8	2,0	2,2	2,5	2,7	2,9	3,0	3,1	3,2	3,4	3,5		
$f_{ctk,0.95}$ [Mpa]	2,0	2,5	2,9	3,3	3,8	4,2	4,6	4,9	5,3	5,5	5,7	6,0	6,3	6,6		
E_{cm} [Gpa]	27	29	30	31	33	34	35	36	37	38	39	41	42	44		
ϵ_{c1} [‰]	1,8	1,9	2,0	2,1	2,2	2,25	2,3	2,4	2,45	2,5	2,6	2,7	2,8	2,8		
ϵ_{cu1} [‰]	3,5									3,2	3,0	2,8	2,8	2,8		
ϵ_{c2} [‰]	2,0									2,2	2,3	2,4	2, 5	2,6		
ϵ_{cu2} [‰]	3,5									3,1	2,9	2,7	2,6	2,6		
n [-]	2,0									1,75	1,6	1,45	1,4	1,4		
ϵ_{c3} [‰]	1,75									1,8	1,9	2,0	2,2	2,3		
ϵ_{cu3} [‰]	3,5									3,1	2,9	2,7	2,6	2,6		

TABLE 68 – Resistance and deformation properties of the different concrete classes [1].

10.2 Typical example of the input file for Finelg

This example concerns the 5 meters column with 1% of reinforcement subjected to axial force and a basic inclination of 1/100 (5C2).

```
FINELG   102       4
Valeur de calcul

CTRL
  kN   M
   0   0   0      -1  123456       0   0   0   0   0    28.0
    NONL
    SEQP   1
   1   19999                      1           5   0   0
   0   0   0
CTRL_END
SEQP       1
    COMB
   1         1.0     1.0     0.0     0.0     0.0     0.0     0.0
    INCR
 101  -4 115  -4 125  -4
    CREM
     1.0     1.0     1.5
    MOPA
   1  10  -4
    MOPS
 900   3     0.5     1.2       1     0.5
 999   4     0.5     1.2       1     0.5
    NODC
  11
   2
SEQP_END   1
MECA
   1   0    2.10E+08      0.3000      255.00
   2   0    1.95E+08      0.3000
   3   0    3.50E+07      0.2000
   4   0   1.170E+07        0.20
   5   0   2.100E+11
   6   0   2.100E+05
   7   0   1.160E+07
  -7   0   7.500E+05
   8   0   6.444E+06
  -8   0   4.000E+05
   9  27   2.583E+07        0.20   16666.667      0.0021      0.0001
    0.0035    Loi béton Compression
  -9   0   0.000E+00        0.00       0.000       0.000       0.000
    0.000     Loi Béton traction
```

```
  10    2   2.000E+08         0.30  434000.000  727273.000
              Loi acier Armatures
MECA_END
GEOM
   1    0       0.0000         0.00         0.00         0.00         0.00
    0.00       Column
  -1         0.000000     0.000000     0.000000     0.000000     0.000000
    0.00
    FICG
   1   1colonnebrux1%.gci
GEOM_END
COOR    nb nœuds:              11n max:                11
   1    0        0.000        0.000        0.000
   2    0        0.000        0.000        0.500
   3    0        0.000        0.000        1.000
   4    0        0.000        0.000        1.500
   5    0        0.000        0.000        2.000
   6    0        0.000        0.000        2.500
   7    0        0.000        0.000        3.000
   8    0        0.000        0.000        3.500
   9    0        0.000        0.000        4.000
  10    0        0.000        0.000        4.500
  11    0        0.000        0.000        5.000
    APPU
 1111110    0    0    1
 1000000    0    0   11
COOR_END
ELEM    nb elem:       10
   1  87    9    1    1    2    0           A
   2   0    0    0    2    3    0           A
   3   0    0    0    3    4    0           A
   4   0    0    0    4    5    0           A
   5   0    0    0    5    6    0           A
   6   0    0    0    6    7    0           A
   7   0    0    0    7    8    0           A
   8   0    0    0    8    9    0           A
   9   0    0    0    9   10    0           A
  10   0    0    0   10   11    0           A
ELEM_END
CHAR
   1            0.000      8.94400    -1000.000
    CAS
   1   1    1       11
CHAR_END
END
```

References

[1] Comité Européen de Normalisation. EN 1992-1-1 : Eurocode 2 : Calcul des structures en béton - partie 1-1 : Règles générales et règles pour les bâtiments. 2004.

[2] Comité Européen de Normalisation. EN 1992-2 : Eurocode 2 : Calcul des structures en béton - partie 2 : Ponts en béton - calcul et dispositions constructives. 2005.

[3] Fib : fédération internationale du béton. Model code 2010, First complete draft. *fib-Bulletin 55 - 56*, 2010.

[4] Bureau de Normalisation. EN 1992-1-1 ANB : Eurocode 2 : Calcul des structures en béton - partie 1-1 : Règles générales et règles pour les bâtiments - Annexe Nationale Belge. 2010.

[5] British Standards. EN 1992-1-1 UK : UK National Annex to Eurocode 2 : Design of concrete structures - part 1-1 : General rules and rules for buildings. 2004.

[6] Association Française de Normalisation (AFNOR). EN 1992-1-1 NF : Eurocode 2 : Calcul des structures en béton - partie 1-1 : Règles générales et règles pour les bâtiments - Annexe Nationale. 2005.

[7] Comité Européen de Normalisation. EN 1990 : Eurocodes structuraux : Eurocodes : Bases de calcul des structures. 2002.

[8] European Concrete Platform. Eurocode 2 commentary - Brussels. 2008.

[9] Six M. Sicherheitskonzept für nichtlinear Traglastverfahren im Betonbau. *Institut für Massivbau, Technical University Darmstadt*, page pp. 183, 2011.

[10] Calheiros F. Henriques A. A. R. and Figueiras J. A. Safety format for the design of concrete frames. *Engineering Computations*, pages pp. 346–363, 2002.

[11] Schlune Hendrik. Safety evaluation of concrete structures with nonlinear analysis.

[12] Comité Européen de Normalisation. EN 1998-1 : Eurocode 8 : Calcul des structures pour leur résistance aux séismes - partie 1 : Règles générales, actions sismiques et règles pour les bâtiments. 2005.

[13] Comité Européen de Normalisation. EN 1991-1-4 : Eurocode 1 : Actions sur les structures - partie 1-4 : Actions générales - Actions du vent (+ AC :2010). 2005.

[14] MSM Department – University of Liège and Engineering Office GREISCH. FINELG : Nonlinear finite element analysis program. User's Manuel Version 9.0. 2003.

[15] De Ville De Goyet V. Problèmes non linéaire en génie civil. *Cours universitaire (Université de Liège)*, 2014.

[16] Somja H. Legrand E. Hansoulle T. Puffet J.F., De Ville De Goyet V. CINELU, Programme de calcul des courbes d'interaction ELU et de vérification des sections béton armé, acier ou structures mixtes - version 42. 2007.

List of Figures

List of Tables